Synthetic, layered nano-particles for polymeric nanocomposites (PNC's)

Utracki, L. A.; Sepehr, M.; Boccaleri, E.

Publisher's version / Version de l'éditeur:
https://doi.org/10.1002/pat.852
Polymers for Advanced Technologies, 18, 1, pp. 1-37, 2007-01-08

POLYMERS FOR ADVANCED TECHNOLOGIES
Polym. Adv. Technol. 2007; **18**: 1–37
Published online in Wiley InterScience (www.interscience.wiley.com) DOI: 10.1002/pat.852

PAT

Review

Synthetic, layered nanoparticles for polymeric nanocomposites (PNCs)

L. A. Utracki[1]*, M. Sepehr[1] and E. Boccaleri[2]

[1]National Research Council Canada, Industrial Materials Institute, 75 de Mortagne, Boucherville, QC, J4B 6Y4, Canada
[2]Università del Piemonte Orientale "A. Avogadro", Dipartimento di Scienze e Tecnologie avanzate, Alessandria, Italy

Received 21 July 2006; Revised 2 October 2006; Accepted 3 October 2006

This review discusses preparation and use of the synthetic layered nanoparticles in polymer matrices, i.e., in the polymeric nanocomposites (PNCs). Several types of synthetic or semi-synthetic layered materials are considered, namely the phyllosilicates (clays), silicic acid (magadiite), layered double hydroxides (LDHs), zirconium phosphates (ZrPs), and di-chalcogenides. The main advantage of synthetic clays is their chemical purity (e.g. absence of amorphous and gritty contaminants, as well as arsenic, iron, and other heavy metals), white to transparent color that assures reproducibly of brightly colored products, as well as a wide range of aspect ratios, $p = 20$ to ≤ 6000. Several large scale production facilities have been established. The synthetic clay and LDH industries are oriented toward big volume markets: catalysis, foodstuff, cosmetics, pharmaceuticals, toiletry, etc. The use of these materials in PNCs is limited to synthetic clays and LDHs, mainly for reinforcement, permeability control, reduction of flammability, and stabilization, e.g. during dehydrohalogenation of chlorinated macromolecules. The use of lamellar ZrPs and di-chalcogenides is at the laboratory stage of functional polymeric systems development, e.g. for electrically conductive materials, catalysts or support for catalysts, in photochemistry, molecular and chiral recognition, or in fuel cell technologies, etc. Copyright © 2007 John Wiley & Sons, Ltd.

KEYWORDS: polymeric nanocomposites; nanoparticles; clay; layered double hydroxides; matrix

AUTHORS' BIOGRAPHIES

Dr Leszek A. Utracki was born and educated (up to Habilitation) in Poland. After the post-doctoral stage at USC in Los Angeles with Robert Simha he settled in Canada. His passionate research interest has been within the field of thermodynamics, rheology and processing of multicomponent, multiphase polymeric systems. During the 55 years in the profession he has published several hundred articles, book chapters, books, patents, etc., which has placed him on the ISI list of Highly Cited Researchers. He is co-founder and past President of the Canadian Rheology Group and the Polymer Processing Society (International). He has also organized and served as the Series Editor of the books' series *Progress in Polymer Processing*, as well as being editor and member of editorial boards of several research journals.

Dr Maryam Sepehr obtained her B.Sc. in Chemical Engineering from Polytechnic of Tehran, her M.Sc. in Physics and Material Engineering from École des Mines of Paris, CEMEF. In 2003 she completed her Ph.D., under the supervision of Professor Pierre J. Carreau in the Department of Chemical Engineering of École Polytechnique in Montreal with a thesis on the rheological study of short fiber suspensions. Currently she works as a post-doctoral fellow at the Industrial Material Institute, National Research Council Canada, on the preparation, compounding and characterization of thermoplastic nanocomposites with Professor Leszek A. Utracki in the Structural Polymers and Composites Group.

**Correspondence to*: L. A. Utracki, National Research Council Canada, Industrial Materials Institute, 75 de Mortagne, Boucherville, QC, J4B 6Y4 Canada.
E-mail: leszek.utracki@nrc.ca

Dr Enrico Boccaleri received his degree in Chemistry *cum laude* in 1996, and Ph.D. in 2001, both from Torino University. At the end of the same year he became researcher in the field of Inorganic and Materials Chemistry at the Università del Piemonte Orientale—Faculty of Science, in Alessandria. Currently, he is associated with the Molecular Spectroscopy and Solid State Chemistry laboratories. His research interests are focused on the synthesis, characterization and functionalization of inorganic and organic/inorganic hybrid nano-structured materials. More specifically, his basic and applied studies concern one-dimensional (layered inorganic materials, e.g. layered double hydroxides, or synthetic clays), two-dimensional (e.g. carbon nanotubes, CNTs) and three-dimensional (e.g. polyhedral oligomeric silsesquioxanes, POSS).

INTRODUCTION

The layered materials of interest to polymeric nanocomposite (PNC) technology should have platelets from *ca*. 0.7–2.5 nm thick.[1] A partial list of candidates is given in Table 1. The average interparticle spacing between layers depends on the extent of intercalation, and mineral concentration, generally the higher the mineral concentration the smaller the spacing.

Since polymeric nanocomposites are mainly used as structural materials, currently the preferred layered materials are phyllosilicate clays of the 2:1 type, more precisely smectites, and in particular montmorillonite (MMT), and hectorite (HT) shown in Fig. 1. Chemical structures of these clays have also been published by Itoh *et al.*[2], and Greenwell *et al.*[3], respectively. The layer surface has 0.25 to 1.2 negative charges per unit cell and a commensurate number of exchangeable cations in the interlamellar galleries. For the anionic clays (e.g. smectites) the ion concentration is usually expressed as the cation exchange capacity (CEC), which ranges from about 0.5 to 2 meq/g; for cationic layered compounds (e.g. layered double hydroxides, LDHs; see Fig. 1), the equivalent measure is the anion exchange capacity (AEC), which ranges from about 0.5 to 6 meq/g. The aspect ratio of commercial MMT-type organoclay is about $p = d/t \approx 280$, where d is the diameter, and t is the clay platelet thickness. An average smectite clay platelet is about 1 nm thick, 150 nm wide and 500 nm long. The aspect ratio of commercial synthetic clays ranges up to 6000. The concentration of such (fully exfoliated) nano-material required for the production of PNCs with significantly improved performance ranges from 5 ppm to about 10 wt% (for the high barrier properties).

In natural clays there are three types of primary contaminants: presence of platelets welded together by a crystallographic fault (frequently doublets and short stacks or tactoids may also be present), presence of grit (*ca*. 0.3 to 2 wt% mostly of quartz particles at least 300 nm in diameter), and presence of amorphous silicates. Thus elaborate purification methods are required (e.g. see Part 2.2.3 of ref. 1).

While MMT is abundant and relatively inexpensive its main drawback is that it is a mineral with variable composition, and numerous contaminants that are extremely difficult to eliminate. The variability of PNCs has been frequently blamed on structural (particle size distribution, and aspect ratio) as well as chemical (surface reactivity) variability. Consequently, there is a growing interest in synthetic or at least semi-synthetic layered materials with well-controlled physical and chemical properties. While the experiments with these systems are essential for the development of basic knowledge of intercalation and exfoliation, only a few synthetic layered materials have been used for the manufacture of PNCs.

The organoclays and PNCs are usually characterized by means of X-ray diffraction (XRD), transmission electron microscopy (TEM) and scanning electron microscopy (SEM) methods. These tools indeed provide information about the structure and the degree of clay dispersion. However, these methods are unable to assess the basic forces responsible for the dispersion, the clay/intercalant/polymer interactions.

Table 1. Layered nano-particles for the potential use in PNC

Smectite clays	Montmorillonite (MMT), bentonite (BT), nontronite, beidellite, volkonskoite, hectorite (HT), saponite, sepiolite, stevensite, sauconite, sobockite, svinfordite, kenyaite
Synthetic clays	e.g. hectorite, $MgO(SiO_2)_s(Al_2O_3)_a(AB)_b(H_2O)_x$, (where AB is a ion pair, namely NaF)
Layered silicic acids	Kanemite, makatite, octosilicate, magadiite, kenyaite, layered organo-silicates
Other clays	Micas, vermiculite, illite, ledikite, tubular attapulgite, etc.
Mineral layered hydroxides	e.g. brucite: $Mg(OH)_2$, or gibbsite: $Al(OH)_3$
Layered double hydroxides (LDHs)	$[M^{+2}_{(1-X)}M^{+3}_X(OH)_2]^{Y+}(A^{n-Y/n})\ mH_2O$, e.g. $Mg_6\ Al_{3\cdot4}\ (OH)_{18\cdot8}\ (CO_3)_{1\cdot7}\ H_2O$; or $Zn_6\ Al_2\ (OH)_{16}\ CO_3\ nH_2O$
Layered alumino-phosphates	e.g., mineral ALPO (berlinite), $Al_4(PO_4)_3(OH)_3 \cdot 9H_2O$ (vantasselite), or from hydrothermal synthesis of $H_3PO_4 + Al(OH)_3$ with structure-directing agents
M^{+4} phosphates or phosphonates	M^{+4} = Ti, Zr, or Sn; e.g., α-form: $Zr(HPO_4) \cdot 2H_2O$; γ-form: $ZrPO_4O_2P(OH)_2{\cdot}2H_2O$; λ-form; $ZrPO_4XY$ (X and Y are anionic or neutral ligands), etc.
Chlorides	$FeCl_3$, FeOCl, CdI_2, $CdCl_2$
Chalcogenides	TiS_2, MoS_2, MoS_3, $(PbS)_{1.18}(TiS_2)_2$
Cyanides	$Ni(CN)_2$
Oxides	$H_2Si_2O_5$, V_6O_{13}, $HTiNbO_5$, $Cr_{0\cdot5}V_{0\cdot5}S_2$, $W_{0\cdot2}V_{2\cdot8}O_7$, Cr_3O_8, $MoO_3(OH)_2$, V_2O_5, $VOPO_4$-$2H_2O$, $CaPO_4CH_3$-H_2O, $MnHAsO_4$-H_2O, $Ag_6Mo_{10}O_{33}$, etc.
Others	Graphite, graphite oxide, boron nitride (BN), etc.

DOI: 10.1002/pat

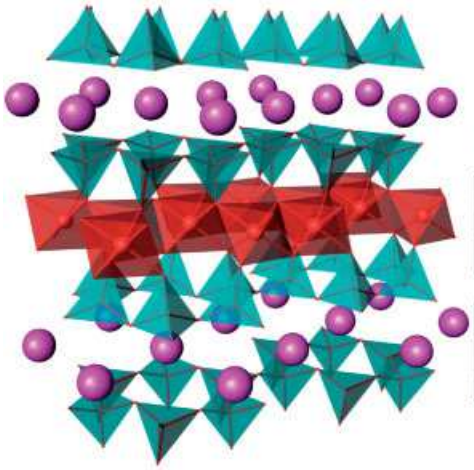

Talc

	Framework element	Vicariant element
T	Si	-
O	Mg (occupancy 3/3)	-
T	Si	-
interlayer	none	

Pyrophyllite

	Framework element	Vicariant element
T	Si	-
O	Al (occupancy 2/3)	
T	Si	-
interlayer	none	

Hectorite

	Framework element	Vicariant element
T	Si	-
O	Mg (occupancy 3/3)	Li
T	Si	-
interlayer	Na^+/Mg^{2+}...	

Montmorillonite

	Framework element	Vicariant element
T	Si	-
O	Al (occupancy 2/3)	Mg
T	Si	-
interlayer	Na^+/Mg^{2+}...	

Saponite

	Framework element	Vicariant element
T	Si	Al
O	Mg (occupancy 3/3)	
T	Si	Al
interlayer	Na^+/Mg^{2+}...	

Beidellite

	Framework element	Vicariant element
T	Si	Al
O	Al (occupancy 2/3)	
T	Si	Al
interlayer	Na^+/Mg^{2+}...	

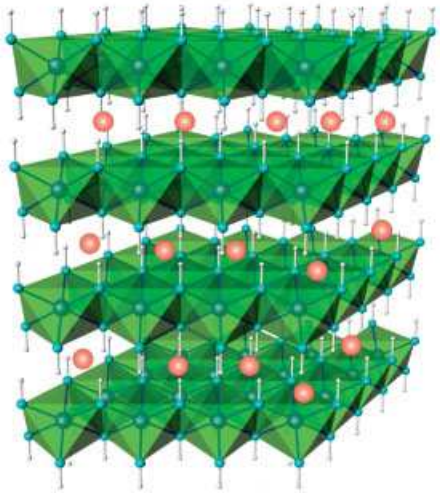

Brucite

	Framework element	Vicariant element
O	Mg (occupancy 3/3)	-
interlayer	none	

Gibbsite

	Framework element	Vicariant element
O	Al (occupancy 2/3)	-
interlayer	none	

Hydrotalcite

	Framework element	Vicariant element
O	Mg/Zn et al.	Al
interlayer	Anions as Cl^-, CO_3^{2-}, NO_3,	

Figure 1. The chemical general structures are respectively for: 2:1 phyllosilicates (top) and LDH (bottom), with the schematic representation of the tetrahedra (T) and octahedra (O) occupancies in natural and synthetic layered nano-fillers.

The rapid progress in NMR provides means for quantification of these interactions, and thus elimination of the guesswork in PNC formulations.

Solid-state ^{1}H, ^{13}C, ^{15}N, ^{19}F, ^{29}Si and ^{31}P magic angle spinning (MAS) NMR spectroscopy has been found useful for measuring interactions between nuclei and between them and the surroundings, and thus the macroscopic behavior of PNCs can be interpreted. The chemical shift (Cs) dipole–dipole interactions, and *J*-coupling are used to elucidate electronic structure surrounding the nuclei, inter-nuclear distances and orientation. For example, Usuki *et al*. demonstrated that the tensile modulus (*E*) is proportional to the Cs value of ^{15}N in the ammonium-clay complex.[4] The shift also provided accurate information about the degree of clay hydration, the interactions engendered by intercalation and the structure of clay-organic matrix complexes. The quadrupole coupling enlarged the list of nuclei to include ^{17}O, ^{23}Na and ^{27}Al, providing means to study chemical bonding.[5]

NMR has been also used to determine polyethylene glycol (PEG) chain dynamics within the interlayer spacing of synthetic mica/MMT.[6] The ^{1}H-NMR line widths and relaxation time versus temperature (*T*) were used to determine the effect of bulk thermal transitions.[7] The ^{13}C cross-polarity/MAS NMR of PEG showed that these macromolecules undergo the helical jump motion of the α transition—the same as within the crystalline phase. The solid-state NMR, of ^{1}H and ^{13}C was used to study poly-ε-caprolactam (PA-6) with 5 wt% organoclay.[8] MMT contained non-stoichiometric amounts of Mg^{2+} and Fe^{3+} ions substituted into the octahedral layer. The paramagnetic contribution of Fe^{3+} ion to T_1^H was used to determine the degree of dispersion, the stability of intercalant, etc.

During the 1980s two-dimensional (2D) NMR spectroscopy was developed. The method originally was used for studying the geometry of molecular dynamics. The rotation of molecules engendered exchange peaks, from which the magnitude of interactions and the molecular rotation angle can be calculated.[9,10] The homo-nuclear and hetero-nuclear 2D correlated solid-state NMR spectroscopy was found to be of particular value in studies of organic-inorganic complex structures.

Sozzani *et al*. determined by means of 2D solid-state NMR the structure and interactions of the $MgCl_2 + EtOH$ adduct (a catalyst support for Ziegler-Natta polymerization).[11] Closer to the PNC technology were more recent publications from the group.[12,13] The object of the study was hectorite pre-intercalated with tetraethyl ammonium (4EA) during a hydrothermal synthesis, HT-4EA of the formula: $(4EA)_{0.66}(Mg_{5.34},Li_{0.66})Si_8O_{20}(OH, F)_4$ with $d_{001} = 1.47$ nm, in agreement with the 0.6 nm diameter of the 4EA ion. The compound was studied using the 2D advanced solid-state,

DOI: 10.1002/pat

Lee–Goldburg homo-nuclear decoupling MAS NMR techniques at the spinning speed of 15 kHz and contact times 2 and 8 msec. The studies indicated close magnetic communication between C, H, and Si atoms providing evidence of strong interactions between the organic and inorganic parts of the HT-4EA. It is noteworthy that these interactions were stronger than those involving N-atom. This provides further proof that the clay-ammonium ion complexes are formed with delocalized charge. The authors also demonstrated porosity of HT-4EA, and its ability to adsorb gases and vapors.

SYNTHETIC CLAYS

Synthetic clays have been used in PNCs since the very beginning; in 1976 Unitika (now: Unitika Ube Nylon Co., Ltd) started commercial production of PNCs with PA-6 as the matrix (Nylon grade M1030D) by polymerizing ε-caprolactam in the presence of synthetic clay from COOP (now CBC Co.). Currently, these materials are injection molded into covers for Mitsubishi and Toyota cars as well as the bases for the electronic control units under the hood. Table 2 provides a partial list of synthetic clays—not all are commercially available. The interest in synthetic layered nano-fillers is growing. Several reviews on the preparation and properties of synthetic clays are available, namely Barrer and Dicks,[14] Kloprogge,[15] Kloprogge *et al.*,[16] and Carrado and co-workers.[17,18] Preparation and use of LDH and layered M^{+4} phosphates or phosphonates have also been described, respectively, by Duan and Evans,[19] and by Alberti *et al.*[20]

Synthetic clays—methods of preparation

Synthetic clays have been developed mainly in a search for catalysts, with 2D porous structures and acidic properties, comparable to the three-dimensional (3D) zeolites. Synthetic smectites and related phyllosilicates have been prepared in a number of ways, as described in numerous patents and articles. The methods can be assigned to three categories:

1 Semi-synthetic, prepared by modification of such minerals as, talc or obsidian. The mineral crystalline structure is modified by partial replacement of Mg^{+2} in the octahedral layer by Na^+ or Li^+ (e.g. see Orlemann[21]). For this purpose Li_2CO_3 or Na_2CO_3 may be used. When Na_2SiF_6 or LiF are used, the fluoro hectorite (FH) or fluoro mica (FM) is obtained. The fluoride (*ca.* 5 wt%) partially replaces the –OH groups on the clay surface, and thus modifies its reactivity.[22]
2 Fully synthetic, where formation of layered silicate starts with a variety of metal oxides that provide suitable composition, e.g. $(Si_4O_{10})_2$ $(Mg_{6-x}Li_x(OH)_{4-y}F_y$, for crystallization of layered silicates. Several sub-categories can be distinguished:
   a The low temperature, hydrothermal process that starts with aqueous solutions of suitable salts co-precipitated into slurry, which in turn is hydrothermally treated (boiling under reflux under autogenous pressure in a sealed autoclave) for 10 to 20 hr to cause crystallization. Washing (to remove amorphous materials) and drying at 110 to 25°C completes the process.[23–27] Furthermore, the hydrothermal crystallization in the presence of fluoride anions provides a fast synthetic route for the preparation of MMT,[28] beidellite, saponite,[29] and clay-like organosilicates.[30]
   b The high temperature melt process, starts with fine powders of suitable salts (e.g. Li_2O, MgO, SiO_2 and MgF_2), mixed in proper proportions, heated at 1300°C for 3 hr and then allowed to cool for 10 hr. The reaction mass is dispersed in water and the solid contaminants sedimented, yielding synthetic HT stacks of *ca.* 2–5 nm thick, and 20–80 nm long.[31]
   c Co-precipitation of di-valent and tri-valent metal ions in alkaline, aqueous medium at $T \cong 95$°C, under flow of N_2. Considering the wide choice of metal ions (e.g. M^{2+} = Fe, Co, Ni, Mg, Cu, Zn, Mn, Cd, Ba, Be, Hg, Pb, Sn, Sr, Ca; M^{3+} = Al, Fe, Co, Mn, Ga, Ru, Cr, V, In) and that of anions, the process might produce a great variety of the co-organized LDHs with diverse physical and chemical characteristics.[32]

Low temperature, sol-gel method for LDH preparation has been proposed with short time (10 to 30 min) microwave irradiation replacing the hydro-thermal treatment. Starting with Al-acetyl-acetonate and either Mg-ethoxide or Mg-acetyl-acetonate, LDHs with different characteristics are obtained.[33]

3 Templated synthetic, using organic templates, which after synthesis may be pyrolyzed, or left in as intercalants (non-commercial).[17,18,34]

As shown in Table 2, several types of synthetic clays have been synthesized. Thus, for example, Hénin[23] crystallized MMT at $T = 20$ to 100°C (the reaction rate increased with T), starting with diluted salt solutions (few mg/l). Later it was found that only at higher at high temperatures(T) and pressures(P) MMT might be produced on a large scale. For this reason, the commercial synthetic clays are not MMT, but primarily FH, FM, or LDHs, all prepared at low T and P, and which crystallize under much less rigorous conditions—the HT synthesis takes place under aqueous reflux, at high pH, and in the absence of Al^{3+}.

The natural HT has a significantly smaller aspect ratio than MMT, namely $p < 100$, but its fully synthetic homologue prepared at low T, e.g. synthetic FH, has even smaller, nearly circular flakes with $p = 10$ to 50. As described by Yano *et al.*,[35] the semi-synthetic FM can be prepared with high aspect ratio, e.g. $p < 6000$. Similarly as it is the case for MMT (see Fig. 1), the basic structural unit of HT consists of two tetrahedral silicate layers that sandwich a central magnesium oxide octahedral layer. Whereas in MMT the CEC arises from isomorphous substitutions in the octahedral layer of Mg^{+2} for Al^{+3}, in HT it originates from the substitution of Li^+ for Mg^{+2}. The fully synthetic clays prepared in the molten state also can be produced with high aspect ratio: $p \leq 6000$. The aspect ratio of the LDH material has rarely been cited. However, judging by the published micrographs the aspect ratio in processed PNC is smaller, namely $p \leq 100$ nm.[19,36] The advantages and disadvantages of natural and synthetic clays are summarized in Table 3.

DOI: 10.1002/pat

Table 2. A partial list of manufacturers of synthetic clays

No.	Company	Synthetic clay	Clay type
1	UNICOOPJAPAN, is now: CBC Co. Ltd., Mr Tetsuo Wakisaka, wakisaka@cbc.co.jp	Somasif^{TM} ME100 fluoro-mica (FM) or fluoro-hectorite (FH), intercalated grades are available Lucentite^{TM} SWN is lithium magnesium sodium silicate; intercalated SAN and SPN grades are available	Montmorillonite-type; CEC $\cong$1 meq/g; $d_{001} = 0.95$ nm; pH = 9–10 Na-hectorite; pH = 10–11
2	Laporte Industries, Ltd., Luton U.K./SCP, P.O. Box 44, Gonzales, T X 78629 Cheryl Evans, Phone: 830-672-1997; Fax: 210-672-7206; http://www.laponite.com/	Laponite LRD or RD was developed by Laporte more than 30 years ago, and has been manufactured at the Widnes site since 1985. It is either Na-Li-Mg-silicate, or Na-Li-Mg-fluorosilicate	Hectorite, SYnL–1; 25 × 10 nm;
3	Süd Chemie AG; Sabine Kern Mgr. Sales; Ostenriederstr. 15, 85368 Moosburg; Phone: +49-8761-82-369; Fax: +49-8761-82-713; sabine.kern@sud-chemie.com, www.sud-chemie.com	Optigel SH is synthetic expandable mica; composition (%): SiO_2: 57–61 MgO: 25–29 Li_2O: 0.5–0.9, Na_2O: 2.5–3.5, aspect ratio = 20–50; no commercial use for polymers.	Optigel SH is hectorite, SYnH-1; density: 2.5 g/cm^3.
		Hydrotalcite (LDH) is used as sorbent for acidic byproducts in production of PP or PVC, but not for nanoreinforcement.	This LDH is a synthetic aluminium-magnesium-hydroxycarbonate,
4	Kunimine Industries Co., Ltd. 1-10-5, Iwamoto-cho, Chiyoda-ku, Tokyo 101-0032; Fax +81 3 3866-2256; Mr. H. Matsudo Matsudo@kunimine.co.jp	Sumecton®-SA; CEC = 0.997 meq/g; $d_{001} \cong 1.3$ nm. The company also produces natural MMT: Kunipia F and 3MODA-MMT, 2M2ODA-MMT Kunipia T and Kunipia D, respectively	Na-Saponite;
5	Topy Co., Ltd; 5-9, Mica division; Dr Shun-ichi OHTA, Akemi-cho 1, Toyohashi-shi, Aichi, 441-8510, JAPAN Phone: +81-532-25-4415; Fax: +81-532-25-4416 s-oota@topy.co.jp. http://www.topy.co.jp/	Li-taeniolite is no longer produced. Synthetic tetrasilicic mica is produced by high-temperature melting method. An intercalated grade of this material was developed for PP. The aspect ratio is $p = 1000$–5000.	CEC = 2.6 meq/g; synthetic mica
6	FCC INC NO.79 Moganshan R.D., Zhejiang, China, 310005; Phone: 86-571-8805-1375/86-138-5726-7820; Fax: 86-571-8882-2631 http://www.nanoclay.net Contact: Mr Frank Lim, Business Manager.	SUPLITE-MP and -RD are sold by the tones as rheological additives for aqueous formulations, to increase viscosity and thixotropy.	SUPLITE-MP is synthetic hectorite;
		SUPLITE–RD has chemical activity, e.g. as a polymerization catalyst, or PVC stabilizer.	SUPLITE-RD is synthetic layered hydroxides (LDHs),
7	Sasol Germany GmbH; Paul-Baumann Strasse 1, D-45764 Marl, Germany. Phone: +49-2365-49-5371 marlotherm@de.sasol.com	Pural MG30, MG50, MG63HT, MG70; Mg-Al type LDH with different Mg:Al ration. Mainly used as PVC stabilizer against the dehydrochlorination.	Hydrotalcite; specific surface area 16 m^2/g, aggregates ca. 300 nm diameter.
8	Chamotte Holdings (Pty.) Ltd., 33 Louress Street, South Africa; Phone: +27 11 805-1916	Mg_2Al-CO_3 type of LDH from pilot plant; synthesis based on mineral MgO contaminated by Al, Ca, Fe & Ni	To be used for PVC as a stabilizer against dehydrochlorination
9	Akzo-Nobel	LDH	Designed for PNC
10	Corning, Inc., Dr G. H. Beall (now at Southwest Texas State University)	Fluoro hectorite, $Li_{1.12}[Mg_{4.88}Li_{1.12}]Si_8F_4$ or fluoro phlogopite $KMg_3(AlSi_3O_{10})F_2$	No longer produced
11	NL Industries; Baroid Division, idp@baroid.com	Barasym SMM-100, composition (%): SiO_2: 49.7 Al_2O_3: 38.2, TiO_2: 0.023, Fe_2O_3: 0.02, MgO: 0.014, Na_2O: 0.26, K_2O: <0.01, Li_2O; 0.25, F: 0.76, S: 0.10;	Muscovite-type mica-MMT, CEC = 0.7 meq/g; SYn-1; no longer produced

Note: The three synthetic clays: SYn-1 = synthetic mica-MMT Barasym SSM-100 (250 g/unit); SYnH-1 = synthetic HT Optigel SH (50 g/unit); and SYnL-1–synthetic HT Laponite RD (50 g/unit) are available from: The Source Clays Repository, Purdue University. Several other manufacturers of LDH for the use as PVC stabilizer against dehydrohalogenation are known, e.g. Toda Kogyo Corp., Kisuma Chemicals BV, Kyowa Chem. Ind.

DOI: 10.1002/pat

Table 3. Relative merits of natural versus synthetic clay

Clay	Advantages	Disadvantages
Natural	Well-known technology; Availability; Price: US$ 1600/ton in 2001	Variability of composition; difficult purification; poor reproducibility of PNC performance; crystallographic defects that prevent total exfoliation; variable color; used with toxic and thermally unstable intercalants
Synthetic[a]	Control of composition and shape; high aspect ratio: $p \leq 6000$; colorless and non-toxic; reproducibility of PNC performance	Developing technology; crystallization control might be difficult; limited sourcing; Price: US$ 2300/ton in 2001

[a] The term ''synthetic'' is not always exact, as some these clays are based on a mineral precursors, which may suffer from similar disadvantages as those listed for the natural clays. For example, talc (magnesium silicate hydroxide: $Mg_3Si_4O_{10}(OH)_2$) may be contaminated by serpentine, dolomite, magnesite, quartz, pyroxenes, olivine, biotite, amphiboles, etc. Similarly, when the natural brucite, $Mg(OH)_2$ is used for the production of LDH, it might be contaminated with grits and heavy metals.

Table 4. Properties of synthetic clays from COOP

#	Property	Somasif™	Lucentite
1	Counterion	Na^+	Li^+
2	Particle size (μm)	5 to 7	
3	Specific surface area (m^2/g)	9	
4	Brightness (%)	90 <	>95
5	Density (g/ml)	2.6	
6	Thermal resistance (°C)	800	700
7	Cation exchange capacity (meq/g)	1.2	1.01
8	pH in water	9 to 10	10 to 11
9	Grades (ammonium intercalant)[a] (see also Appendix)	ME-100 (none);MAE(2M2HTA), MTE(M3OA), MEE(MC2EG), MPE(M2EPG)	SWN(none), SPN(M2EPG), SAN(2M2HTA)
10	Aspect ratio, p[b]	≤6000	≈50
11	Type	Fluoromica (FM)	Hectorite (HT)

Note: Somasif™ composition (wt%): Si = 26.5, Mg = 15.6, Al = 0.2, Na = 4.1, Fe = 0.1, F = 8.8.
[a] Abbreviations of the quaternary ammonium intercalants are provided in the Appendix.
[b] Information provided by COOP on 18 January 2005.

Somasif and Lucentite synthetic clays from COOP

COOP, then UNICO, UNICOOPJAPAN, and now CBC Co. Ltd manufactures three types of synthetic clays: Somasif™, Micromica, and Lucentite—the two former are semi-synthetic, while the latter is fully synthetic.

Somasif™ and Micromica are prepared by introducing alkali metal into interlamellar talc galleries. This is accomplished by heating talc with an alkali fluoro silicate for several hours in an electric furnace. When Na_2SiF_6 is used, the product, Somasif™, is readily expandable, high aspect ratio phyllosilicate, with a structure similar to the mineral MMT. The hydrophilic Somasif™ ME may be intercalated with quaternary ammonium salts to make it hydrophobic. By contrast, when K_2SiF_6 is used, the product, Micromica, is a non-swellable, and has low aspect ratio, $p \cong 20$ to 40. The products are colorless. Evidently, for the application in PNC only Somasif™ can be used. Selected properties are listed in Tables 4 and 5.

Table 5. Somasif ME and MAE (sodium fluoro mica and FM-2M2HTA)

No.	Property	ME-300	ME-100	ME-100F	MAE
1.	Particle size (μm)	15–20	5–7	1–3	
2.	Aspect ratio, p	>5,000	5,000	<5,000	
3.	CEC (meq/g)	1.10	1.20	1.20	
4.	Interlayer spacing, d_{001}, (nm)		0.95		3.1

The method for producing semi-synthetic FM was patented by Tateyama *et al*.[22] Accordingly, a powdery mixture of 10 to 35 wt% alkali silicofluoride as the main component (Na_2SiF_6 optionally with LiF) and natural talc is heated for about 1 hr at $T = 700$ to 900°C. The product has the composition: $\alpha MF \cdot \beta(aMgF_2 \cdot bMgO) \cdot \gamma SiO_2$ where M is an alkali metal (Li, Na, K), and $0.1 \leq \alpha \leq 2$; $2 \leq \beta \leq 3$; $3 \leq \gamma \leq 4$; $a + b = 1$ are coefficients. For example, composition of swellable FM may be: talc/LiF/Na_2SiF_6 = 80 : 10 : 10; or talc/Na_2SiF_6/Al_2O_3 = 70:20:10, i.e. $NaMg_{2.5}Si_4O_{10}$ $(F_\alpha OH_{1-\alpha})_2$ with $0.8 \leq \alpha \leq 1.0$. Replacing Na by K makes the product non-swellable. Besides composition, the heating temperature greatly affects swellability and the interlayer spacing. Thus, FM produced at $T = 700$–750°C shows the XRD peak at $d_{001} = 0.91$ nm, while that produced at $T = 780$–900°C at $d_{001} = 1.61$ nm. Selected properties are listed in Table 4.

COOP has also produced hydrothermally a fully synthetic HT (Lucentite) from magnesium silicates and alkali salts. Again, the crystalline product is that of phyllosilicate, i.e. similar in structure to MMT, with the chemical composition of $Na_{0.33}(Mg_{2.67}Li_{0.33})Si_4O_{10}(OH)_2$. These low aspect ratio materials are characterized by high brightness (transparency in products), and low level of impurities. The hydrophilic Lucentite SWN might be intercalated with quaternary ammonium salts to make it hydrophobic. Selected properties

DOI: 10.1002/pat

Table 6. Lucentite SWN and SAN [sodium fluoro mica (Na-FM); $d_{001} = 0.95$ nm]

No.	Property	SWN	SAN
1.	Particle size (μm)	15–20	5–7
2.	Aspect ratio, p	~50	~50
3.	CEC (meq/g)	0.65	1.20
4.	Interlayer spacing, d_{001}, (nm)	1.27	1.79

are listed in Tables 4 and 6. The non-intercalated Na-FM (Somasif ME) is offered in three grades: ME-300, ME-100, and ME-100F (see Table 5). Larger talc particles are used as the staring material for ME-300 than those for ME-100F. Grinding ME-100 engenders ME-100F. These three grades of Somasif differ by the aspect ratio, and by CEC. The aspect ratio of well-dispersed ME-100 is $p \cong 5000$, while ME-300 is expected to have larger aspect ratio than that. However, since it is difficult to disperse large clay platelets, determining the exact value of p is not straightforward. All the grades listed in Tables 4–6 are commercially available. On request the company will produce clays intercalated with another intercalant.

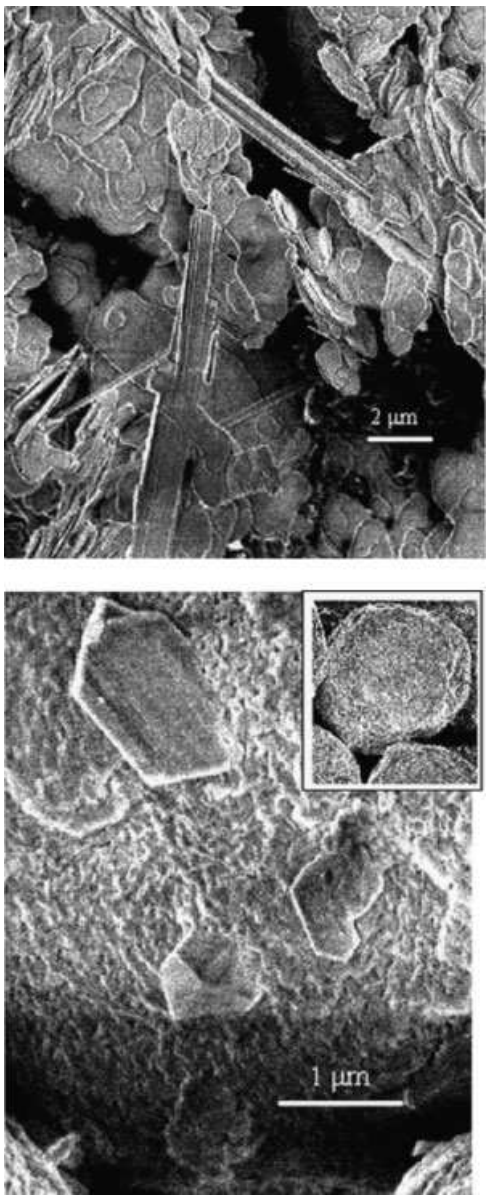

Figure 2. Low voltage (2 kV) SEM of Somasif ME-100 (top, 5 k magnification), and Lucentite SWN (bottom, 20 k magnification). The insert in the right top corner shows the spherical aggregates of Lucentite (diameter ≈ 11 μm) at magnification 4 k.

Low voltage SEM micrographs of Somasif ME-100 and Lucentite SWN are shown in Fig. 2. The micrograph of Somasif ME-100 indicates the presence of large platelet aggregates, but as high voltage SEM showed, the individual platelets are not very large. At the same time, the clay contains fiber-like particles, some over 30 μm long. Since the microanalysis reveals that the composition of clay aggregates and fiber-like particles is the same, the difference of morphology originates in the local diversity of crystallization conditions. The presence of these very long fibers may explain the statement: ''During dispersion, the fairly large isotropic mica particles of average diameter around 5000 nm are broken down into much smaller anisotropic nanoparticles resembling short fiber reinforcement of 500 nm length and 20 ± 50 nm diameter''.[37] Breaking FM plates of *ca*. 5000 nm diameter into 20–50 nm thick ''fibers'' seems rather improbable for the employed dispersing method. Furthermore, the same laboratory reported that after melt processing Somasif ME with PP + PP-g-MA [poly(propylene) (PP) gratted with maleic anhydride (MA)], the FM platelets were ≥750 nm long and *ca*. 200 nm wide (hence: $p \geq 437$).[38]

The SEM micrographs of Lucentite SWN have another surprise—the platelets are supposed to be *ca*. 50 nm in diameter. However, as seen in Fig. 2 the synthetic clay comes in the form of spherical aggregates, *ca*. 10 ± 2 μm in diameter, encrusted with crystals 1 to 3 μm long. However, these crystals might be of residual water-soluble salts.

Laponite LRD or RD from Laporte Industries, Ltd.

Laponite synthetic clays are HTs and FHs, prepared in a reaction between Mg, Li, and Na-silicate salts, which results in partially crystalline, monodispersed in size discs, 0.92 nm thick and *ca*. 25 nm long, with a density of 2.57 g/ml, and surface area of *ca*. 800 m^2/g. CEC of Laponite RD is listed as 0.95, while the value of CEC = 0.48 meq/g is published by Kaviratna *et al*.[39] The crystalline structure is that of tri-octahedral smectite, similar to HT.[15,40] Nine hydrophilic grades are manufactured at the old site in the UK: Laponite B, D, DF, JS, RD, RDS, S, XLG, and XLS. Grades B, DF, RD, and XLG swell in water, while the others dissolve in it (see Table 7). Laporte Industries does not sell organically modified grades.

The idealized chemical formula for Laponite RD is $[(Si_8(Mg_{5.34}Li_{0.66})O_{20}(OH)_4] \cdot Na_{0.66}$. The layered sodium lithium magnesium silicates may be modified with F^-. These clays are used in shear-sensitive, water based formulations, e.g. toothpastes, creams, glazes, etc. The grades listed in Table 7 hydrate and swell in water or in aqueous solutions of alcohols, producing clear and colorless colloidal dispersions. The standard products are also supplied with added $Na_4P_2O_7$. Pricing and delivery time depend on the local distributor. Their data and MSDS sheets are available from: www.laponite.com.

DOI: 10.1002/pat

Table 7. Properties of synthetic Laponite clays from Laporte/SCP

No.	Property	B (FH)	D	DF	RD (H)
2	Particle size (μm): <2% above	250	250	250	250
3	Specific surface area (m^2/g)	330	370	370	370
4	Moisture (%)	<10	—	3 to 10	<10
5	Bulk density (g/ml)	1	1	1	1
6	Solubility in water	Swells	Swells	Swells	Swells
7	CEC (meq/g)	?	?	?	0.95
8	pH in water (2% solution)	9.4	9.8	9.7	9.8
9	Composition (wt%): SiO_2	53–55	59.3	59–60	59–60
	MgO	25–26	27.4	27–29	27–29
	Li_2O	1.3–1.5	0.8	0.6–0.8	0.7–0.9
	Na_2O	3–4	2.9	2.2–2.9	2.2–2.9
	F	5–6	0.3	0.25–0.35	—
	Loss on ignition (%)	9–11	9.2–9.8	8–9	9.2–9.8
10	Aspect ratio: $p = d/t$	25	27	27	25–35
11	Applications	Thixotrope	Toothpastes	Toothpastes	Glazes

Optigel and Sorbacid from Süd Chemie AG

Optigel SH is sodium-magnesium silicate, used as thickener for alkaline aqueous products (pH 6 to 13). Its composition (in wt%) is: $SiO_2 = 57$ to 61; $MgO = 25$ to 29; $Li_2O = 0.5$ to 0.9; and $Na_2O = 2.5$ to 3.5. It is a white powder, 95% passing through 325-mesh screen; specific surface area $A_{sp} = 450 \pm 50\ m^2/g$; density $\rho = 2.5\ g/ml$; bulk density $= 850 \pm 50\ g/l$; and $p = 20$–50. Its application is for personal care goods (toothpaste, ointments, creams, etc.), as well as industrial, and household cleaners.

Optigel SH does not reinforce polymers, but it may reduce permeability. It is not used in any commercial plastic material. Süd Chemie has two other series of Optigel gellants for water-based systems: inorganic C-series, and organically modified W-series (for semi-gloss emulsions). However, both these series are based on ''specially activated natural MMT'' with low aspect ratio. Similarly like Laponite, Optigel forms clear, transparent gels ''with excellent brightness''. For the use in polymers, Süd Chemie offers a range of Nanofil organoclays, based on natural MMT with quaternary ammonium ions, e.g. di-methyl di-octadecyl ammonium chloride (2M2ODA), di-methyl-benzyl-octadecyl ammonium chloride (2MBODA), etc.

Süd Chemie also manufactures LDH Sorbacid® for controlling dehydrohalogenation of poly(vinylchloride) (PVC). In addition, the company sells Ciba product, Hycite® 713, an acid scavenger for polyolefins. Both these materials are pseudo-hydrotalcites: $[Mg_{1-x}Al_x(OH)_2](CO_3)_{x/2} \cdot nH_2O$ ($0.25 < x < 0.33$). In polyolefins Hycite 713 neutralizes residual acids liberated by catalysts, or other decomposition products. The LDH has high absorption capacity for acids, causes lower water carry-over and shows no bleed-out effect.

Sumecton® from Kunimine Industries Co., Ltd

Sumecton-SA from Kunimine Industries is a synthetic, cation-exchangeable Na-saponite, colorless and pure, dispersible in water: $[(Si_{7.2}\ Al_{0.8})(Mg_{5.97}Al_{0.03})O_{20}(OH)_4]^{-0.77} \cdot (Na_{0.49}Mg_{0.14})^{+0.77}$, with $p = 50$; $A_{sp} = 750\ m^2/g$; and the CEC $= 0.997$ meq/g (CEC $= 0.71$ meq/g was quoted in several publications). On the basis of these values, the average area per anionic site is calculated to be $1.25\ nm^2$, and thus the average distance between anionic sites on the clay surface (square array) is about 1.12 nm.[41] The interlayer spacing was estimated as $d_{001} = 1.3$ nm, increasing upon intercalation up to 2.6 nm. High voltage SEM images of Sumecton SA are shown in Fig. 3.

Kunimine Industries also produces natural clays: Na-MMT (Kunipia-F) with CEC $\cong 1.2$ meq/g. Intercalated organoclay grades are also available, namely Kunipia-T with tri-methyl octadecyl ammonium chloride (3MODA), Kunipia-D with 2M2ODA. The inorganic content and d_{001} are: 67.8 and 56.3 wt%, and 2.07 and 3.00 nm respectively. The aspect ratio ranges from 80 to 1120, with an average of $<p> = 320$.

Synthetic mica from Topy Industries, Ltd

Taeniolite is a naturally occurring phyllosilicate mineral (e.g. in Mt. Ste. Helene, QC), discovered in 1900 in Greenland, having idealized formula: $KLiMg_2Si_4O_{10}F_2$, and several impurities, such as: Ti, Al, Fe, Mn, Na, H_2O. Solid-state synthesis of taeniolite requires relatively low temperature of 700°C. It may also be obtained in a hydrothermal reaction. Synthetic Li-taeniolite (tetra-silicic Na-FM with the formula: $NaMg_{2.5}Si_4O_{10}F_2$, or $Na(Mg_2Li)Si_4O_{10}F_2$) was produced by Topy Industries. The clay has been used in several studies.[42–44] Reacting it with Ca or Mg salt increased the interlayer spacing from $d_{001} = 1.23$ to 1.47 nm.[45] However, Topy Industries no longer produces Li-taeniolite.

More recently, the company developed technology for the production of fully synthetic Na-tetrasilicic micas by reacting SiO_2, MgO, and Na_2SiF_6 in the molten state at $T > 1500$°C. Depending on the composition, either swelling, or non-swelling synthetic clay may be obtained (see Table 8). Production of Na-tetrasilicic mica results in the crystalline product contaminated by non-crystalline by-products and other impurities that can be eliminated by dissolution and centrifugation. The aspect ratio of purified material ranges from $p = 1000$ to 5000. Low voltage SEM micrograph of the material is presented in Fig. 3.

In addition, Topy Industries developed (purified) organoclays based on the synthetic tetrasilicic mica for greases and/or for polymeric nanocomposites (e.g. with PP) intercalated with 3MODA (4C-Ts), and with 2M2ODA (4CD-Ts), respectively. The Na-tetrasilicic mica is available in boxes 20 kg each, whereas the organo-mica in boxes 10 kg each, for US$450/10 kg box (FOB Japan).

DOI: 10.1002/pat

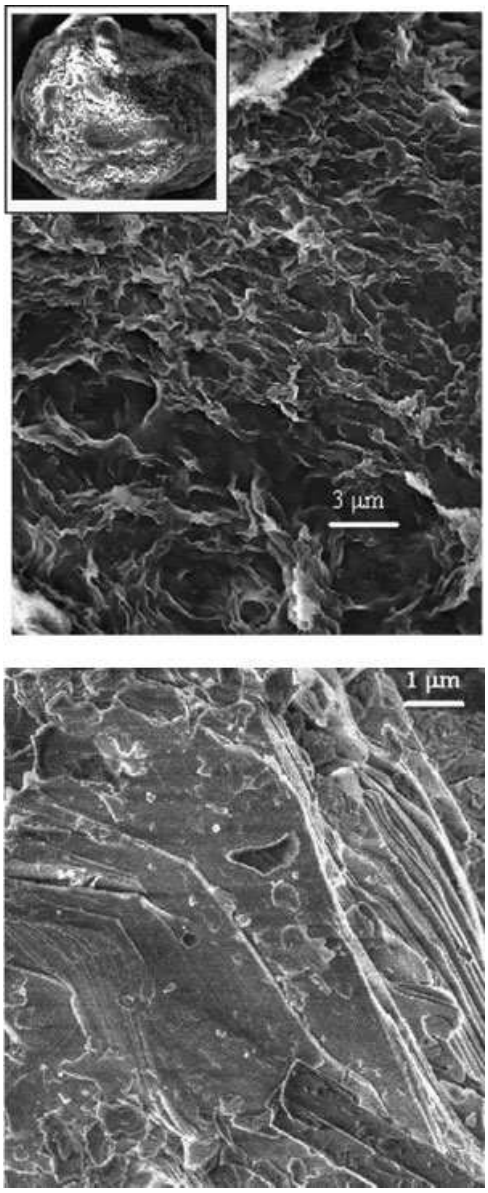

Figure 3. (Top) High voltage SEM micrograph of Sumecton SA at × 3 k magnification displaying aggregates of clay platelets. An insert shows a primary particle *ca.* 62 μm diameter. (Bottom) Low voltage SEM micrographs of Topy synthetic, non-purified Na-tetrasilicic mica at × 10 k. The synthetic clay forms large aggregates of high aspect ratio rectangular platelets.

Suplilte's: synthetic HT and LDH from FCC

FCC produces large quantities of two synthetic materials, to be used mainly as rheological additives, i.e. to increase viscosity of aqueous systems, and make them thixotropic (see Table 2).

Suplite-MP is a highly purified synthetic HT, free of silica and other contaminants. It is to be used in water based systems, such as paints, inks, polymeric solutions, etc. It is sold in 25 kg bags (minimum order = 1 ton). The material is similar to Laponite-RD, and Optigel-SH.

Suplite-RD is a synthetic LDH, formed by alternating charged brucite-like layers, separated by layers containing anions and water molecules. The material might be used as a catalyst for chemical reactions of interlayer molecules, a rheological additive in water based system, including inks, color pigments, personal care products, as nano-sized additives to polymers, flame retardants, stabilizers (replacing PbO), HCl scavengers, etc.

Lithium fluoro hectorite from Corning Glass, Inc.

This synthetic clay with the molecular composition: $Li_{1.12}[Mg_{4.88}Li_{1.12}]Si_8F_4$, CEC = 1.22 meq/g, $p = 2000$, has been described in several scientific papers.[22,46–49] Dry clay had $d_{001} = 0.97 \pm 0.01$ nm, with H_2O monolayer increasing to 1.24 ± 0.01, and with bilayer to 1.52 ± 0.01 nm. The patent described preparation of a variety of compositions, including lithium fluoro hectorite.[50] The process comprised: (1) ball-milling the ingredients; (2) heating them at 1450°C for 5 hr without stirring; (3) forming the melt into a ribbon, which crystallizes after 4 hr at 700°C; (4) immersing the product overnight in H_2O with stirring; (5) removing the solid contaminants; (6) drying the decanted suspension. Small quantities of the material were produced in the 1970s, but at present the material is not available.[51]

Barasym SMM-100 from NL Industries; Baroid Division

In the 1950s, Mellon Institute conducted explorative research on synthetic clays, sponsored by the National Lead Co.[52] A hydrothermal method produced HT: $[(Li_xMg_{6-x})Si_8O_{20}(OH)_4]^{x-} \cdot Na^+$ from SiO_2, MgO, Li_2O (or LiF) and Na_2O. The process was similar to that described earlier. However, SiO_2 was obtained as silica gel by hydrolysis of $SiCl_4$, and refluxing was carried out for up to 7 days at ambient pressure. The commercial production of Barasym® was conducted at 250–300°C with pH ≥ 8, under autogenous water vapor pressure for 12 to 72 hr.[53] The Barasym SSM-100 properties are published,[54–57] namely CEC = 1.4 meq/g, $A_{sp} = 133.66 \pm 0.72\ m^2/g$. The material is no longer produced.[58]

Synthetic silicic acids

This monoclinic mineral of the formula: $NaSi_7O_{13}(OH)_3 \cdot 4(H_2O)$ is found in brines with high pH and silica content. Along with kanemite ($NaHSi_2O_5 \cdot H_2O$), makatite ($Na_2Si_4O_9 \cdot$

Table 8. Synthetic micas from Topy Industries, Ltd

Clay type	Composition	Swelling	Grade	p
Fluoro phlogopite	$KMg_3AlSi_3O_{10}F_2$	No	PDM	25–400
K-tetrasilicic mica	$KMg_{2.5}Si_4O_{10}F_2$	No	PDM-K	
Na-hectorite	$Na_{0.33}Mg_{2.67}Li_{0.33}Si_3O_{10}F_2$	Yes	NHT	
Na-tetrasilicic fluoro mica	$NaMg_{2.5}Si_4O_{10}F_2$	Yes	DMA	≤5000
Organo-mica		Yes	4C-Ts; 4CD-Ts	≤5000

DOI: 10.1002/pat

H_2O), octosilicate ($Na_2Si_8O_{17} \cdot H_2O$), and kenyaite ($Na_2Si_{20}O_{41} \cdot H_2O$) it belongs to the phyllosilicate (layered) silicic acid group. It is white translucent to opaque, relatively soft, lamellar, with density $\rho = 2.25$ g/ml, and has a molecular weight, Mw = 550.66 g/mol. Described by Eugster,[59] it has been used mainly as a base for the preparation of mesoporous catalyst.[60]

The silicic acids have been synthesized by hydrothermal methods.[61–64] For example, sodium magadiite (Na-MAG) was produced by heating for 4 weeks at $T = 100°C$ aqueous suspension of SiO_2 with NaOH, or by combining silica gel with NaOH solution in an autoclave, and heating the mixture with stirring (at 150°C for 42 hr or at 180°C for 20 hr) under autogenous pressure. Next, the suspension was centrifuged, the solid product washed with water, and then air-dried at room temperature.[65] Another method involved combining Na_2SiO_3 and H_2SiF_6 solutions, than stirring at 70°C. After 48 hr of reaction, the precipitate was filtered, washed and dried.[66] The new process was reported to be more economic. Structural diversity of MAG has been documented by Scholzen *et al*.[67]

The layered silicic acids (MAG, kenyaite, octosilicate/ilerite and kanemite) have been also prepared hydrothermally with good control of platelets dimensions,[68] by means of templated preparations that led to organomodified materials,[69] using a one-pot method with structure directing agents,[70] or by using solid-state reactions.[71] Beneke *et al*. also reported syntheses of layered lithium sodium silicate (silinaite).[72] The results are promising as the material can be tailored for specific applications, e.g. by insertion of other cationic metals. In MAG and kenyaite an isomorphous substitution of Si with B and Al has been successfully performed, as well as them being grafted with organic or metallic ions.[73–75] Using trialkoxysilanes and inorganic salts in water solutions Schwieger *et al*. prepared in a one-step method layered Al^{3+}, Mg^{2+}, Ni^{2+} and Ca^{2+} organosilicates using extremely mild conditions (aging for 24 hr at 40°C).[76]

Post-functionalization of the silicic acids by grafting on the surface silanol groups offers interesting prospects for their use in PNCs.[77] A large variety of layered structures has been prepared and modified with the goal for polymer reinforcement.[78–80] In particular, the synthetic homologues of naturally occurring materials have been prepared and often functionalized by chemical grafting. For example, ilerite was silylated with alkoxy silanes with different pendant groups, either aliphatic and perfluorinated, also bearing amino and thiol terminated organic substituents.[81]

The recent Garces and Lakso's patent[82] defines the optimum conditions for the production of MAG in terms of: the molar ratios of NaOH to SiO_2 (ranges from 0.48 to 0.52) and that of H_2O to SiO_2 (ranges from 25 to 39), as well as the reaction temperature (ranges from 140 to 170°C); the reaction takes about 24 hr. The method produces >50% of lamellar (platy) synthetic MAG. The material might be converted to the acid form, and then either heated to produce quartz-like plates, or alkylated (e.g. with butanol) to produce an organophilic material.

Similar structures were prepared at $T \leq 70$°C by Chastek *et al*.[83] Starting with tetraethyl orthosilicate (TEOS), and hexadecyl trimethoxy silane (HDTMOS) lamellar mesostructured silicates (LMS) were produced. Alternatively, in the presence of aluminum chloride hexahydrate ($AlCl_3 \cdot 6H_2O$), a lamellar mesostructured aluminosilicates (LMASs) was obtained. Both types were characterized as layered structures with covalently attached hexadecyl functional groups. The interlayer spacings, $d_{001} = 4.8$–4.9 nm, could be further increased (to *ca*. 5.2 nm) by addition of tetra ethoxy silanes during the synthesis.

Synthetic organoclays by hydrothermal method with templates

Carrado[17] prepared synthetic HT of the formula $Ex_{0.66}[Li_{0.66}Mg_{5.34}Si_8O_{20}(OH, F)_4]$, starting with the precursor composition of 0.32 R, 1.0 LiF, 5.3$Mg(OH)_2$, 8 SiO_2, nH_2O, where R is a mono-valent organic salt and Ex is an exchangeable cation (Ex = Li, *R*). The process begins by dissolving 0.72 mmol of organic salt in water and adding 4.8 mmol LiF with stirring. Separately, 24 mmol $MgCl_2 \cdot 6H_2O$ is dissolved in water and mixed with 32 ml of 2 N NH_4OH to crystallize fresh $Mg(OH)_2$. After removing excess ions the crystals are added to the organic-LiF solution, and stirred for about 15 min before 0.036 mol silica sol is added. The 2 wt% solid suspension is stirred under reflux for 40–48 hr. Solids are isolated by centrifugation, washed, and air-dried. The product, Li- or R-HT, has CEC ≅ 0.8 meq/g, $d_{001} = 1.48$ nm, and platelet size of $L_a = 19.5$ nm (natural HT has $L_a = 42$ to 52 nm).

Another method involves sol-gel hydrothermal transformation of TEOS or organo-tri-alkoxy silane, namely phenyl-tri-ethoxy silane (PTES).[17] Aqueous slurries of LiF, $Mg(OH)_2$, and the silane are refluxed for 2–5 days. The organic content in the resulting PTES-HT was *ca*. 20–25 wt%. The phenyl groups are directly bonded to HT via Si–C. The ^{29}Si-NMR indicates the presence of $RSi(OMg)(OSi)_2$ and $RSi(OMg)(OSi)(OH)$. XRD gave $d_{001} = 1.30$ and 1.39 nm for, PTES- and TEOS-based clays respectively. The organoclays were stable at $T \leq 400$°C. The method may be used to produce synthetic clays with bonded to the surface compatibilizing intercalant molecules.

A layered alumino-phosphate with a structure mimicking the naturally occurring kanemite (also known as ALPO kanemite) was synthesized using the hydrothermal method and *n*-alkylamines as templates. The layered structure was obtained as organophilic structure with *d*-spacing linearly growing with the length of intercalant aliphatic chain.[84]

The potential for the use of these materials in PNCs is excellent, and hopefully, the interest in them will intensify.

Other synthetic nano-fillers

The sol-gel transition method has been used to generate a wide variety of synthetic nano-fillers, including metal, metal oxides (e.g. Cr_3O_8, V_2O_5, SiO_2), layered chlorides (e.g. FeOCl), chalcogenides (e.g. MoS_2), functional or structural nano-fillers, and others.[1,85] There is rich literature on the use of nano-sized SiO_2, carbon black (CB), graphite, carbon fibers, carbon nanotubes (CNTs), and polyhedral oligomeric silsesquioxanes (POSSs). Polymer intercalated layered zirconium phosphates (ZrPs) have been produced.[86,87] More recently, rod-like synthetic, unmodified boehmite (γ-Al_2O_3) was dispersed in caprolactam. The polymerized specimens doubled the modulus at *ca*. 5 wt% loading.[88]

DOI: 10.1002/pat

Table 9. Mechanical properties of PA-6 and based on Its PNC

			Ube		Unitika	
Property	ASTM	Units	PA-6	PNC	PA-6	PNC
Tensile strength, σ	D-638	MPa	78	89	79	91
Tensile elongation, ε_b	D-638	%	100	75	100	4
Flexural strength, σ_f	D-790	MPa	108	136	106	155
Flexural modulus, E_f	D-790	GPa	2.80	3.52	2.84	4.41
Impact strength, NIRT	D-256	J/m	64	49	48	44
HTD (18.56 kg/cm^2)	D-648	°C	75	140	70	172
HTD (4.6 kg/cm^2)	D-648	°C	180	197	175	193
H_2O permeability, P_{H2O}	JIS Z208	g/m^2 24 hr	203	106	—	—
Density, ρ	D-792	kg/m^3	1140	1150	1140	1150

Data from Ube Industries, Ltd., 2002, and Unitika Plastics, 2004.

PNC BEHAVIOR WITH SYNTHETIC CLAYS

PNC with Somasif™

General—intercalation

Somasif™ ME100 is more often quoted in the scientific and patent literature than any other synthetic clay. Frequently, in the publication the clay is not fully identified, but simply called ''fluoromica from COOP'' or ''Somasif'' without identifying the grade. FM has been used by Unitika to reinforce PA-6 based PNCs since 1976. By contrast, Toyota Central R&D Laboratories developed a similar composition (licensed to Ube) starting with MMT pre-intercalated with ω-amino dodecanoic acid. Properties of these two commercial PNCs are listed in Table 9. One of the FM advantages is the reproducible neutral color, thus the products may be brightly colored with pigments or dyes.

In Somasif™ ME100, the negative charges of the layers are balanced by Na^+ ions (Na-FM). The CEC as cited by the manufacturer is 1.2 meq/g, while its value reported by Zanetti *et al.*[89] ranges from 0.7 to 0.8 meq/g. Earlier, these authors intercalated FM with octadecylamine (ODA) and ω-amino-dodecanoic acid (ADA), following the published procedure.[90] The interlayer spacing increased from the Na-FM value of $d_{001} = 0.95$ to 2.4, and 1.7 nm respectively. Reichert *et al.*[91] intercalated FM with protonated alkyl amines, namely butyl (C_4), hexyl (C_6), octyl (C_8 or OA), dodecyl (C_{12} or DDA), hexadecyl (C_{16} or HDA), and octadecyl (C_{18} or ODA). The intercalation with these primary ammonium ions expanded the interlayer spacing from 0.95 to 1.98 nm (see Fig. 4).

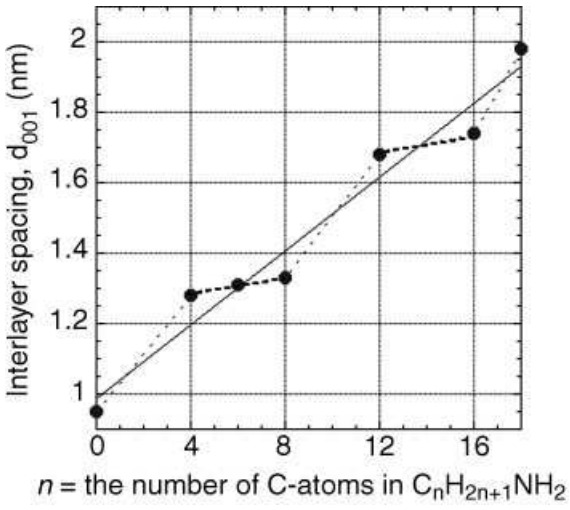

Figure 4. Somasif ME-100 intercalated with primary amine salts, $C_nH_{2n+1}NH_2 \cdot HCl$. The interlayer spacing step-wise increases with number of carbon atoms in the amine, n. The dependence may be approximated as: $d_{001} = 0.988 + 0.052n$; $r = 0.980$.[91]

Polyamide matrix

Yasue *et al.*[92] patented PNCs based on polyamide (PA) (PA-6, -66, -46, -12) with 0.1 to 20 pph FM. To prepare reinforced PA, free from the customary reduction of toughness in standard composites, and without the expensive and time consuming pre-intercalation, the non-intercalated FM was dispersed in a monomer or monomers that subsequently were polymerized. If required, the initial polymerization could be followed by the solid-state reaction. The new material might contain the customary additives and reinforcements. The patent also describes the preparation and properties of FM. Thus, the material may be obtained by heating a mixture of talc with sodium and/or lithium silicofluoride(s) or fluoride(s) under N_2 at $T = 700$ to 1200°C for 5 to 6 hr. In the process Na^+ and/or Li^+ ions are intercalated into the silicate layers of talc (see Fig. 1) to induce formation of the counter-ion layer with the expanding characteristics. The desired interlayer spacing of FM should be $0.9 \leq d_{001}$ (nm) ≤ 2.0.

The compositions of six FM used in the studies are listed in Table 10. The mechanical strength, toughness, heat resistance, and dimensional stability of PNCs containing 5 wt% of these FMs are also given. Incorporation of FMs improved the tensile strength heat deflection temperature (HDT), dimensional stability and reduced the water absorption of PA-6 and PA-66. Within the experimental error, the relative viscosity (i.e., PA MW) and impact strength remained unchanged, while the elongation at break seriously decreased. The cited values of strength and HDT are smaller than what could be expected for 5 wt% clay loading. Thus, most likely exfoliation of FM was only partial. Of the six tested FM compositions M5 shows the best performance.

Kim *et al.*[93] dispersed Somasif ME-100 in ADA, which was then polymerized. TEM revealed that FM formed *ca.* 150 nm

DOI: 10.1002/pat

Table 10. Composition of FM and performance of PA-6 and PA-66 comprising 0 or 5 wt% of FM

	PA-6							PA-66						
	None	M1	M2	M3	M4	M5	M6	None	M1	M2	M3	M4	M5	M6
Talc (wt%)	—	80	80	80	80	80	80	—	80	80	80	80	80	80
Na_2SiF_6	—	20	—	6	10	16	6	—	20	—	6	10	16	6
Li_2SiF_6	—	—	20	—	10	2	6	—	—	20	—	10	2	6
K_2SiF_6	—	—	—	—	—	2	—	—	—	—	—	—	2	—
NaF	—	—	—	6	—	—	—	—	—	—	6	—	—	—
Al_2O_3	—	—	—	8	—	—	8	—	—	—	8	—	—	8
Performance of dry composition														
η_r	2.6	2.6	2.6	2.7	2.5	2.5	2.4	2.4	2.3	2.4	2.3	2.2	2.2	2.3
σ (MPa)	73	79	78	78	78	79	76	78	84	83	83	84	84	83.3
ε_b (%)	180	31	30	28	46	52	68	110	27	31	29	31	27	21
NIRT	3.3	3.5	3.1	3.4	2.9	3.8	2.7	4.6	4.2	4.4	4.3	4.5	4.2	4.4
HDT (°C)	55	121	120	122	116	121	118	74	153	150	150	155	153	154
Performance of wet composition														
H_2O (wt%)	5.8	3.1	3.0	3.1	3.0	3.1	3.1	3.8	2.1	2.0	2.0	2.0	2.1	2.0
Δl (%)	1.2	0.7	0.7	0.7	0.6	0.7	0.6	0.8	0.5	0.5	0.5	0.4	0.5	0.5
σ (MPa)	33	59	58	58	59	59	60	53	68	69	69	68	68	66.7
ε_b (%)	>200	56	53	55	95	150	140	180	46	42	40	47	46	42
NIRT	4.5	4.5	4.7	4.5	4.8	4.2	4.4	5.6	5.2	5.0	5.2	5.1	5.1	5.0

Note: η_r = relative viscosity of PA at 25°C, $c = 1$ g/dl in phenol/tetra-chloro ethane; σ = tensile strength, ε_b = strain at break, NIRT = notched Izod impact strength at room temperature, HDT = heat deflection temperature under load of 18.6 kg/cm^2; H_2O = water absorption; $\Delta/$ = dimension change.

thick stacks in the PA-12 matrix. During injection molding of PNC the stacks aligned parallel to the injection molding direction, while the PA-12 lamellae oriented perpendicular to them. The studies of *in situ* deformation under the high voltage TEM showed that the clay stacks tilt perpendicular to the direction of applied load, what might indicate strong bonding between macromolecules and FM. The localized damage at the polymer/clay interface induced cavitation and fibrillation. The main micro-mechanical mechanism was identified as microvoid formation inside the stacked silicate layers. The high specific surface area of the clay and covalent bonding of the PA-12 chains to the clay surface noticeably altered the local chain dynamics. Macromolecular chain tethering to two clay platelets (bridging) was also postulated.

Melt compounding of PA-12 (weight average molecular weight $M_w = 126$ kg/mol) with 4 wt% of Somasif ME-100 and Somasif MAE in a single-screw extruder (SSE) demonstrated the need for pre-intercalation.[94] Whilst compounding with ME-100 increased its $d_{001} = 0.96$ to 0.99 nm, that of MAE increased from 3.40 nm to greater than 8.8 nm, indicating extensive exfoliation. However, incorporation of ME-100 increased the matrix crystallinity by *ca*. 6%, while that of MAE decreased it by 36%. Similarly, the melt viscosity was differently affected—ME-100 increased the melt viscosity whereas MAE decreased it. Evidently, the presence of the intercalant di-methyl di-(hydrogenated tallow) ammonium chloride (2M2HTA) significantly affected the PNC performance. Plasticization of the matrix by 2M2HTA reduced stiffness, dimensional stability and barrier properties, but improved the elongation at break.

Showa Denko patented rigid, flame-resistant PNCs containing: (1) PA, (2) clay complexed with triazine, (3) fibrous reinforcements and (4) flame retardant.[95] The clay complex was obtained by inserting a triazine ($C_3H_3N_3$) or its derivative (melamine, cyanuric acid, and melamine cyanurate) into the interlamellar galleries of, e.g. Somasif ME-100. The four basic components of the formulation could be dry blended before melt-compounding. Conventional additives may also be added. Thus, dispersing FM in H_2O at 60°C, adding melamine and HCl and stirring for 1 hr caused precipitation of the complex particles with *ca*. 5 μm diameter. XRD confirmed expansion of the interlayer spacing from $d_{001} = 0.96$ to 1.28 nm. The procedure was repeated with MMT (Kunipia-F; CEC = 1.19 meq/g). The organoclay with 15 wt% of melamine showed $d_{001} = 1.30$ nm. Larger values of d_{001} were obtained by either replacing melamine with a melamine cyanurate and/or by using excess intercalant. For the sake of comparison FM was also intercalated with 2M2ODA. At 40 wt% of the organic content the interlayer spacing was $d_{001} = 3.5$ nm.

Patent test results are summarized in Table 11. The first four compositions are based on the invented intercalant (melamine or its derivative), the last three are for reference. It is interesting that melt compounding of PA-66 with slightly intercalated clays (nos. 1 to 4) gives better results than clay with 2M2ODA, the ''classical'' quaternary ammonium intercalant (no. 5). The first four compositions also outperformed the references for flame resistance (V-0 according to the UL-94 standard), mold deposition, bleed-out, and appearance are concerned. Owing to good appearance and ease of processing the new compositions may be used, e.g. for the electric and electronic parts, in automotive applications, in house appliances, mechanical parts, etc.

Lew *et al.*[96] melt compounded PA-12 with pre-intercalated FM (CEC = 2 meq/g; $d_{001} = 3.4$ nm) in a SSE at $T = 185$ to 225°C and screw speed $N_s = 12.5$ to 50 rpm. All compositions contained well intercalated ($d_{001} \cong 2.1$ nm) short stacks. The authors considered reduction of melt viscosity in PNCs as a sign of delamination, which appeared to cause a plasticizing effect. However, as neither the type of intercalant, nor its

DOI: 10.1002/pat

Table 11. Properties of PA-66 containing 1 phr of modified clay and 15 phr of glass fibers (GF)[95]

No.	Organoclay or other filler	d_{001} (nm)	Flex modulus (MPa)	HDT (°C)	Deformation (mm)	Relative shrinkage (TD/MD)
1	FM + m	1.28	6.3	245	0.5	1.94
2	MMT + m	1.30	6.1	244	0.7	1.86
3	FM + mc	1.50	6.2	244	0.7	1.96
4	FM + 2xm	1.35	5.9	240	1.0	2.12
5	FM + 2M2ODA	3.5	5.8	230	1.2	1.88
6	Talc	0.96	6.0	243	1.0	2.13
7	Nil	—	5.6	244	6.2	2.30

Note: FM = Somasif ME-100; MMT = Kunipia-F; m = melamine; mc = melamine cyanurate; 2M2ODA = di-methyl -di-octadecyl ammonium chloride; 2x = twice stoichiometric; phr = ''per hundred weight parts of resin''.

concentration is given this interpretation cannot be taken seriously. The results also indicated that (at least during SSE compounding) smaller polymer particles in the polymer/organoclay mixture enhance the degree of clay dispersion.

Effect of incorporation of FM and its pre-intercalated version, Somasif MEE, on modulus, creep compliance, physical aging of PA-6, and moisture absorption has also been studied.[97] Addition of FM increased the modulus and reduced the creep compliance—the properties depended on clay concentration. The FM presence had little effect on the physical aging. Incorporation of 5 wt% exfoliated FM reduced the creep compliances by more than 80%. Furthermore, when T increased from 23 to 80°C, for PA-6 the creep increased by a factor of 12, while for PNC by a factor of three. Thus, the use of PNC instead of unfilled matrix is advantageous for the time dependent deformation behavior. Incorporation of FM into PA-6 also reduced the rate of moisture absorption (by a factor of three at 10% loading), but not the final amount of absorbed H_2O (the equilibrium absorption may take several years). The fracture behavior of PNC depends on the type and concentration of clay, the moisture content, and the aging time. Addition of clay usually reduces the ductility. However, in a series of PA-6 compositions with Nanomer I30TC, Cloisite® 30B, and Somasif MEE, the latter was found the most ductile.

PNC brittleness is a common problem—as the modulus increases the impact strength decreases.[1] It seems that the material can absorb only a specific amount of energy; hence large enlongation at break (ε_b) for low modulus and strength, or low ε_b for the inverse system. This problem has been elegantly and radically solved in polymer blends by inducing co-continuity of phases.[98] Blending seems to be a good way to solve the low ductility problem in PNCs as well. Nylon M1030D from Unitika Co. (containing 4 wt% of ME-100—see Table 9) was melt-blended with acrylonitrile-butadiene-styrene (ABS) copolymer and a compatibilizer: poly(octene-co-ethylene) grafted with maleic anhydride (POE-g-MA).[99] The impact strength increased with the addition of compatibilizer at various ABS copolymer compositions, while the modulus, tensile strength and HDT decreased. The results seem to indicate migration of the compatibilizer to the clay surface, forming soft domains between it and the PA-6 phase.

The effect of clay content on crystallinity of PA-6 was studied.[100] The resin was melt compounded with ME-100 pre-intercalated with methyl-coco-di-polyethylene glycol ammonium (MC2EG). The organoclay content was 0, 4, 8, and 12 wt%. All PNC's were fully exfoliated with local interlayer spacing decreasing with concentration from 61 to 28 nm. Films with clay platelets oriented parallel to the film surface were prepared by hot pressing. According to XRD, at low clay content the crystal lamellae were perpendicular to the clay surface, while at high loading parallel to it. The results suggest macromolecular stretching at low clay loadings.

To evaluate the relative merits of various clays, PA-6 was melt compounded with 1.14 wt% of clay (inorganic part). The compounding line comprised SSE with the extensional flow mixer (EFM).[101] Figure 5 displays TEM micrographs of PNCs compounded using the same protocol, amount of clay, and magnification. It is noteworthy that Somasif MAE, Cloisite® 15A, and Lucentite SAN, were pre-intercalated with 2M2HTA. In agreement with TEM, the XRD of these compounds indicated short stacks of the former, and full exfoliation for the other two systems. The best mechanical properties were obtained for Somasif, the worst for Lucentite—what might be expected considering the clay aspect ratios, namely < 5000, 280, and about 50 respectively.

Polyolefin matrix

Kawasumi *et al.*[103] compounded PP, PP-g-MA (Yumex 1001), and either MMT or FM pre-intercalated with ODA that increased the interlayer spacing to $d_{001} = 2.2$ nm. The blend of PP with PP-g-MA was reported miscible. The compositions were dry blended, compounded in a twin-screw extruder (TSE) at $T = 210$°C and then injection-molded. XRD scans indicated the presence of only few short stacks (confirmed by TEM). Dispersion of FM was slightly better than that of MMT, and correspondingly the storage modulus of FM was higher. Thus, the best overall performance was obtained for PNC containing: PP, PP-g-MA, and FM-ODA.

Heinemann *et al.*[104] prepared polyolefin (PO)-based PNCs by the melt compounding or reactive methods. Three clays were used: unmodified FM, unmodified HT (Optigel), and pre-intercalated MMT. Melt compounding with high-density poly(ethylene) (HDPE) decreased the intensity of the XRD peak, and reduced the organoclay spacing from $d_{001} = 1.96$ to 1.41 nm. When HDPE was polymerized in the presence of the clays the XRD also indicated reduction of the peak intensity and the interlayer spacing. The E value of PNCs prepared by the polymerization and compounding methods depended on the M_w value and the branching index (N, defined as number of branching C per 1000 C-atoms). The original results were fitted to the relation:[1]

DOI: 10.1002/pat

Figure 5. PA-6 melt compounded with 1.14 wt% of organoclay: (from top to bottom) Cloisite® 15A, Somasif MAE, and Lucentite SAN. The TEM magnification is the same, 200 k (see the 100 nm scale bar).[102]

$$logE = a_o + a_1 logM_w - a_2 N \quad (1)$$

At constant value $M_w = 100$ kg/mol, E decreased with N. The neat resin had the lowest modulus, the synthetic PNC

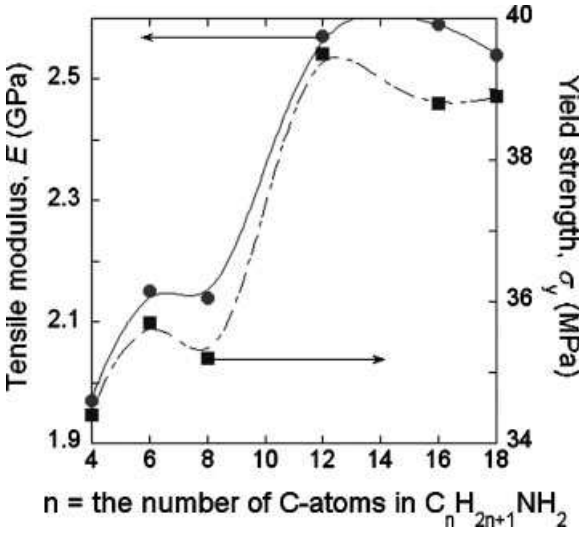

Figure 6. PP/FH PNC prepared by melt compounding of PP + PP-g-MA + FM intercalated with C_nH_{2n+1}-NH_3^+. Data for 5 wt% FH and Hostaprime HC5 compatibilizer.[91]

the highest, and the compounded PNC an intermediate. Efficiency of the compounding method decreased with N (as well as with M_w). This is reasonable, since TSE is unable to provide long mixing time required for the diffusion controlled exfoliation. Polymerization efficiency in the presence of unmodified FM was order of magnitude higher than that for MMT-type organoclays.

The work was continued by Reichert *et al.*[91] who melt-compounded at $T = 190$ to 230°C PP with 0, 5, or 10 wt% of FM pre-intercalated with primary ammonium ions (see Fig. 4), and with 20 wt% of PP-g-MA. As shown in Fig. 6, only dodecyl ammonium chloride (DDA), hexadecyl ammonium chloride (HDA), and ODA amines produced dispersible organoclays; the systems with other organoclays behaved as microcomposites. The performance was sensitive to the type of compatibilizer—good results were obtained for Hostaprime HC5 and poor for Epolene E43. The interlayer spacing increased with MA content. PP with 20 wt% PP-g-MA, and 10 wt% of FM (pre-intercalated with either HDA or ODA) gave the best performance. TEM and atomic force microscopy (AFM) indicated that full exfoliation has not been achieved.

Reichert *et al.*[105] observed that compounding PP + PP-g-MA with FH-C_4 produced micro-composites, while with FH-C_{18} yielded exfoliated PNCs. However, the morphology was also controlled by the compatibilizer and processing T, namely annealing the sample at 200°C converted exfoliated PNC into a micro-composite.[105] The thermal and flammability behaviors of these systems were studied as well.[106] In comparison to the matrix behavior, the micro-composites did not show improvement of thermal stability. By contrast, PNCs containing FH-C_{18} had higher thermal oxidation temperature and lower thermal degradation rate, with high char yield that enhanced the ablative effects. A detailed study using isothermal thermogravimetric analysis (TGA) measurements highlighted also the chemical catalytic effects due to the silicate and strongly acidic sites formed by

DOI: 10.1002/pat

thermal decomposition of the protonated amine silicate modifier. Furthermore, incorporation of 10 wt% FH-C_{16} into PP/PP-g-MA increased the tensile modulus from 1490 to 3460 MPa and of yield stress from 33 to 44 MPa. These results support Reichert *et al.*[91] observations that organoclays with shorter than C_8 paraffinic chain leads to poorly performing micro-composites.

Oya *et al.*[107] examined the role of the clay type and that of a secondary intercalant on the degree of dispersion and mechanical properties of PNCs with PP. Thus, FM, MMT and mica (MC) were intercalated with di-methyl-hexadecyl-octadecyl ammonium chloride (2MHDODA). The organoclay was dispersed in toluene solution of di-acetone acrylamide (DAAM = the second intercalant) with a free radical *N,N'*-azo-bis-isobutyronitrile (AIBN) initiator. After polymerization of DAAM a solution of PP-g-MA was added, the product was precipitated, washed, dried, and finally melt compounded with PP. In parallel, PNC was similarly prepared without DAAM—only intercalation was obtained. The best dispersion was obtained for doubly intercalated FM, but the best mechanical properties at 3 wt% of clay loading were those of PNC with MC. The difference most likely originated in large aspect ratio and relative high modulus of MC platelets. In conclusion, MC may be a better nano-filler than FM, but performance of PNC with MMT, although the poorest, was still acceptable.

Morgan and Harris[108] investigated the effect of intercalant excess (in organoclay) on the degree of clay dispersion in PP matrix, the mechanical properties, and flammability. The organoclay (FM-2M2HTA) was repetitively washed with water, filtered, dried, ground into fine powder, and then the particles with diameter $d < 120\ \mu m$ were subjected to Soxhlet extraction with ethanol for up to 4 days. Dried and ground organoclay was melt compounded with PP and PP-g-MA in an internal mixer, at 190°C. The XRD indicated sharp changes after 1 day of extraction and smaller thereafter. The original spectrum displayed multiple peaks with spacing ranging from *ca.* 1.2 to 5.6 nm, with the principal peak at about $d_{001} = 3.6$ nm. After extraction the main peak moved to lower spacing (2.8 nm), became sharper and reduced in intensity, while the peak at 3.6 nm decreased in intensity to a shoulder. Harmonics of these two were also apparent. Thus, removal of adsorbed intercalant reduced the interlayer spacing and made it more regular. The effect of intercalant extraction on flex modulus and the notched Izod impact strength at room temperature (NIRT) are shown in Fig. 7. The increased stiffness is accompanied by enhanced brittleness—NIRT is reduced by 35 to 45%. In short, extraction affects the interlayer spacing, which in turn modifies the PNC performance. There was a significant reduction of the peak heat release rate (PHRR) = 1435 kW/m^2 for (PP + PP-g-MA) to 498 kW/m^2 for PNC with no extracted organoclay, and to PHRR = 519 to 491 kW/m^2 for the systems containing organoclay extracted for 1 to 4 days.

Owing to high crystallinity and relatively large difference of density between the molten and solid state, the PP films are known for high permeability to gases and vapors. Gorrasi *et al.*[109] studied the effect of FM on the transport properties of CH_2Cl_2 and *n*-C_5H_{12} vapors through syndiotactic poly (propylene) (sPP) film containing up to 20 wt%

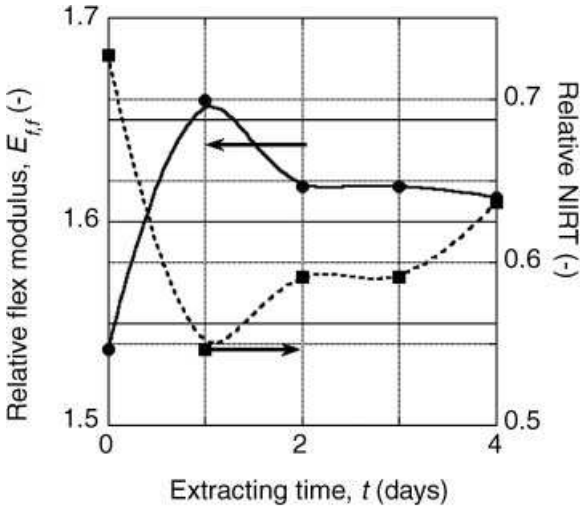

Figure 7. Relative flexural modulus and NIRT for PNC containing extracted organoclay. The relative magnitude refers to the corresponding performance of the matrix, namely PP + PP-MA.[108]

FM-ODA. The system was compatibilized by addition of (isotactic) iPP-g- MA. Permeability of CH_2Cl_2 decreased with organoclay loading up to 10 wt% to a plateau—reduction by a factor of 40 was obtained. By contrast, permeability of *n*-C_5H_{12} vapors tended to decrease all the way to 20 wt% organoclay, but the effect was significantly smaller—reduction by a factor of 10 at 20 wt% loading. The effect was assigned to reduction of the diffusion rates. Significantly, at the latter loading the tensile modulus increased from about 300 to 800 MPa.

In the PNC monograph[1] there are several tables listing the tensile modulus versus clay loading that were used to generate Figure 133. The aim was not to prove or disprove any of the reviewed theories, but rather to see how the best PNCs perform in amorphous polymer matrix (polystyrene, PS), in semi-crystalline end-tethered exfoliated matrix (PA-6), and in semi-crystalline not tethered matrix with a compatibilizer (PP). In these systems MMT was used with an average aspect ratio $p = 200$ to 300. The results indicated that independently of the matrix the relative modulus (E_R) doubles at the clay content of about 5 wt%. The PNC with FM instead of MMT had lower E_R, most likely caused by lower aspect ratio, p. For dilute systems E_R increased with clay concentration:[1]

$$E_R \equiv E/E_m = 1 + [\eta]\phi = 1 + aw; \quad w \leq 8\ wt\%$$
$$[\eta] = 2.5 + 0.025(p^{1.47} - 1) \tag{2}$$

Here the reinforcing factor [η] is the hydrodynamic volume, which for monodispersed hard spheres ($p = 1$) equals 2.5. The parameter $a = [\eta]/(100\rho_f/\rho_m) \simeq [\eta]/314$. The lowest predicted value for hard spheres is $a = 0.008$. For poorly exfoliated PP, PA-6 and polylactic acid (PLA) the values of E_R increase with $a = 0.07$ that corresponds to $p = 93$. For fully exfoliated, best performing systems $a \approx 0.20$ equivalent to $p = 200$. The latter value is close to the expected for the commercial organoclays with MMT. The values for PP

DOI: 10.1002/pat

reinforced with FM can also be approximated by eqn (2) with $a = 0.13$ equivalent to $p = 150$.

Rubber nanocomposites (RN)

Elastomer-based PNC are in an initial stage of development.[110,111] Usually, pre-intercalated clay is incorporated into rubber via solution, latex, or melt compounding methods. While the solution method is expensive, the latex process is attractive as most rubbers are produced as lattices, and the inorganic Na-clay can be dispersed in water. Natural and synthetic clays might be used. Comparing performance of rubber filled with non-dispersed clay with that of latex mixed with Na-MMT or Na-FH showed better performance for the system with synthetic clay—surprisingly, the tensile modulus was nearly twice as high as that for Na-MMT. Melt mixing of epoxidized rubber showed that non-intercalated Na-FH outperformed Na-MMT, but that it was inferior to pre-intercalated MMT-ODA.

Thermoplastic polyester (PEST) matrix

Kaneka Corp. has been developing PNCs with thermoplastic polyester (PEST) as the matrix for a decade.[112–117] The aim has been to provide PNC with 0.1 to 50 wt% of clay, well dispersed in PEST or bisphenol-A polycarbonate (PC). As an example, Na-MMT (from Yamagata) or Na-FM was dispersed in water, then (2-aminoethyl)amino-propyl trimethoxy silane was added, and the mixture agitated for 2 hr. In dry precipitate with MMT and FM, the interlayer spacing was respectively: $d_{001} = 2.6$ and 1.8 nm. Next, slurry of the treated clays was dispersed in a monomer, water was distilled off at $T \cong 120$°C, and polycondensation under vacuum conducted at 280°C. Thus prepared PNC with poly(ethylene terephthalate) (PET), poly(butylene terephthalate) (PBT), or PC as a matrix were exfoliated ($d_{001} > 10$ nm). The performance was evaluated in terms of HDT and flexural tests. The three functions, flexural modulus, E_f, flexural strength, σ_f, and heat deflection temperature (HDT) showed similar increases with increasing clay (inorganic part) content. At clay concentration exceeding 5 wt% the improvements begun to be less pronounced. Comparing the performances of PNCs with MMT and FM in the PET matrix, the following numbers were reported: $d_{001} > 10$ and 8 nm; TEM average platelet diameter $<d> = 71$ and 389 nm; HDT = 169 and 156°C; flexural strength 160 and 150 MPa; flexural modulus = 6.64 and 6.02 GPa, respectively. It seems that during the process the large aspect ratio FM was not fully exfoliated, what reduced its effectiveness. By contrast, properties of PNCs with PC as the matrix were with MMT and FM were respectively: $d_{001} = 4.8$ and > 10 nm; HDT = 156 and 164°C; flexural strength = 148 and 156 MPa; flexural modulus = 3.05 and 3.98 GPa; now FM clearly outperformed MMT.

Imai *et al.*[118] developed a new intercalating compound, which may bind to PEST macromolecules and act as a molecular repair agent. The logic for selecting this route was the observation that the key to high mechanical performance of a composite is the stress transfer from matrix to the reinforcing particles. In the case of nanocomposites, the clay must be exfoliated and strongly bonded to the matrix. The new intercalant should react with PEST, bond to clay, and be stable at the polymerization temperatures ($T \approx 275$°C). The selected compound was:

i.e. a dimethyl isophthalate (DIP) substituted with the

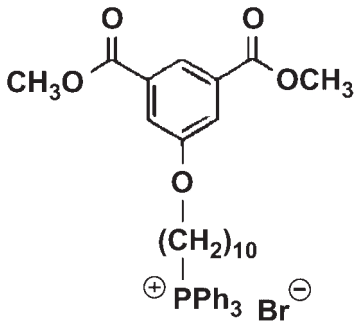

tri-phenyl-phosphonium group. In the study, FM was intercalated with the modified DIP, increasing $d_{001} = 0.96$ nm of FM to 3.20 nm. The PNCs were prepared by polymerizing bis-hydroxy-ethyl terephthalate in the presence of the FM-DIP, with Sb_2O_3 as a catalyst at 275°C under vacuum for 3 hr. XRD of the product showed a residual peak at $d_{001} = 1.53$ nm. Thus, intercalation with DIP was not uniform. NMR confirmed bonding between the organoclay and the matrix. The flexural modulus increased with clay loading from 3.5 (PET) to 6.3 GPa at organoclay loading of 8 wt%. This improvement confirms good dispersion of FM in PET and the strong interactions between the two components.

Biodegradable polyesters: polylactic acid (PLA), polycaprolactone (PCL)

In 2002 several articles from Okamoto's laboratory were published on the polylactic acid (PLA)/layered silicate systems.[119,120] Thus, PLA was melt compounded in a TSE at 190°C with MMT, ''smectite'' and FM—all pre-intercalated with quaternary phosphonium bromides (e.g. tri-butyl-hexadecyl phosphonium bromide 3BHDP). Upon intercalation the interlayer spacing ($d_{001} = 1.2$–1.25 nm) less than doubled, and then increased after compounding to ≤ 2.69 nm (for FM). Considering O_2 permeability and modulus, the performance increased in the order: MMT, FM, ''smectite''. Ray *et al.*[120] studied the clay effect on PLA crystallinity. Melt compounding of PLA with 4 wt% Somasif MEE was carried out in a TSE at 210°C, which increased d_{001} from 2.1 to 3.1 nm, and reduced the PLA M_w from 177 to 150 kg/mol. The total crystallinity increased by *ca.* 4%, melting point temperature (T_m) was unchanged, crystallization temperature (T_c) increased by 28°C, and glass transition temperature (T_g) decreased by 4°C. The mechanical properties of PLA significantly improved—flex modulus, storage modulus and flex strength at 25°C increased by: 26, 25 and 9%, respectively, while the rate of PLA biodegradability by *ca.* 60%.

Chang *et al.*[121] solution-blended PLA with MMT or FM, both pre-intercalated with HDA. The tensile strength at 4 wt% loading was $\sigma = 28$ and 44 MPa, and the tensile modulus (at 8 wt% loading) was $E = 274$ and 633 MPa, respectively for MMT and FM.

DOI: 10.1002/pat

Finally, caprolactone (CL) was bulk-polymerized at 170°C in the presence of traces of water and 0, 10, 30 and 50 wt% of FM. Low molecular weight polycaprolactone (PCL) was obtained: $M_w = 5.36$–22.4 kg/mol. The clay increased lactone hydrolysis and polymer chain growth rates. XRD indicated that monomer and polymer diffused into inter-lamellar galleries, but their height remained small, namely 0.87 and 0.78 for CL and PCL, respectively. The results suggest that PCL chains are flatly arranged onto each side of silicate platelet creating pseudo bi-layers inside the gallery.[122]

Styrenics and acrylics matrix

Hoffmann *et al.*[123] intercalated FM with either 2-phenylethylamine (PEA, $M_n = 121$ g/mol) or with an amine-terminated PS (ATPS; $M_n = 5.8$ kg/mol; $M_w/M_n = 1.33$):

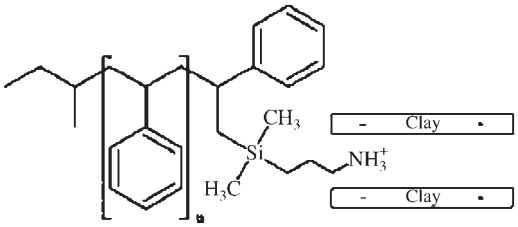

PNCs were prepared by compounding 5 wt% of these organoclays with PS in a micro-compounder at 200°C. The interlayer spacing of PNC with FM-PEA did not increase, but the one prepared with FM-ATPS became exfoliated. In the PNC the clay platelets of *ca*. 1 nm thick were about 600 nm long and 100 nm wide, what gives $p = 276$ to be compared with $p \leq 5000$ reported for ME-100. The presence of FM-PEA slightly increased the storage modulus of the matrix while that of the exfoliated FM-ATPS created an elastic network that had strong effect on the rheological behavior. Thus, one may control the degree of intercalation/exfoliation by varying the chain length of the intercalant. This experimental finding confirms the theoretical conclusions by Balazs and her colleagues,[124,125] and by Kim *et al*.[126] regarding the use of long-chain end-functionalized compatibilizers. Its MW should be just above the entanglement molecular weight: $M_e < M_w$.

Another set of PS-based PNC was prepared by Morgan and Harris via solvent blending with sonication.[127] Na-MMT and Na-FM were pre-intercalated with 1,2-di-methyl-3-*n*-hexadecyl imidazolium bromide (2MHDI), dispersed in chlorobenzene solution of PS at concentrations of *ca*. 1.0 and 2.5 wt% (inorganic content). After sonication their interlayer spacing hardly changed, namely $d_{001} = 3.23$ and 3.37 nm for MMT, and 3.28 and 3.17 for FM. Thus, MMT and FM showed comparable peak positions, but the diffraction peak height for the PS/FM system seemed to be smaller than that for PS/MMT. Accordingly, TEM micrographs showed micron-sized aggregates in all systems. The work was continued by Zhao *et al*.[128] The dynamic mechanical frequency scans were presented for all the samples. Judging by constancy of the value of $T_g = 104.0 \pm 0.4$°C (for PS = 103.2) the interaction between organo clay and the matrix was weak. In immiscible systems the apparent yield stress might be used as a measure of the intensity of interactions between the dispersed domains. The effect is created by the formation of a 3D structure that breaks down at higher stresses or frequencies.

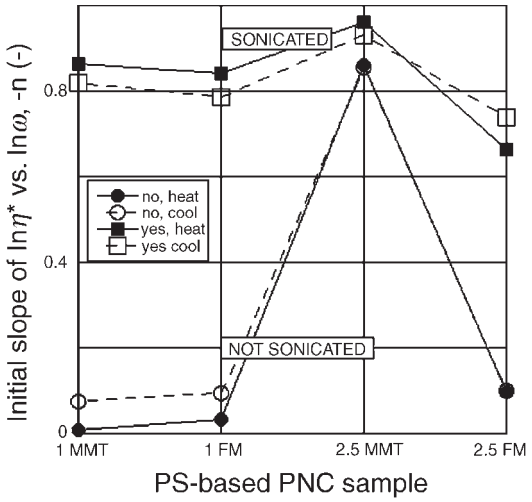

Figure 8. Negative values of the slope, $n = \partial \ln \eta^* / \partial \ln \omega$, for four PS-based PNC containing 1 or 2.5 wt% of mineral clay of the MMT or FM type. In the legend "no" and "yes" corresponds to no or yes to sonication, while heat and cool indicate that the master curve was obtained upon heating or cooling.[128]

Thus, one might use the initial slope of the complex viscosity as an indicator of interactions between the dispersed domains. In Fig. 8 the negative values of the slope (as reported by the authors) are plotted versus composition for the sonicated or not compositions. The isothermal frequency scans were measured at 10°C intervals between $T = 160$ and 260°C, either increasing or decreasing the temperature. Excepting the sample containing 2.5 wt% MMT, all other non-sonicated specimens behave almost like micro-filled composites. The sonicated ones showed significant yield behavior, nearly independent of the clay type or content. This is surprising as at low clay concentration even fully exfoliated particles should be able to rotate freely (thus no yield stress), while at higher concentration, when rotation is no longer possible, rheology will show significantly higher yield stress. One possible explanation of these results might be that during sonication the intercalant was partially removed from the clay platelets. As a consequence, the PS was adsorbed and solidified on the clay platelets, greatly increasing the effective filler loading. Similar explanation was recently offered for the behavior of PNC's based on PA-6 or PP.[101] Independently of the explanation, PNC with 2MHDI-modified clays, combined with high-energy sonication, resulted in better dispersion than that in the PNCs with di-methyl-benzyl-hexadecyl ammonium chloride (2MBHTA)-modified MMT. Judging by the values of n, there is no serious difference in behavior for PNC with MMT or FM, although the former clay showed higher yield stress than the latter. Since the original aspect ratio of FM is higher than that of MMT, the information may suggest that FM is more fragile that MMT, and easier breaks down during sonication.

Comparative work was carried out by Chu *et al*.[129] The authors prepared PNC based on SAN with MMT or FM pre-intercalated with either 2M2HTA, methyl tallow di-hydroxy ethyl ammonium chloride (MT2EtOHA), tri-

DOI: 10.1002/pat

phenyl *n*-hexadecyl phosphonium (3PHDP), or 2MHDI. PNCs were prepared by melt compounding SAN with *ca*. 5 wt% organoclay at 210°C. All compositions were intercalated with d_{001} ranging from 2.85 to 3.51 nm. As far as the degree of dispersion is concerned, MT2EtOHA was the best, with 3PHDP following closely. The latter one also engendered better thermal stability and reduced flammability; FM reduced flammability better than MMT. This conclusion was found applicable to PS-based PNCs as well.[130]

Panek *et al*.[131] studied dynamics and microstructure of intercalants [tri-methyl hexadecyl ammonium bromide (3MHDA), and tri-butyl-hexadecyl phosphonium bromide (3BHDP) with head- or tail-attached electron paramagnetic resonance (EPR) probes] in FM-organoclays dispersed in PS. The authors compression molded ($T = 433$ K for 30 min at 70 MPa) fine mixtures of PS/organoclay = 3:1. In the presence of PS the interlayer spacing of ME-100 with 3MHDA increased from $d_{001} = 2.21$ to 3.38 nm, whereas with 3BHDP the interlayer distance virtually did not change. The ^{31}P MAS NMR and electron spin echo envelope modulation (ESEEM) have also been used. The data for ME-100 indicated the presence of Fe^{3+} ionic impurities that most likely came from talc. Bimodal dynamics was observed over broad ranges of surfactant loadings and temperatures, in the presence or absence of PS. This could be related to a bimodal distribution of intercalant head-group distance from clay surface. The data also indicated close proximity of PS to intercalants' tail ends.

Epoxy (EP) matrix

Zilg *et al*.[132] attempted to find relationships between the mechanical properties and the EP-based PNC composition, clay type, and concentration. The EP was synthesized from diglycidyl ether of bisphenol-A (DGEBA) cured with hexa-hydro-phthalic anhydride ($T_g > 100$°C). Three clays were used: (1) FM (Somasif ME-100), (2) Na-MMT (Süd Chemie), and (3) HT (synthetic hectorite; Optigel SH). The clays were pre-intercalated with: DDA, di-methyl di-dodecyl ammonium chloride (2M2DDA), tri-methyl dodecyl ammonium bromide (3MDDA), methyl dodecyl di-polyethylene glycol ammonium chloride (MDD2EG), ADA, 2M2ODA, 2MBODA, and bis(aminopropyl)-terminated oligo(propylene glycol). Upon intercalation the interlayer spacing of FM increased from $d_{001} = 0.94$ to 1.74 nm (with MDD2EG), and then upon matrix polymerization to $d_{001} = 6.79$ nm. At loadings $\geq$5 wt% FM was more difficult to disperse than MMT, while small HT plates exfoliated quite readily. The observation correlates with the aspect ratios, namely $p \cong 5000$, 300 and 25, respectively.

Enhanced toughness was associated with the formation of dispersed anisotropic laminated nanoparticles consisting of intercalated silicates. The authors reported that d_{001} increased with the onium salt alkyl chain length, and that the primary amines increased d_{001} more than the quaternary ones. During curing, the former probably reacted with the EP that the latter were unable to do. For HT intercalated with 2MBODA TEM showed randomly dispersed individual platelets, suggesting exfoliation. Some mechanical properties of the EP-based PNC are presented in Fig. 9. The initial tensile modulus and elongation at break (not shown) were drastically reduced by addition of clay. Surprisingly, intercalation did not improve the performance—the tensile strength and fracture energy of compositions with neat clays is higher than that that with organoclays. The best fracture toughness was observed for FM.

EP-based PNC were prepared using FM pre-intercalated with ODA, 1-methyl-2-norstearyl-3-stearinoacid-amidoethyl-di-hydro-imidazolinium methyl-sulfate (W75), hydroxy-ethyl-di-hydro-imidazolinium chloride (HEODI), or ricinyl di-hydro-imidazolinium chloride (RDI).[133] The matrix was tetra-glycidyl 4,4′-di-amino-di-phenyl methane (TGDDM) cured with 4,4′-di-amino diphenyl sulfone (2DS). Once the organoclays were dispersed in the matrix, the gallery increased for FM-ODA, FM-HEODI and FM-RDI, but decreased for the immiscible FM-W75. The FM-ODA is known to produce organoclays that can be exfoliated during EP curing (at $T \leq 200$°C; $T_g > 240$°C), while FM-imidazolium organoclays are known for their thermal stability. While FM had no influence on curing, FM-W75, FM-HEODI or FM-RDI reduced the exothermal peak by 6°C and FM-ODA, by 11°C. Thus, all intercalants catalyzed the curing, but the di-hydro imidazolines were not as effective as ODA. This suggests that FM-ODA could lead to the best exfoliation, if not for the thermal decomposition of ammonium ions (see Table 12). None of the produced PNC was fully exfoliated. SEM micrographs showed clay aggregates (some as large as 20–30 μm), especially for FM-W75 and FM-ODA.

In Fig. 10 (left) the relation between the tensile modulus and clay content is displayed. The least squares fit to eqn (2) is shown by lines. In Fig. 10 (right) the parameter *a* of eqn (2) is plotted versus d_{001} (see Table 12). The result for FM-W75 is the worst, falling out of correlation for other compositions. The performance of PNC with FM-RDI is the best, with the two other organoclays not far behind. It is also significant that neat FM shows a good performance. At 4 vol% clay loading the modulus increased by 35%. The fracture energy for all the intercalated systems was found to be higher than that for the micro-composite with FM, but again the data for FM-W75 were the lowest and these of FM-RDI the highest. At 5 vol% clay the fracture energy was nearly twice as large as that for the neat matrix resin.

Fröhlich *et al*.[134] prepared high-performance EP-based PNC using either FM or FM-ODA, and six-arm star poly(propylene glycol-*b*-ethylene glycol) (PPEG). The hydroxyl end groups of the latter compound were modified, yielding on average two pendant stearate chains, two phenol groups, and two hydroxyl end groups, which controlled polymer polarity. The phenol end groups ensured covalent bonding between liquid polymer and EP resin. TEM showed that the PNCs comprised intercalated clay stacks and PPEG spheres dispersed in EP, engendering a complex behavior. For example, the coefficient of thermal expansion for PNC was higher than that for the neat matrix. The T_g value ranged from 204 to 242°C. The relative modulus, E_R, reached its maximum value of 1.12 for 5 wt% of PPEG and the same amount of FM-ODA. The relatively high fracture toughness of the neat resin, $K_{1c} = 1.34$, was not necessarily preserved in PNC: $K_{1c} = 1.13$ to 1.52 MPa/m. SEM of the fractured surfaces revealed extensive matrix shear yielding for the neat resin, whereas the predominant fracture mode of the

DOI: 10.1002/pat

Table 12. Organic content and interlamellar spacing[133]

Materials	CEC (meq/g)	Interlamellar spacing, d_{001} (nm)	
		In organoclay	In epoxy[a]
FM	—	0.94	—
FM-ODA	0.99	1.9	4.0
FM-W75	0.67	3.2	2.5
FM-HEODI	0.90	2.2	4.1[b]
FM-RDI	1.10	2.5	7.5[c]

[a] At 5 wt% clay, cured as indicated in the text.
[b] In ordered places.
[c] Irregular distribution.

hybrid nanocomposites was crack bifurcation and branching. In short, addition of FM was somehow overshadowed by that of PPEG, thus the effect of FM intercalation by ODA did not play the expected role. However, the ME-100 presence in the EP contributed to the overall good presence.

Polyurethane matrix

Kosiński *et al.*[135] prepared polyurethane (PU)-based PNC for fibers or films by dispersing clay in a PU solution in dimethyl acetamide (DMAC) then agitating the suspension until sufficient exfoliation took place, forming fibers or films by spinning or casting, respectively. The solution could contain dyes and/or other additives. The clay was either MMT or FM (CEC = 0.5 to 2 meq/g), intercalated with onium ions to generate interlayer spacing of $d_{001} \geq 1.4$ nm. The patent

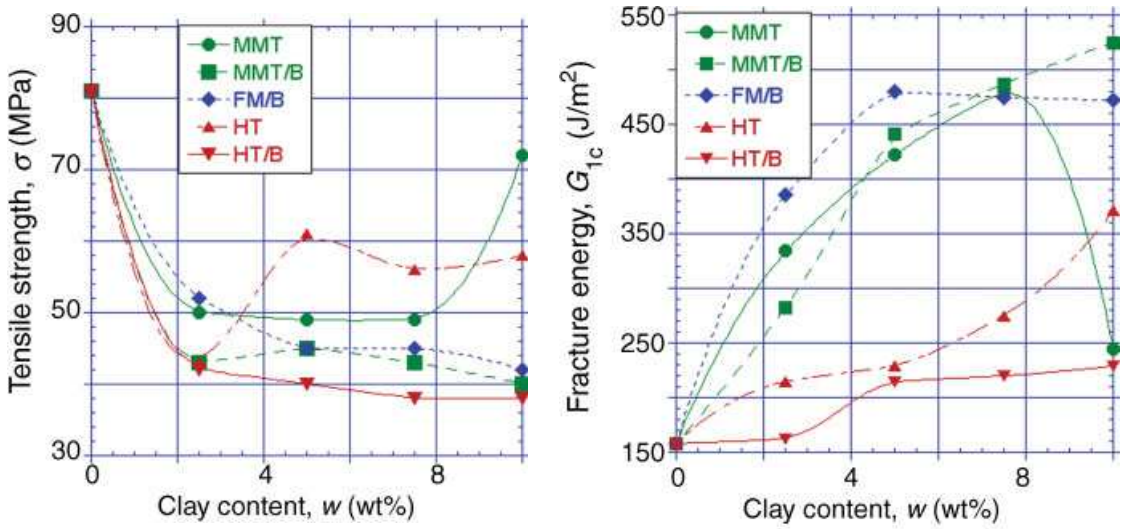

Figure 9. Tensile strength and fracture energy of the EP-based PNC: MMT, not intercalated purified bentonite; MMT/B, MMT intercalated with 2MBODA; FM/B, fluoro mica intercalated with 2MBODA; HT, not intercalated synthetic hectorite; HT/B, synthetic hectorite intercalated with 2MBODA.[132]

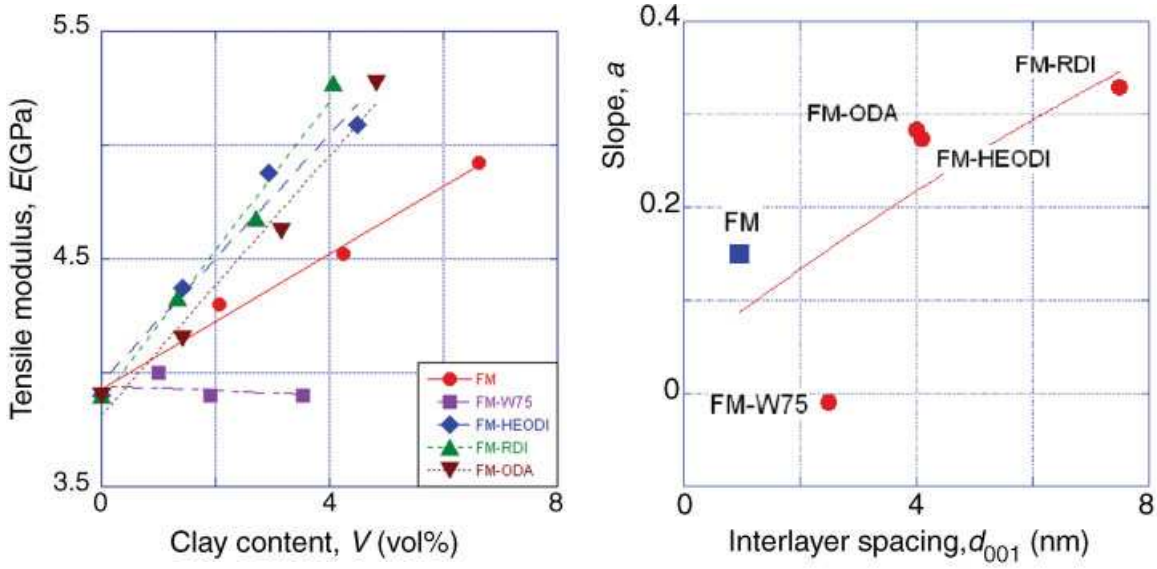

Figure 10. Left figure displays the tensile modulus versus FM content for EP-based PNCs. The right figure shows the relation between slopes of the *E* versus *V* dependence (shown in the left figure), and the d_{001} values from Table 12.[133]

DOI: 10.1002/pat

focused on the segmented PU (for Spandex), with 0.1 to 12 wt% clay having $d_{001} \geq 3.5$ nm. For example, MMT was intercalated with aqueous solution of dehydro-abietyl ammonium and Nile Blue dye. The organoclay-dye pigment had $d_{001} = 2.2$ nm and it contained about 5.2 wt% of Nile Blue bonded to the clay. In comparison to PU formulations without clay, the PNCs showed greater dyeability and dye-fastness, namely 25 times deeper blue, and 2–3 times stronger yellow absorptions. Since addition of MMT-type organoclay may cause yellowing, a small amount of pre-dyed clay may be needed to offset this effect. Evidently, this problem does not exist for FM.

PNC were prepared by pre-intercalating ME-100 with MDD2EG, dispersing 2.5, 5, 7.5, and 10 wt% of the organoclay in tri-hydroxy-terminated-PPG (poly- or oligo-propylene glycol), adding curing agent (*N,N*-dimethyl-benzylamine), and then curing the system with di-isocyanato-di-phenyl-methane.[37] At 80°C the presence of organoclay slightly reduced the reaction rate. At 10 wt% of clay loading the interlayer spacing of FM ($d_{001} = 0.9$ nm) increased to 8.8 nm. TEM showed well dispersed stacks, and FM particles resembling ribbons, 500 nm long, and 20 to 50 nm wide. Since the nominal aspect ratio, $p \leq 5000$, severe clay attrition was postulated. However, it is possible that the used FM was similarly contaminated with long fibers as that shown in Fig. 2 (top).

As shown in Fig. 11, the tensile strength and elongation at break increased with organoclay content, at least up to 7.5 wt% FM. There is clearly an advantage of having FM pre-intercalated, even though only intercalation was achieved. PNC with 5 wt% FM (as neat FM or pre-intercalated FM) had the relative tensile modulus, tensile strength and elongation at break equal, respectively: 0.97 and 0.75; 1.37 and 2.12; 1.49 and 3.23; hence MDD2EG acted as a toughening agent.

Rossetti[136] studied flammability of PNCs with PP, PU, and EP as the matrix. Different organoclays were used—based either on ME-100 or MMT (Cloisite® series). The flammability reduction was observed for all systems containing 10

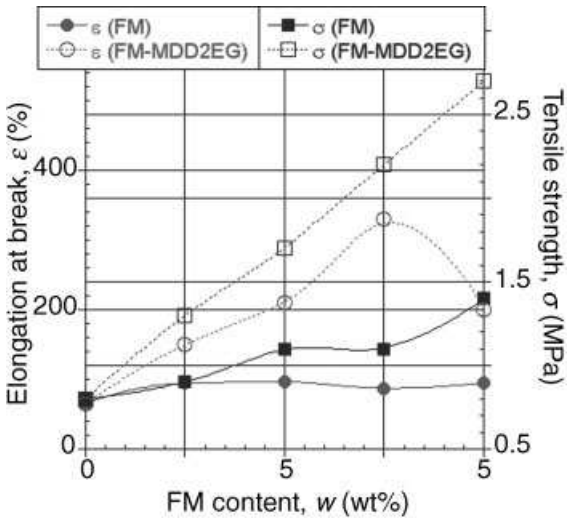

Figure 11. The elongation at break and tensile strength versus clay content for PU with neat FM and FM pre-intercalated with MDD2EG.[37]

wt% organoclay. The effect for PP and PU could be expected from the earlier report.[137] However, for EP Rossetti observed a significant reduction of the mass-loss rate (MLR). The latter systems were prepared by dispersing FM (pre-intercalated with $C_nH_{2n+1}NH_3^+Cl^-$, where $n = 4$, 8, 12 or 18) in DGEBA crosslinked with an anhydride. FM with C_4 did not change flammability of EP, but the three other organoclays reduced the MLR by about 40%, and the maximum T from 133 to 108°C.

Poly(ethylene–co–vinyl acetate) (EVAc) matrix

Zanetti *et al.*[89,90,138] melt compounded (in a mini-compounder or internal mixer) EVAc-12 or EVAc-19 with ME-100 pre-intercalated with ODA or ADA. The degree of clay dispersion depended on the matrix and intercalant, namely in EVAc-19 exfoliation was obtained for FM-ODA, whereas d_{001} was unchanged for FM-ADA. The materials also behaved differently in thermogravimetric tests and cone calorimetry. Under thermo-oxidative conditions FM-ODA accelerated de-acetylation of the EVAc-19, while FM-ADA did not significantly affect the decomposition of the matrix polymer. Similarly the cone calorimetry of the well dispersed nanocomposites with FM-ODA indicated reduction of peak heat release rate (PHRR), whereas there was hardly a difference between EVAc-19 with and without FM-ADA.

In addition to the two FM organoclays the authors also used MMT pre-intercalated with methyl hydrogenated tallow di-hydroxy ethyl ammonium chloride (MHT2EtOH) or 2M2HTA. Melt compounding EVAc-19 with these organoclays resulted in exfoliation for MMT-MHT2EtOH, while intercalation ($d_{001} = 3.8$ nm) for MMT-2M2HTA. The TGA weight loss in air of these systems was similarly improved.[139] The rheological measurements were more sensitive to the aspect ratio and platelets distribution. Overall, better results were obtained with MMT-MHT2EtOH than with the FM-ODA.

Bellucci *et al.*[140] compared the mechanical behavior of EVAc-19 with natural and semi-synthetic clays. The polymer was compounded with FM-MHT2EtOH and MMT-2M2HTA. The effect of purification of organoclays on the performance was examined. Since the FM-organoclay was fully exfoliated, purification did not affect the interlayer spacing. By contrast, in the intercalated MMT-2M2HTA system removal of impurities reduced d_{001}. The rheological measurements were more discriminatory showing the highest apparent yield stress for purified FM-organoclay. PNC with purified organoclays was stiffer and more brittle—the highest tensile modulus was obtained for PNC containing purified FM-MHT2EtOH organoclay, and the lowest (but still 25% higher than the matrix) for the one with non-purified MMT-organoclay. The elongation and tensile strength at break were similar for all nanocomposites, but the tensile yield stress was the highest for PNC with FM-MHT2EtOH (Somasif MEE).

PNC with Lucentite

By contrast with large number of PNC preparations with Somasif, those with other synthetic clays are far less common. Thus, for Lucentite only one patent was found. The reason for the use of this synthetic clay was not to

DOI: 10.1002/pat

Table 13. Natural and synthetic clays used in the study[147]

Name	Type	Exchangeable cation	Modifier loading (%)	CEC (meq/g)	Platelet size (nm)	Al/Mg/Fe content (%)
Gel White GP	MMT	Ca^{2+}, Na^{+}	0	0.90–0.92	>100	14.7/3.2/0.8
TSPP-GP	MMT	Ca^{2+}, Na^{+}	2	0.90–0.92	>100	14.7/3.2/0.8
Cloisite®-Na	MMT	Na^{+}	0	0.926	75–100	19.2/2.1/4.3
TSPP-CL	MMT	Na^{+}	4	0.926	75–100	19.2/2.1/4.3
Laponite RD	HT	Na^{+}	0	0.60	25–35	0/27.5/0
Laponite RDS	HT	Na^{+}	8.24	0.60	25–35	0/26/0
Laponite B	FM	Na^{+}	0	0.60	25–35	0/27/0
Laponite S	FM	Na^{+}	6.18	0.60	25–35	0/25/0
Laponite JS	FM	Na^{+}	10.12	0.60	25–35	0/22.2/0
Somasif ME-100	FM	Na^{+}	0	1.20	<5000	0/25.6/0
TSPP-ME-100	FM	Na^{+}	1	1.20	<5000	0/25.6/0

Note: HT = synthetic hectorite; FM = fluoro mica; TSPP = 4-sodium pyrophosphate. The values of CEC, average platelet size, and content of Al_2O_3, MgO, and Fe_2O_3 in clay, are from the clay provider.

reinforce, but rather to change the rheological behavior of the polyol solution during preparation of rigid PU foams.[141] Higher viscosity of the thixotropic system stabilized a dispersion of flame retardants [Sb_2O_3, $Al(OH)_3$, CB, or melamine], while on shearing dramatically reduced viscosity facilitated foaming. The resulting hard PU foam had good dimensional stability and fire-resistance.

More recently, Si *et al.*[142] compared performances of polymethyl methacrylate (PMMA)-based PNCs with MMT (18 wt% Cloisite® 6A) or HT (16-wt% Lucentite SPN). The melt compounded specimens were intercalated. TEM micrographs showed the presence of large clay aggregates in the form of ribbons. PNC containing MMT were yellowish and partially opaque, whereas that with HT was as optically clear and colorless as the matrix polymer. In comparison to MMT, HT was less efficient for increasing rigidity and T_g, but significantly more so for flammability reduction.

PNC with Laponite

The synthetic Laponite® has low aspect ratio ($p \approx 25$–35), is chemically pure and free from contaminants. It is an efficient rheology controlling agent for waterborne systems, which gives colorless, transparent, and highly thixotropic gels. Several studies on the effect of Laponite in PNC have been published.

McCarthy *et al*. used synthetic HT (Laponite), $Na_4P_2O_7$ and a hydrophilic, air curable EP resin. The system has been designed as a flexible, antistatic film for polymeric substrates [e.g. poly(ethylene) (PE)], and for multilayer food pouches.[143]Kaviratna *et al*[39]. studied the dielectric properties of MMT, Laponite FH, and ME-100 FM with Na^{+}, Li^{+}, and Cu^{2+} as counterions. The dielectric behavior was mainly controlled by the counterion charge-to-radius ratio. Intercalation of PEG into Laponite enhanced Li^{+} ion conductivity in rechargeable lithium batteries.[144] Inan *et al*.[145] studied effects of Laponite on char formation and flame-retardation of its PNC with PA-6.

Shemper *et al*.[146] investigated the effects of Laponite RD on photo-polymerization kinetics and coating properties of MHMA in the presence of hydroxylated dimethyl acrylate crosslinkers. The clay auto-accelerated the reaction, thus high rates and conversions were achieved. XRD did not show any peak for the interlayer spacing—either in neat clay or in PNC containing 10 wt% Laponite. Similarly the TEM micrographs indicated a lack of organization of the clay layers. Incorporation of the clay improved coating hardness.

PMMA was prepared by emulsion polymerization with cationic initiator in the presence of 3MHDA, followed by mixing with aqueous clay slurry and hetero-coagulation the mixture via cooling it to –20°C.[147] The clays included MMT, Laponite, and ME-100 (see Table 13). XRD and TEM indicated that the PNC morphology depended on the clay concentration and colloidal stability. The nanocomposites from Gel White GP and Laponite were well dispersed at ≤ 5 wt% clay loading. Although modification of clay with $Na_4P_2O_7$ improved the colloidal stability, it did not enhance exfoliation. Exfoliated nanocomposites showed good morphological stability during solution or melt processing. According to the differential TGA the presence of Fe or Al improved PMMA thermal stability, with the former being more effective. It has been postulated that PNC thermal stability is related to the *p*-controlled barrier properties, but here there was no correlation with the clay dimensions.

Sun *et al*.[148] dispersed in styrene Laponite RD with 3MHDA, oil-soluble initiator, non-ionic surfactant and co-stabilizer. After ultrasonication the mixture was emulsion polymerized into PS latex with 200 nm diameter spherical particles, containing up to 7.8 wt% well dispersed clay.

The mechanical properties and structures of aqueous gels (nanocomposite gels), consisting of 80–90 wt% water, poly-(*N*-isopropylacrylamide) (PNIPA) and Laponite XLG were studied.[149] After drying, the interlayer spacing was measured. The compositions containing < 50 mmol/l were exfoliated, while those at clay content ≥ 100 mmol/l were intercalated. Characteristically, full shape recovery after elongation was observed only for low concentrations. The tensile properties, E and σ, increased with clay content, reaching 1.1 MPa, and 453 kPa, respectively, with small loss of elongation at break (ε_b was reduced from about 1000 to 800%). The relative fracture energy increased to 3300 (comparing with a conventional gel). Upon elongation of gel with 250 mmol clay per litres of H_2O, σ increased to 3.0 MPa. On the basis of the mechanical and optical properties it was concluded that an organic/inorganic network structure existed in the full range of clay content. It is certain that clay is not covalently bonded to the polymer, but at lower

DOI: 10.1002/pat

Table 14. Interlayer spacings of the pre-intercalated MMT-type clays

Clay	CEC (meq/g)	Area/cation (nm^2)	d_{001} (nm)			
			ODA	2ODA	3ODA	4ODA
Nanofil 757	0.68	1.87	1.82	2.45	3.25	—
Cloisite® Na	0.88	1.44	—	2.51	3.48	—
Optigel CK	0.90	1.41	1.85	2.66	3.58	3.94
Optigel CMO	1.00	1.27	2.14	3.28	3.84	—

concentration the randomly oriented single clay platelets are enclosed within the aqueous polymer network. The presence of the critical clay concentration: $50 < c_{cr} < 100$ mmol/l, is related to the critical overlap concentration of encompassed volumes equal to the maximum packing volume fraction of hard spheres, $\phi_m \approx 0.62$.[98] Assuming circular clay platelets with diameter of 35 nm and density 2.57 g/ml (see earlier section), the two c_{cr} limits leads to reasonable values $0.334 < \phi_m < 0.658$.

In a recent patent, Galiano *et al*. functionalized Laponite RD with sulfonic groups using plasma treatment. The compound was added to Nafion, and the composition was either cast or extruded into membranes with improved protonic conductivity. Their hydration capability was found improved by the presence of the nanofiller, especially at higher T (e.g. 80–100°C).[150]

In short, Laponite has been used with polymers for catalytic activity, increased hardness and stiffness, or improved performance of soft aqueous gels. The clay can also be used for rheology control during emulsion or polycondensation reactions. Similar uses can be found for other clays of this type listed in Table 2.

PNC with Optigel

Synthetic HT (Optigel SH) was used in the cited work on EP-based PNCs by Zilg *et al*.[132] The authors investigated correlations between PNC composition, type of clay (FM, MMT, and HT), its concentration and mechanical properties. Neat clays and organoclays were examined. At 5 wt% of clay content FM was difficult to disperse, MMT dispersed easier, while HT exfoliated—note the correlation with the aspect ratio. The mechanical properties of four series of EP-based PNC are summarized in Fig. 9. Surprisingly, there is little improvement of properties by intercalation—the tensile strength of PNC's with neat MMT or FH is higher (mid-concentrations) than that with organoclays. The best fracture toughness was reported for FM and MMT, either intercalated or not. Surprisingly, at >3 wt% loading PNC with HT had the best tensile strength at the lowest fracture energy.

PNCs were prepared by melt-compounding in an internal mixer high-density poly(ethylene) (HDPE) with clays (note different CEC) pre-intercalated with ODA, 2ODA, 3ODA, or 4ODA.[151] As shown in Table 14, d_{001} increased with CEC and number of ODA groups of the intercalants. At the constant volume fraction of inorganic clays the mechanical performance correlated with d_{001}, but not with the clay type or aspect ratio. For Optigel-CK–2ODA system, the relative modulus linearly increased with the clay volume fraction—35% higher modulus at 2.8 vol% was reported. Substituting these values to eqn (2) gives the aspect ratio, $p = 59$. This is modest, but reasonable for this non-exfoliated synthetic clay.

PNC with Sumecton-SA

Polymerization of ε-caprolactam in the presence of synthetic Na-saponite (Sumecton-SA) resulted in full exfoliation.[152] The presence of clay increased the crystallization rate of the α-form. At 2.5 wt% clay loading the relative tensile and flexural moduli increased to: 3.06 and 1.12, respectively, with the Charpy impact strength reduced from 6.2 to 6.1 kJ/m, and HDT increasing from 65 to 76°C at 264 psi.

PNC with synthetic magadiite (MAG)

The interlayer spacing of intercalated clays depends not only on the type of clay and intercalant, but also on T and P. The measurements conducted on aqueous suspensions indicated that in most cases as T or P increases d_{001} decreases.[61,153] Figure 12 displays d_{001} versus T plot for organo-MAG; squares represent MAG-di-methyl-di-tetradecyl ammonium chloride (2M2TDA) behavior (filled for heating, open for cooling), while circles represent tetra-decyl ammonium chloride (TDA)-ammonium amine complex [$C_{14}H_{29}N^+H_3 \cdot C_{14}H_{29}NH_2$]. As shown, d_{001} variations with T depend on the ammonium radical; the primary ammonium intercalant seems to be more sensitive to T than quads. The authors suggested that these changes are caused by molecular

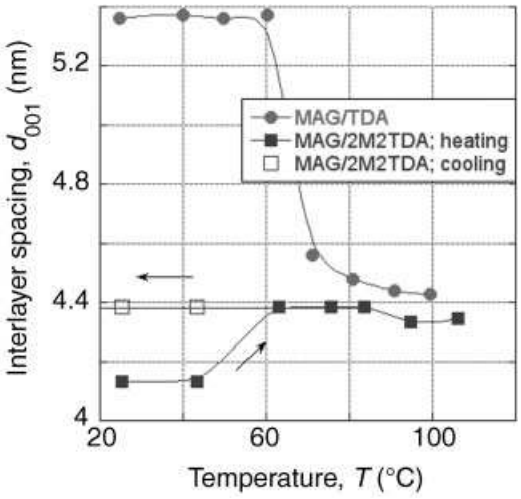

Figure 12. Interlayer spacing, d_{001}, as a function of temperature, T, for MAG intercalated with salts of tetradecyl ammonium and complexed with tetradecyl ammonium (TDA) or with di-methyl di-tetradecyl ammonium (2M2TDA); open squares show values after cooling.[153]

DOI: 10.1002/pat

rearrangement of the ammonium ions, melting *n*-paraffin groups, or hydration.

Since 1994 Pinnavaia and coworkers published a series of articles on the use of EP compounds as the second intercalant of layered materials.[154–157] To achieve organoclay exfoliation in glassy EP involved heating pre-intercalated layered nanofiller with EP resin at $T = 200$–$300^{o}C$. For example, synthetic Na^{+}-MAG was ion-exchanged in the presence of amine with ammonium ions, $CH_3(CH_2)_{17}NH^{+}_{3-n}(CH_3)_n$ where $n = 0$–3.[158] For the primary amine (ODA) $d_{001} = 3.82$ nm was determined. As the number of methyl groups increased from $n = 1$ to 2 and 3, d_{001} decreased to 3.74, 3.20 and 3.41 nm, respectively. Next, an organo-MAG was added to Epon 828 and Jeffamine [PPG-bis(2-aminopropyl ether)], stirred for 60 min, degassed and cured. When the curing time was > 5 min, full exfoliation was obtained (EP contained ≤15 wt% organoclay). Good exfoliation was obtained for MAG intercalated with either primary or secondary onium ions ($n = 0$ or 1), but for higher amines ($n = 2$ or 3) intercalated systems were obtained with $d_{001} = 7.82$ and 4.10 nm, respectively. The observed effect of the intercalant structure was interpreted in terms of acidity that accelerates the curing reaction within the interlamellar galleries, which results in delamination. The acidity of, e.g., ODA is reduced by the presence of methyl groups (especially for $n = 2$ or 3). It is also possible that N–H of the primary and secondary ammonium ions may be able to react with EP, and thus causing an expansion of the intergallery space. EP nanocomposites with MAG showed great improvement in tensile modulus and strength. The enhancement of tensile strength depended on the degree of exfoliation, e.g. at 10 wt% of MAG the tensile strength increase by a factor of 4.8, 3.5, and 2.3 for the exfoliated, ordered exfoliated and intercalated system, respectively ($n = 1$–3). The transparency and high barrier performance makes these PNCs attractive as packaging materials and protective films.

Effects on the curing kinetics were also observed during UV-curing. MAG in either sodium form or organo-modified were dispersed at 5 wt% by sonication in 3-4 epoxycyclohexylmethyl-3′-4′-epoxycyclohexylcarboxylate, then 2 wt% of cationic photo initiator (triaryl sulphonium hexafluoroantimoniate) was added, and the system was UV-cured. Despite that the dispersion did not show any change of d_{001} (for neither the unmodified nor the organophilic MAG) the curing kinetics (followed with FT-IR) had a long induction time. Incorporation of Na-MAG was ineffective, while the presence of organo-modified MAG resulted in high conversion.[159]

Intercalation of MAG has been also carried out by silylation of interlayer silanol groups with organo-chloro silanes with different functionality[81] that resulted in covalent bonding between organic molecules and clay surface. Thus, first MAG was dispersed in a solution of tri-methyl dodecyl ammonium (3MDDA) ($d_{001} = 2.79$ nm), then the product was added to a toluene solution of either octyl-dimethyl-chloro-silane ($C_8H_{17}(CH_3)_2SiCl$; **1**) or octyl-tri-chloro-silane ($C_8H_{17}SiCl_3$; **2**). The reaction involved de-intercalation of 3MDDA, which reduced d_{001} to 2.33 and 2.18 nm, for **1** and **2** respectively. The grafting density of the organo-silyl groups was 1.84 and 1.94 per $14SiO_2$ (molar ratio), respectively, and the organo-silyl groups formed monolayers. The two pre-intercalated MAGs showed different reactivity and alcohol sorption behavior. The new organoclays with better thermal and chemical stability could be used to form PNCs.

MAG, prepared in a hydrothermal reaction that gave CEC = 2.2 meq/g, and thickness of the silicate layer of 1.12 nm[160] was intercalated with photochromic *p*-(*ω*-dimethyl-hydroxyethyl amino-ethoxy)-azo-benzene cation:

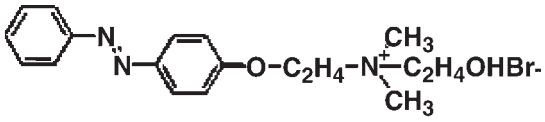

The intercalant isomerized when UV-irradiated, resulted in reversible changes of d_{001} from 2.69 to 2.75 nm.

Wang *et al.*[161] prepared PNCs with MAG, pre-intercalated with di-methyl-(*p*-vinyl benzyl)-hexadecyl ammonium chloride (2MVBHDA; VB-16). The compound was dispersed in styrene, and then the bulk polymerized at 60 to 80°C for 48 hr. The interlayer spacing of MAG, $d_{001} \approx 1.5$ nm, increased to >8.8 nm, suggesting exfoliation. However, TEM micrographs showed the presence of large, micron-size, clay aggregates. The high magnification micrographs seem to indicate that the individual MAG platelets are about 150 nm large. The relative modulus (at 3 wt% loading?) was $E_R = 1.4 \pm 0.1$, and the relative peak stress $\sigma_R = 3.4 \pm 1.2$. From the relative modulus eqn (2) gives for the effective MAG aspect ratio value of $p \approx 150 \pm 25$. The thermogravimetric and cone calorimetry analyses indicated that PNC and PS had similar degradation onset and the pathway, thus MAG is not a flame retardant for PS. This conclusion was found also applicable to PNCs based on thermoset vinyl ester,[162] or to EVAc.[163]

Morgan *et al.*[164] prepared a series of EVAc-based PNCs with 5 wt% of MAG, pre-intercalated with inorganic (H^{+}, Na^{+}, Ca^{2+}, Mg^{2+}) and organic ($2M2HTA^{+}$) cations. All compositions comprised 58 wt% of $Mg(OH)_2$ and 6 wt% of maleated linear low density poly(ethylene) (LLDPE-*g*-MA) compatibilizer. The composites were prepared by melt compounding in an internal mixer at 170°C. Owing to high solid content (*ca.* 40 vol%) the clay dispersion was poor—the best ($d_{001} = 4.4$ nm) for MAG-2M2HTA, the worst ($d_{001} = 1.35$ nm) for MAG-Ca. EVAc is known for high flammability—its PHRR = 1632 kW/m^2. Incorporation of 63 wt% of $Mg(OH)_2$ reduced this value to 188, while replacement of 5 wt% of $Mg(OH)_2$ by intercalated-MAG changed the PHRR = 131 to 255 kW/m^2—the former value for H-MAG, the latter for Na-MAG. As the authors noted, H-MAG should be considered non-ionic silica, which during the flammability tests may form silicate glass that reduces mass transfer to flame, thus flammability.

PNC with synthetic, laboratory—scale made silicates

Synthetic saponites,[165–167,169] polymer-containing Mg-silicate-HT,[167,168] and HT[169] were synthesized using modified hydrothermal methods. The reactants were added sequentially, and after *ca.* 4 hr of aging, crystallized hydrothermally for 72 hr at 240°C. The resulting clays were pre-intercalated

DOI: 10.1002/pat

by two methods: (1) during ''one-pot'' synthesis,[167] adding 3MHDA directly to gel at a ratio 3MHDA/Na = 3 to ∞; (2) standard ion-exchange by suspending the pristine clay in 3MHDA or ODA aqueous solution at approximately pH $\approx$ 3. The suspensions were stirred at 70°C for 36 hr and the final products was filtered and dried.

PP with synthetic organoclays (saponites or hectorites) was prepared by melt blending in an internal mixer at 190°C for 3 min with a screw speed of 60 rpm.[170] For comparison, neat PP and its PNCs with fully inorganic synthetic clays or MMT-2M2HTA have been compounded under similar conditions. The thermal degradation in air was found related to the degree of clay dispersion. The thermal degradation temperature, T_d (defined by the maximum rate of weight loss in TGA), of the PP-based PNC was higher than that of the neat PP, $T_d(PP) = 330°C$. Thus, PNC containing synthetic saponite pre-intercalated with 3MHDA in the ''one-pot'' method showed $\Delta T_d = T_d - T_d(PP) = 44°C$, that ion-exchanged with ODA had $\Delta T_d = 61°C$, while PNC with for PP/MMT-2M2HTA: $\Delta T_d = 51°C$. It is noteworthy that PP containing mineral Na-saponite also showed enhanced thermal behavior: $\Delta T_d \approx 40°C$.

Quite different results were obtained when saponite was replaced by HT. The PNC containing HT-3MHDA showed the maximum rate of thermal degradation at $T_d = 328°C$, comparable to $T_d(PP) = 330°C$. This result can be ascribed to the different surface properties of the two synthetic clays. In saponite, Al $\rightarrow$ Si substitution in the tetrahedral sheets leads to the formation of Brønsted acid sites, that as shown by FT-IR is similar to most acid zeolites.[167] By contrast, such a surface acidity is absent in synthetic HT.

With low temperature hydrothermal treatment of basic silicate solutions, Pinnavaia and Xue prepared synthetic saponite with low aspect ratio.[171] The material (without any modifier) was dispersed in EP by ultrasonication at 90°C, and then cured with different curing agents to give rubbery or glassy PNC. As illustrated by data in Table 15, the elastomeric matrix nanocomposites showed greatly improved mechanical performance.

PNC with layered double hydroxides (LDHs)

Introduction

Clay is a generic term for hydrous silicate particles less than 2 μm in diameter, rich in silicon and aluminium oxides and hydroxides as well as structural water. From the point of view of PNC technology, of main interest are crystalline (natural or synthetic) clays with layered structure that can be exfoliated. However, besides clays there are other layered materials that might be used for the same purpose.[1] Of these, the LDHs are gaining notoriety—at present, over 100 patents on LDH synthesis and its application are published annually.

LDHs have been known since 1842. Natural LDH, namely hydrotalcite, pyroaurite, and stichtite [$Mg_2M^{3+}{}_2(OH)_{16}CO_3 \cdot 4H_2O$ with $M^{3+} = Al^{3+}$, Fe^{3+}, and Cr^{3+}, respectively] exist in small quantities and are highly contaminated. The first LDH synthesis was described by Feitknecht,[172] and patenting activities started in the 1960s.[173] Clearfield *et al*. studied intercalation of several types of LDHs with sodium dodecyl sulfate (Na-DDS) and thermal stability of the adduct.[174] The decomposition of LDH-DDS complex started at 180°C with evolution of $C_{12}H_{24}$. However, the structure of LDH was reported stable up to 250–300°C.

LDH might be tailored to produce functional materials with properties required for specific applications, e.g. as precursors for magnets, heat retention additive in horticultural plastic films, flame retardants, HCl absorbing agents for poly(vinyl chloride) (PVC) and other halogenated polymers or POs, adsorbing agents for dyes, pigment dispersion stabilizers for coloring polymers, in biology and medicine for the storage, delivery and controlled release of pharmaceuticals and other biomolecules, as sensing materials for determination of water level, toxic additives, as biosensors, for electrodes, as catalysts for polymerization or decomposition of noxious gases, etc.[184] LDHs are commercially manufactured (e.g. by FCC in China, Süd Chemie and Sasol in Germany, Ciba in Switzerland, Akzo Nobel, Dulso Šal'a, Slovakia, and Reheis Chemical Co. in the USA) from purified salts, or minerals such as brucite, $Mg(OH)_2$, or quasi-crystalline boehmite, AlO(OH),[175] mainly as acid-absorbers, and catalysts for molecular conversions and reactions.

LDHs, also known as hydrotalcite-like anionic clays, or mixed metal layered hydroxides. Their general chemical composition is:

$$[M(II)_{(1-x)}M(III)_x(OH)_2]^{y+}(A^{n-y/n}) \cdot mH_2O$$

where M(II) is the M^{+2} cation (e.g. Mg^{2+}, Zn^{2+}, Ni^{2+}, Fe^{2+}, Cu^{2+}, Co^{2+}, Ca^{2+}, or Mn^{2+}), M(III) is M^{+3} cation (e.g. Al^{3+}, Fe^{3+}, Cr^{3+}, Co^{3+}, Ni^{3+}, Sc^{3+}, Y^{3+}, In^{3+}, La^{3+}, Th^{3+}, Ti^{3+}, V^{3+}, Sb^{3+}, Bi^{3+}, Mn^{3+}, Ga^{3+}), $y = 1–2$; $n = 1–10$; and A^{n-} is organic or inorganic anion of charge n, e.g. $A = Cl^-$, Br^-, NO_3^-, CrO_4^{2-}, $Cr_2O_7^{2-}$, $B_4O_7^{2-}$, MoO_4^{2-}, SeO_3^{2-}, SiO_3^{2-}, SO_3^{2-}, SO_4^{2-}. Idealized structures and dimensions of MgAl-LDH are displayed in Fig. 1. The x value generally ranges from 0.15 to 0.5 and determines the layer charge density and the anion

Table 15. Tensile properties of glassy or rubbery EP—saponite PNCs sonified at 90°C[171]

Matrix type	Saponite (wt%)	Modulus, E (GPa)	Strength, σ (MPa)	Strain at break, ε_b (%)
Glassy	0.0	2.9	66	4.3
Glassy	2.1	3.1	68	5.7
Glassy	5.4	3.1	70	8.9
Glassy	9.4	3.8	73	5.4
Rubbery	0.0	2.8	0.6	24.9
Rubbery	2.1	3.8	1.2	38.7
Rubbery	5.5	5.6	1.8	38.0
Rubbery	10.9	7.7	2.7	39.2

DOI: 10.1002/pat

exchange capacity (AEC). It is noteworthy that LDHs have cationic character, by contrast with the anionic clays. Furthermore, their AEC = 0.5 to 6 has much greater span than clays CEC = 0.5–2. The structure of the LDH is similar to that of brucite, in which isomorphous replacement of a part of the divalent cations by trivalent cations occurred. The composition crystallizes in layers formed by the edge concatenation of $Mg(OH)_6$ octahedra. As cations in clays, the interlayer anions in LDH can be exchanged by other anions, dyes or biomolecules containing ionisable acidic groups.[176–178] LDHs have been discussed in several edited books[19,179,180] and reviews.[36,181–184] They are also discussed in the PNC monograph.[1]

Costantino *et al*.[185] prepared a series of iso-structural LDHs of the type Mg-Al, Zn-Al, and Ni-Al with diverse properties. The synthesis offered the possibility of modification of the inorganic lamella, and improved its interactions with the polymeric chain by suitable anionic exchange. The organo-modifiers increased the interlayer spacing from 0.89 to several nanometers. A structural model, considering the composition, the charge density, and the gallery height, suggests that for long alkyl chain carboxylic acid anions (e.g. stearate, C_{18}) a monofilm of inter-digitated alkyl chains is formed.

During the last few years the computer simulation of LDH structures provided better insight into the interlayer properties and dynamics.[3,186] The use of computational methods provides information on the spatial arrangement, dynamics of molecular vibrations that help interpretation of XRD, FT-IR, NMR, or neutron diffraction studies. It is noteworthy that owing to the variation of electron density in LDHs the 00n XRD peak intensity not necessarily decreases with n, but spectrum modeling provides the correct assignment. The computations also lead to such quantities as, e.g. interlayer spacing, chemical reactivity, or diffusion coefficients, which might be compared directly with the experiments.

For the production of PNCs, LDH might be intercalated by: (1) monomers, e.g. aniline, pyrrole, ω-aminoacid, methyl methacrylate, vinyl-benzene sulfonate, vinylpyrrolidone, vinyl acetate, etc. (2) extended polymer chains, e.g. PEG, *p*-sulfonated polystyrene (PSS), polyaniline (PANI)-sulfonate; (3) co-precipitation in the presence of a polymer. Furthermore, LDH/polymer PNCs have been prepared by two-step surfactant-mediated incorporation, hydrothermal treatment, reconstruction, or restacking.

Few PNCs with dispersed LDHs have been evaluated for mechanical performance. These systems are thermally more stable than the pristine organic compounds, and might be used in applications requiring enhanced flame-retardance. A large variety of LDH/polymer systems may be tailored considering the highly tunable interlayer composition coupled to the choice of the organic moiety. DNA may be stabilized in the interlayer space of $[Mg_2AlNO_3]$ as a gene reservoir. Some of the intercalated polymers show excellent physical properties, e.g. conductivity (PANI), insulation (PS), ion-gate behavior [polypyrrole (PPY)], etc. However, these are difficult to process because of lack of mechanical strength. Numerous studies focused on the use of conductive polymers for capacitors, rechargeable battery materials, or in electrochromic windows. Some difficulties for replacing in PNCs the natural or synthetic clays by LDHs still remain. The LDH usually has a small aspect ratio ($p < 80$), and specific surface area ($A_{sp} < 100\,m^2/g$), the platelets are thin (about 0.5 to 0.8 nm), and fragile. The LDH concentration needed for generating desired performance has been significantly higher than that of clay. Furthermore, at $T \approx 240$–$300^\circ C$ LDHs thermally decompose, loosing the crystalline structure.[187] Diverse LDHs have been incorporated into polymers such as: PANI, poly(vinyl alcohol) (PVAl), PSS, poly(vinyl sulfonate) (PVS), polyacrylate (PAC), poly(acrylic acid) (PAA), PPY, PEG, polyimide (PI), elastomers, poly(α,-β-asparatrate), etc.[181,182] In most cases the LDH-type nanocomposites with high LDH content showed small interlayer spacing, $d = 1.3$–3.7 nm.

LDH with vinyl or acrylic polymers

The template method was used for the preparation of PNCs comprising MgAl-LDH and PSS or PVS as the matrix.[188] Aqueous solutions of a sulfonated polymer, $Mg(NO_3)_2$, $Al(NO_3)_3$, and NaOH were mixed together for 24 hr at 65°C, and then filtered, washed and dried. The XRD interlayer spacing, $d = d_{003}$ of LDH (0.77 nm) increased to 1.27 and 2.1 nm for PNC with PVS and PSS, respectively. TGA weight loss for these three compositions was 42.1, 55.1 and 59.9 wt%, respectively. The loss corresponds to dehydration at 50–220°C, and dehydroxylation at $T \geq 240^\circ C$. TEM indicated that in LDH the elongated platelets formed aggregates 200 to 300 nm long, whereas the LDH-PSS were composed of aggregated equilateral clusters, *ca*. 25 to 50 nm in diameter. Thus, the presence of anionic polymer affected LDH crystallization.

Moujahid *et al*.[189] prepared PNCs with LDH by *in situ* polymerization. Thus, first two types of LDH were prepared by co-precipitation: $Zn_{0.67}Al_{0.33}(OH)_2Cl_{0.33} \cdot 0.75H_2O$ and $Cu_{0.68}Cr_{0.32}(OH)_2Cl_{0.33} \cdot 0.92H_2O$. Next, Cl^- was exchanged for an acidic monomer vinyl benzene sulfonate sodium salt (VBS) or amino-benzene sulfonate (ABSu), which in turn were *in situ* polymerized at $T = 473$ K. Incorporation of the monomers increased the interlayer spacing from 0.776 to 1.80 nm (VBS) or 1.54 nm (ABSu). The polymerization was studied by ^{13}C cross-polarization (CP)- MAS NMR or electron spin resonance (ESR). The resonance peak associated with the vinyl group disappeared from the VBS/ZnAl-LDH spectrum, and resonance peaks similar to PSS/LDH appeared. The thermal treatment of ABSu/CuCr-LDH was found to depend on the presence of O_2; in air a narrow signal, characteristic of free radicals, was observed. More interesting are fully exfoliated PNCs with ZnAl-LDH dispersed in PS matrix, prepared by *in situ* emulsion or suspension polymerization.[190] The key to exfoliation was the use of *N*-lauroyl-glutamate surfactant and long-chain spacer (e.g. *n*-hexadecane). It is noteworthy that only intercalated systems were obtained using sodium dodecyl sulfate (SDS) as a surfactant, or shorter spacer (e.g. *n*-octane). The exfoliated ZnAl-LDH platelets were dispersed on a molecular level even at LDH concentrations of 10 and 20 wt %. The PNCs showed water loss at $T > 85^\circ C$, but when the 50% weight loss was used as a criterion, the decomposition temperature of the exfoliated PNC with a 5 wt % LDH was about 28°C higher than that of neat PS.

DOI: 10.1002/pat

Vieille *et al.*[191] also used the templating reaction for incorporating VBS or PSS into LDH. Two LDHs were used: LDH1 = $Zn_2Al(OH)_6Cl \times nH_2O$ and LDH2 = $Ca_2Al(OH)_6Cl \times nH_2O$. The reaction conducted at 65°C at pH ≈ 11 expanded the interlayer spacings for LDH1 and LDH2 from $d = 0.78$–0.79 nm, to 1.82–1.77 for VBS, and 1.93–1.92 nm for PSS. ^{13}C CP-MAS NMR indicated similar peak shifts for both LDHs, suggesting similar electrostatic bonding energies. However, the *in situ* polymerization of VBS molecules inside the intergallery spaces of LDH1 was quite different than that in LDH2; for the former the polymerization started at 120°C and was completed at 200°C, whereas for LDH2 the polymerization started at 180°C, and to complete it required $T > 200$°C. The thermal stability of the PNCs with LDH1 was better than of these with LDH2.

Significant reduction of the thermal degradation of PS was obtained incorporating a Zn/Al-LDH (chloride form) modified with benzene phosphonate anions.[192] The amount of organic intercalant ranged from 25 to 88% of the AEC. The organo-modified LDH was intercalated by the benzene phosphonate grafted on the lamellae surface. The PNCs were prepared by the co-solvent method dispersing 5 wt% nanofiller in PS. The XRD of cast films showed almost total disappearance of the LDH diffraction peaks, suggesting exfoliation. The thermogravimetric study of the composites under air, compared with the pure polymer matrix in air and nitrogen, showed stabilization of the thermooxidative degradation of PS; the best performance was obtained for about 40% anionic substitution. In this case, the degradation in air was comparable to that of neat PS under N_2.

Camino *et al.*[193] compared flammability and mechanical properties of EVAc, with EVAc containing 50 wt% of either $Mg(OH)_2$, $Al(OH)_3$, AlO(OH) or MgAl-LDH. The samples were melt-compounded in an internal mixer at $T < 150$°C (to avoid decomposition of LDH). The EVAc with LDH showed the highest value of the limited oxygen index (LOI = 29.5 vol%), the longest delay time to reach the peak temperature ($\Delta t_{max} = 191$ sec) and the lowest peak temperature ($T_{max} = 115$°C). This behavior could be due to the heat absorption within a temperature range of Al and Mg hydroxide decomposition. Furthermore, char retained an intumescent compact surface up to the end of the test. The tensile tests indicated that as far as the elongation at break and ultimate strength are concerned, the LDH system behaved similarly to other fillers. The authors concluded that: ''... to achieve useful flame-retarding properties in EVA polymer, the overall filler loading needed must be higher than 50-wt%''. Similarly, Jiao *et al.*[194] investigated the flame-retardancy of EVAc-LDH. The PNCs were prepared by melt compounding 0–150 phr LDH with EVAc on a two-roll mill at $T = 120$°C. LOI increased linearly with LDH content, doubling its value at *ca.* 100 phr. Incorporation of 120 phr LDH reduced PHRR of the system by a factor of 10. TGA also indicated increased thermal stability of the EVAc copolymer. The flame retardation effect of LDH was larger than that of a nano-sized $Mg(OH)_2$, currently used as a flame depressant. However, to achieve these benefits required 60 wt% or more of LDH, which greatly reduced the mechanical performance.

As these examples demonstrate, MgAl-LDH prepared by co-precipitation with organic reagents might provide specific performance. It is noteworthy that these examples deal with PNCs that by virtue of the reactive agent are bonded to the LDH surface, and that the preparation did not involve heating the system above 200°C. Similarly, MgAl-LDH modified with dodecyl sulfate (DDS) was dispersed in acrylic monomers by high-shear stirring at 70°C.[195] The suspension containing 1 to 10 wt% LDH-DDS was polymerized by free radical initiation at $T = 120$°C. The TEM and XRD suggested a partial delamination (short stacks with 2–5 plates remaining), which resulted in enhanced thermal stability. However, the weight loss in TGA that started at 50°C was greatly accelerated at *ca.* 250°C. Similarly, MgAl-LDH-$(PEG)_2$-PO_3OH has been prepared by template method, and then mixed with PEG and $LiClO_4$.[196] The systems were exfoliated, and the LDH platelets acted as nucleating agents for PEG. A significant enhancement of conductivity was obtained.

Fischer *et al.*[197] used a designed block copolymer as a compatibilizer for immiscible mixtures of a polymer/layered material. The authors tested the concept using, e.g. PMMA with *ca.* 5 wt% of synthetic Na-saponite, or MgAl-LDH. The samples were prepared by melt compounding in a mini-TSE at 160°C for 5 min. For saponite the PMMA-*b*-PEG, and for LDH the PMMA-*b*-PMAA copolymers were used. The relative modulus of these PNCs was, respectively, $E_R = 1.4$ and 1.7; relative elongation at break 0.33 and 0.53; and relative strength 0.62 and 1.06. From E_R an average platelet diameters can be calculated as 64 and 296 nm, respectively.

Recently, Costache *et al.* have reported that the thermal stability of PMMA with LDH require that the latter is exfoliates; incorporation of 7 wt% pre-intercalated LDH did not improve stability over the effects of CNTs or MMT/MHT2EtOH[198].

LDH with polycondensation-type polymers

Full exfoliation during PA-6 polycondensation in the presence of LDH was described by Fischer and Gielgens.[199] To accomplish this task, the LDH was treated with ≥20 wt% of organic intercalant, having organic groups that are either miscible or reactive with the matrix. Furthermore, at least 5% of these anions contain a second charge-carrying group. The preferred anions are of carboxylic, sulfonic or phosphonic acids, while the charge-carrying group is cationic, e.g. ammonium, phosphonium, or similar. Presence of the latter groups repels the LDH sheets helping the exfoliation. According to authors of this patent, the suitable polymeric matrices are: PA, PO, PEST, PC, TPU, vinyl polymers, and polyepoxides. The PNC might be prepared by either melt compounding organo-LDH with molten polymer in a TSE or by dispersing it in monomer, which then is polymerized. Unfortunately, the document does not fully support these broad statements. For example, PC is known to be acid/base sensitive, and melt compounding PC in the presence of hydroxyl groups, might induce its hydrolytic degradation, leading to significant losses of mechanical, thermal, and flammability performance. The following patent[200] provided an example. First, $[Mg_6Al_2(OH)_{16}][CO_3 \cdot 4H_2O]$ (AEC =

DOI: 10.1002/pat

4 meq/g) was dispersed in aqueous solution of α,ω-amino-undecanoic acid at 80°C, and reacted for 3 hr. Next, the purified condensate was mixed with ε-caprolactam and 10% H_2O, heated to 260°C and polymerized. The PA-6/LDH melt was transparent, suggesting exfoliation, confirmed by XRD.

LDHs of the type Mg_3Al/4-dodecyl benzene sulfonate (DBS) = $Mg_{0.75}Al_{0.25}(OH)_2(DBS)_{0.25} \cdot 0.44H_2O$, and Mg_6Al/DBS = $Mg_{0.84}Al_{0.16}(OH)_2(DBS)_{0.16}$ (Na-DBS)$_{0.08} \cdot 0.44H_2O$ were prepared by the co-precipitation. They were melt compounded with 95 wt% of PA-6 in a mini-TSE at $T = 230$–260°C, and then hot-pressed at 240°C.[201] The AEC of these two LDHs was 1.69 and 1.09 (meq/g), and the interlayer spacing $d_{003} = 2.76$ and 2.83 nm, respectively. The hexagonal platelets with diameter of about 70–200 nm were 0.49 nm thick (i.e. the aspect ratio: $p \approx 500$). The degree of dispersion depended on AEC, the compounding T and stress. Higher degree of dispersion was achieved compounding PA-6 with Mg_6Al/DBS than with Mg_3Al/DBS. It is noteworthy that during compounding with PA-6 the high stresses and T resulted in attrition of the fragile LDH to diameter of *ca*. 40–80 nm. By contrast with clay-containing PNCs, the ones with LDH crystallized at about the same rate and into similar crystalline form as those of neat PA-6.

Similarly, PET was melt-compounded with 0, 1.0, and 2.0 wt% of pre-intercalated LDH.[202] Prior to intercalation the LDH (Mg_3Al-CO_3) was calcinated at 500°C (converting it into oxides), re-dispersed in water solution of DDS, DBS, or octyl-sulfate (OS). The interlayer spacing of these adducts ranged from 2.3 to 2.8 nm. Compounding was carried out in a mini-TSE at 270°C with residence time of *ca*. 1 min. According to XRD the PNCs were exfoliated, but aggregates were evident in the TEM micrographs. The flow behavior of the PNCs indicated presence of weak networks; the mechanical properties were disappointing. The best performing was PET with 2 wt% LDH-DDS—its modulus and strength increased by 7 and 11%, respectively, but the elongation at break decreased by 84%. The effect of LDH addition on the thermal properties was marginal. Thus, either the calcinated LDH did not fully recover its layered structure, or damage to LDH during compounding with PET significantly altered its structure.

LDH with polyolefins

PNCs with PO as the matrix are the most difficult to prepare. Owing to low polarity they do not interact with nanofillers, such as clay, CNTs or LDHs. However, several attempts were made to engender exfoliation in PO matrix, and achieve significant improvement of properties.

Attempt to exfoliate LDH in PE-g-MA started by the synthesis of Mg_3Al-LDH by co-precipitation method, calcination of the product, its re-hydration in DDS aqueous solution, followed by drying, and dispersing in xylene solution of PE-g-MA under reflux ($T \approx 140$°C).[203] At 2 or 5 wt% LDH loading PNCs were exfoliated. The hexagonal LDH platelets were randomly dispersed, and their dimensions were about $0.48 \times 70 \times 70$ nm^3. TGA suggested faster charring (than PE-g-MA) at 210 to 360°C, and greater thermal stability above 370°C. The presence of exfoliated LDH, resulted in a shift of the degradation temperature (in air, measured at 50 wt% loss) by *ca*. 24 to 59°C. The PNCs were found suitable for the use in flame-retardant polymeric compositions. Next, the effect of replacement of Mg_3Al-LDH by Zn_3Al-LDH (platelet diameter *ca*. 50 nm) and PE-g-MA by LLDPE were examined.[204] The PNCs containing 2 to 95 wt% LDH-DDS were also prepared in xylene solution. The compositions containing 2, 5, and 10 wt% LDH were found exfoliated, that with 20 wt% showed a shoulder on XRD trace, and samples containing $\geq$50 wt% LDH had intercalated structures. Significant enhancement of thermal stability was obtained, with a shift of the degradation temperature (measured at 50% weight loss) by 37 to 65°C, and the maximum efficiency for 5 wt%. The mechanical behavior has not been reported.

Costantino *et al*. prepared Zn_2Al-LDH by the co-precipitation method (interlayer distance, $d = 0.758$ nm; specific surface area, $A_{sp} = 24.1$ m^2/g).[205] The LDH was pre-intercalated with sodium stearate, and after drying compounded with medium density PE in an internal mixer at 120°C, rotor speed 60 rpm, and residence time 3 min. PNCs with 5, 10, and 15 wt% of inorganic fraction (calculated as ZnO and Al_2O_3 oxides) were found exfoliated. LDH strongly affected PE flammability; namely incorporation of 5 wt% of LDH reduced PHRR by 55%. This observation was indirectly confirmed later by Qiu *et al*.[206] who compared the thermal stability of LLDPE-based PNCs containing 0 to 10 wt% of either 3MHDA-MMT, Mg_3Al-LDH(DDS), or Zn_3Al-LDH (DDS). The best dispersion and stabilization effect was obtained with the latter adduct.

Costa *et al*.[207,208] synthesized Mg_3Al-LDH by Costantino's *et al*.[205] urea hydrolysis method, followed by calcination at $T = 450$°C, and re-hydration in aqueous solution of sodium dodecyl-benzene sulfonate (SDBS). The PNC samples (containing 2 to 10 wt% of the adduct, and twice as much of the compatibilizing MAH-g-PE) were melt compounded in an internal mixer at $T = 200$°C. The master batch (MB) was diluted with low density poly(ethylene) (LDPE) to the final composition. XRD and TEM indicated that compounding Mg_3Al-LDH(SDBS) with PE-g-MA, and LDPE hardly changed the interlayer spacing, $d_{003} = 2.96$ nm, and large aggregates of LDH have remained. In the second paper the morphology and flow behavior were studied. TEM and rheology indicated that LDPE/LDPE-g-MA matrix hardly interacts with Mg_3Al-LDH(SDBS). As expected, better interaction was obtained in Mg_3Al-LDH(SDBS) with LDPE-g-MA alone, i.e. without LDPE.

Recently, Ding and Qu reported preparation of exfoliated PP/LDH nanocomposites by melt-compounding.[209] The TGA and dynamic mechanical analysis (DMA) data showed that the PNCs have enhanced thermal stability compared with virgin PP and a PP/MMT nanocomposites. X-ray photoelectron spectroscopy (XPS) and FT-IR results indicated that the photo-oxidation mechanism of PP in the PP/LDH materials is not modified, but the photo-oxidation rate is much lower than that of PP and PP/MMT samples, suggesting better UV-stability. The mechanical properties have not been measured.

The effects of LDH incorporation into PP and PP + PP-g-MA on photostability were recently investigated.[210] Thus, PP

DOI: 10.1002/pat

or PP + PP-g-MA was melt blended with 5 wt% of commercial Mg/Al hydrotalcite (Sasol PURAL MG45-carbonate form). The effects on photo-oxidation ($\lambda > 300$ nm, T = 60°C, in SEPAP 12/24 apparatus) were followed by IR and UV-visible spectroscopy. Furthermore, the same tests were performed using the samples from which the commercial organic photostabilizer was extracted with 1:1 toluene/ethanol mixture. The presence of the hydrotalcite increased the rate of photodegradation and reduced the oxidation induction time (OIT). The oxidation curves of the PNC (IR absorbances at 1712 cm^{-1}) showed increased slopes. This effect was also evident on extracted samples, but here the OIT was almost constant. The reported results indicate the need for evaluation of photostability for outdoor applications.

LDH with thermosets

Hsueh and Chen[211,212] developed successful strategy for the preparation of PNCs with significant enhancement of properties at low mineral content. It involves co-precipitation of $Mg(NO_3)_2$, $Al(NO_3)_3$, NaOH in the presence of a reactive organic agent, followed by filtration, drying, addition of suitable monomers, and polymerization. The reactive organic agent should be selected considering the matrix polymer, e.g. for polyimide (PI)-based PNC, the reactive agent might be amino benzoate (AB), whereas amino laureate (AL) is preferred for EP-based systems. The LDH content ranged from 0 to about 7 wt%. The interlayer spacing of LDH with either AB or AL was $d = 1.5$ or 2.5 nm, respectively. Incorporation of monomers further expanded the intergalleries, while polymerization led to exfoliation. The dimensions of LDH platelets were not cited, but judging by the TEM micrographs they ranged from about 30 to 100 nm in length. The maximum tensile strength and elongation of LDH-AB and LDH-AB/PI occurred at 4 and 5 wt%, respectively. At 5 wt% LDH loading the storage modulus increased by *ca*. 33% and T_g by 38°C. The coefficients of thermal expansion (CTE, below and above T_g) decreased and the thermal properties have improved. The maximum tensile strength of LDH-AL/EP occurred at *ca*. 3 wt% of LDH–AL. At 7 wt% LDH loading the tensile strength and modulus increased by *ca*. 44% and 52%, respectively. The latter value substituted to eqn (2) gives a reasonable value of $p = 78$. Furthermore, with LDH loading T_g and thermal stability increased, and CTEs decreased.

A significant improvement of EP performance with incorporation of MgAl-LDH was also reported by Zammarano *et al*.[213,214] The LDH-containing PNCs showed different mechanism of the thermal degradation that delayed the maximum heat release by ≥50°C, and decreased the weight loss rate. The nanocomposites showed higher flame-retardant properties than conventional flame retardants, and self-extinguishing behavior in the horizontal burn tests. The performance was related to the level of dispersion and the intrinsic properties of LDHs, which resulted in the formation of intercalated layered structure of mixed metal oxides and char. The LDH-containing PNCs showed a reduction of PHRR by 50.6%, compared to 27.1% for conventional agent. A synergetic effect between ammonium polyphosphate and LDH was reported. In the authors recent paper[214] they compared the flame retardancy of EP compositions with *ca*. 5 wt% of either MMT or LDH. The latter was either fully inorganic, or it contained an organic agent grafted during the templating co-precipitation. Only exfoliated LDH-PNCs showed self-extinguishing behavior. The cone calorimeter revealed intumescent behavior and a higher reduction of the PHRR compared to that of MMT/EP system.

PNC with other lamellar materials

To this category belong many materials listed in Table 1, namely synthetic or natural layered alumino-phosphates, M^{+4} phosphates or phosphonates, chlorides, chalcogenides, cyanides, oxides, graphite, graphite oxide, boron nitride (BN), etc. For example vanadium pentoxide was used to enhance stability of the PANI. Thus, Liu *et al*.[215] sorbed anilinium between V_2O_5 lamellae, forming $(C_6H_5NH_3)_{0.4}$ $V_2O_5 \cdot 0.40H_2O$ complex, which subsequently was polymerized into layered PANI/V_2O_5 (by oxidation).

Due to their lamellar structure the mineral or synthetic transition metal di-chalcogenides have been used as lubricants. However, they also might be intercalated by organic molecules into the inter-lamellar galleries, what might significantly alternate the properties. For example, changing the electrochemical potential may force organic intercalate to lay flat, parallel to the di-chalcogenide layers, or alternatively to form single or double layers of perpendicularly oriented molecules. The diversity of di-chalcogenides, intercalants, and generated structures leads to great number of systems currently explored for electrical, magnetic or photo-optic applications.

Within the category of di-chalcogenides MoS_2 has a special position. Its interlayer spacing is small, $d_{001} = 0.615$ nm, but treated with *n*-butyl lithium in hexane results in formation of a complex: $Li_{1.15}MoS_2$.[216] The complex dispersed in aqueous solution of PEG could be exfoliated.[217,218] In the purified dry product the PEG concentration ranged from 21 to 31 wt%, and the interlayer spacing of MoS_2/PEG complex was $d_{001} = 1.45$ nm, corresponding to the polymeric double-layer within the galleries. TGA tests indicated thermal stability up to 255°C. Intercalation with PEG increases electrical conductivity of MoS_2 by four to five orders of magnitude.[219] Unfortunately, the system was not stable, as starting at 90°C MoS_2 catalyzed degradation of PEG that led to loss of conductivity. The degradation depends on composition and PEG molecular weight.[220] In a recent publication, PEG was replaced by poly(acrylonitrile) (PAN) obtaining a more stable $[Li_{0.6}MoS_2(PAN)_{1.2} \cdot 0.5H_2O]$ system, with mixed ionic-electronic conductor properties, which might be used for electrodes in lithium batteries.[221]

Significantly more interesting for PNC are zirconium phosphates (ZrP) and phosphonates. They are relatively inexpensive, thermally stable, and easy to synthesize into pre-intercalated lamellar structures with a desired aspect ratio. Furthermore, they might be prepared in a diverse crystallographic forms with suitable properties for different applications [e.g. $Zr(HPO_4)_2 \cdot 2H_2O$, or $Zr(HPO_4)_2 \cdot H_2O$ have layered form that can be intercalated].[222,223] Upon intercalation with ethylene oxide or PPG the interlayer spacing increases from $d_{001} = 0.76$ up to 1.7 nm. The authors

DOI: 10.1002/pat

suggested application of the complexes in catalysis or electrochemistry. For the former applications, the pillared, mesoporous crystalline pyrophosphate-phosphate, $M^{+4}(P_2O_7)_{1-z}(HPO_4)_{2z}$ (where M^{+4} is tetravalent metal, and $0.05 < z < 0.25$) was suggested.[224]

Exfoliated nanocomposites with α-ZrP (1–8 wt%; platelet diameter *ca*. 100–200 nm) have been obtained for PE, PCL, and PS.[225] The ZrP was pre-intercalated with benzyl amine, propyl amine or 1-amino 5-pentanol. Depending on the type of matrix polymer, different method of PNC preparation was used. Thus, the lyophilized α-ZrP was melt blended with PE; a mixture of lyophilized nanofiller and PCL solution was cast, while the PS solution was mixed with gel of exfoliated α-ZrP in di-methyl formamide or tetrahydrofuran, and then cast. In all cases the XRD and TEM analyses showed full exfoliation of ZrP. Incorporation of α-ZrP significantly changed the polymer thermal behavior in air, with the most significant degradation delay (in comparison to neat polymer) by 50°C for PCL and PS, and 80°C for PE.

Lamellar ZrP ($d_{001} = 1.50$–2.21 nm) was used in polymer electrolyte membranes for fuel cells. The matrix could be sulfonated-poly(ether-ketone) (PEK) or poly(ether-ether-ketone) (PEEK), perfluorosulfonic acid ionomer (Nafion), etc.[226,227] Furthermore, lamellar $Zr(O_3POH)_2$ also have been dispersed in polyacrylamide (PAAm), EP, PS, or poly(vinylidene fluoride) (PVDF), for applications in bio-catalysis, photochemistry, molecular and chiral recognition, as well as in fuel cell technologies.[228]

The diversity of structures and potential application increased by preparation of new one-dimensional zirconium phosphate fluorides, namely $Zr[(NH_4)_2PO_4]_2F_2 \cdot nH_2O$ ($n = 0.5$ or 1.0). These compounds could be converted into other crystallographic forms, such as lamellar α- and γ-zirconium phosphates.[229] Unfortunately, these are not thermally stable, loosing water at $T \geq 80$°C and eventually (at $T \approx 400$°C collapsing into cubic ZrP_2O_7. Preparation, properties, and application of M^{+4} phosphates and phosphonates have been reviewed by Alberti *et al*.[20,230]

Finally, examples of the preliminary, low scale, use of aluminophosphate (ALPO) layered materials for the preparation of PNC should be mentioned.[231] Thus, for example, DDA-ALPO-kanemite and DDA-ALPO-kanemite grafted with vinyl groups on the surface were dispersed in styrene and polymerization was carried either in bulk or in solution. Only the bulk-polymerized vinyl grafted nano-filler gave some evidence of interaction with the matrix polymer—the XRD and TEM showed intercalation. Similarly, Canepa *et al*. melt blended PP with *n*-butyl amine-ALPO-kanemite, partially ion-exchanged with Fe^{3+}, VO^{2+} and Co^{2+}.[232] While non-exchanged ALPO-kanemite gave microcomposites, the metal-exchanged analogues formed intercalated and exfoliated PNC. TGA measurements in air showed an improved stabilization in the order: $Fe^{3+} > VO^{2+} > Co^{2+}$.

SUMMARY AND RECOMMENDATIONS

The synthetic layered nano particles reviewed in this article might be divided into phyllosilicates (clays), and non-silicate layered materials, reserving the term ''clay'' for layered silicates. The main advantage of synthetic clays is their professed chemical purity (e.g. absence of amorphous and gritty contaminants, as well as arsenic, iron and other heavy metals) hence their lethal dose that causes the death of 50% of test animals, $LD_{50} = 31.4$ g/kg. Evidently, for the semi-synthetic clays the purity hinges on the refinement of natural precursors, e.g. talc or brucite. If heavy metal contaminants are present in these precursors, they will remain in the final product (unless a costly post-synthesis treatment is employed).

The synthetic layered nanoparticles are white to transparent that assures production of brightly (and reproducibly) colored articles. Their, aspect ratio varies from *ca*. 20 to 6000. It is noteworthy that as the aspect ratio increases so do the problems associated with exfoliation, thus a balance must be found between the required performances and processability. Processing may also cause attrition that degrades the aspect ratio and performance.

To the category of synthetic clays belong such layered silicates as HT, MC, MMT, MAG, saponite, and their fluorinated and ''templated'' varieties. The three main methods for their synthesis are:

1 Semi-synthetic, as here the main ingredient is a natural mineral, namely talc, brucite or obsidian. Its crystalline structure is suitably modified by substitution of Mg^{2+} by, e.g. Na^+, or by Al^{3+}. The chemical interaction with the matrix polymer can be modified by a partial substitution of –F for –OH, namely reacting talc with sodium fluoro silicate. This method has been used for the most popular in polymer technology synthetic fluoro micas; the Somasif clays. Here, the aspect ratio of clay platelets depends on that of talc; $p < 6000$ has been cited. As the TEM micrograph in Fig. 2 illustrates, two types of crystals (lamellar and fibrous) have been found in the supplied material.
2 Fully synthetic, where the formation of layered silicate starts with a variety of salts or metal oxides that provide suitable composition for crystallization of layered silicates (e.g. Lucentite). There is a great variety of methods that belong to this category, including low-temperature solution method, high temperature synthesis in the molten state, sol-gel process, etc. In addition to clays that can be prepared on this route, here also belongs synthetic MAG, LDHs and phosphates, etc.

   The synthetic clays have roughly a circular symmetry and $p = 10$ to 50. Similar aspect ratios are found in commercial LDHs. Their main application is the control of rheology (thixotropy) in aqueous systems in the food, cosmetics, pharmaceuticals, and paint industries. Exception is melt-synthesized by TOPY tetrasilicic mica with $p = 1000$ to 5000. When used in polymeric systems they often exfoliate at up to 5 wt% clay loading, and disproportionately increase the modulus, namely by a factor of 3.1 at 2.5 wt%. Rarely pre-intercalated grades of these clays are offered. The manufacturers are: COOP (now CBC), Laporte, Süd Chemie, Kunimine, TOPY, FCC Inc., etc.
3 Templated synthetic, based on organic templates (including polymers), which after synthesis may be pyrolyzed, or left in as intercalants (e.g. prepared by Carrado, Chastek or Boccaleri—not commercial yet). Templating offers better control of interactions between the synthetic organoclay and polymeric matrix.

DOI: 10.1002/pat

The synthetic clay industry is oriented mainly toward large volume markets: foodstuffs, pharmaceuticals, cosmetics, toothpastes, etc. The use of these materials in polymers is limited—except for Unitika's use of Somasif in commercial PNC, all other synthetic clays are employed in laboratory-produced PNCs. As the cited reports indicate, COOP/CBC has been the most successful supplier of clays for PNCs—both Somasif (semi-synthetic), and Lucentite (fully synthetic) are offered, intercalated or not. Other choices are the high aspect ratio, fully synthetic TOPY, intercalated for the use in PP, or Sumecton from Kunimine, which in spite of its small $p = 50$, gave surprisingly large enhancement of stiffness. The information assembled here shows that synthetic clays offer better performance than the natural ones, but the advantages are relatively small and ''non uniform'', i.e. dependent on the system, the method of PNC preparation and its processing.

For example, as far as the potential application of synthetic clays for fire retardancy are concerned, the enhancement is similar or better (e.g. saponite) to that found for nanocomposites prepared with natural clays. However, the controlled composition of these materials can afford the possibility to tune the desired parameters (i.e. surface acidity, redox catalytic sites, the crystallite aspect ratio, etc.) that dictate the thermal properties of PNCs. Flammability of LDH-containing PNC requires high level of dispersion (exfoliation). So far MAG has shown a neutral behavior in the flammability tests, but tuning its composition for better crust formation is within reach.

In the category of non-silicate layered materials three types were discussed: the LDHs, di-chalcogenides and lamellar zirconium phosphates. LDH are being produced on a large commercial scale, whereas the others remain laboratory materials.

Parallel with the development of synthetic clay technology there has been rapid progress in the method of synthesis and enhancement of performance of the LDH. Its main application has been in catalysis. In the plastics industry this material has been used as a traditional flame retardant and stabilizer. There is a wide variety of LDH types, dependent on composition and the preparation method. However, the platelets are thin (0.48 nm) and fragile, LDH has been produced with low aspect ratio ($p < 80$), and used at high loading ($\leq 60\%$). During the last few years the LDH/polymer technology changed in the direction of the clay/polymer type, e.g. the layered material with aspect ratio of ca. 500 has been produced. The principal advantage of LDH over clay is its cationic character. Its compatibilization by anionic modifiers is more straightforward than that by cationic type. Templating LDH also adds tailoring capability to the technology. Thus, fully exfoliated PNCs with LDH have been reported even with a PO matrix. There are still problems with this technology, for example, decomposition of intercalants at low temperature, the low dehydroxylation temperature that affects the crystalline structure, and platelet fragility that make processability of the PNC more difficult. However, considering the great number of possible compositions (as well as the crystalline forms) LDHs might seriously challenge clay dominance in PNC technology of the future.

The di-chalcogenides and zirconium phosphates have been designated as the nano-fillers for functional polymeric systems. For example, their use as electrically conductive materials, as catalysts or support for catalysts, in photochemistry, for molecular and chiral recognition, or in fuel cell technologies has been described. However, the lamellar zirconium phosphates have good potential for the use as fully synthetic, reinforcing nano-fillers—they are inexpensive, easy to synthesize in pre-intercalated form (''one pot'' method), large aspect ratios are achievable, and their modulus and decomposition temperature are high.

Acknowledgments

The authors wish to express their thanks to Dr. Alexander B. Morgan from the University of Dayton and to Dr Alberto Frache from the Politecnicodi Torino-Italy for useful discussions, as well as Ms Weawkamol Leelapornpisit from the NRCC/IMI for the TEM and SEM observations.

APPENDIX

Abbreviations

2DS	4,4′-di-amino diphenyl sulfone
^{13}C CP-MAS NMR	^{13}C solid state CP-MAS spectroscopy
^{31}P MAS NMR	^{31}P variable temperature MAS spectroscopy
AB	amino benzoate
ABSu	amino-benzene sulfonate
ADA	ω-amino dodecyl (or lauric) acid
AEC	anion exchange capacity (meq/g)
AIBN	*N,N*′-azo-bis-isobutyronitrile
AL	amino laureate
ALPO	layered aluminophosphate
BT	bentonite
CB	carbon black
CEC	cation exchange capacity (meq/g)
CL	caprolactone
CNT	carbon nanotubes
CP	cross-polarization (in NMR)
Cs	chemical shift (in NMR)
CTE	coefficient of thermal expansion
DAAM	di-acetone acrylamide
DBS	4-dodecyl benzene sulfonate = C_{12} H_{25}-C_6H_4-SO_3
DGEBA	diglycidyl ether of bisphenol-A
DIP	dimethyl isophthalate substituted with the tri-phenyl-phosphonium
DMAC	dimethyl acetamide
DTG	differential thermogravimetric analysis
EFM	extensional flow mixer
ESEEM	electron spin echo envelope modulation
ESR	electron spin resonance
FH	fluoro hectorite
FM	fluoro mica
FT-IR	Fourier transform infrared spectroscopy
HDT	heat deflection temperature (under load of 18.6 kg/cm)
HDTMOS	hexadecyl trimethoxy silane
HT	hectorite
LD_{50}	lethal dose that causes the death of half of test animals.

DOI: 10.1002/pat

LDH	layered double hydroxide
LMAS	lamellar mesostructured aluminosilicate
LMS	lamellar mesostructured silicate
LOI	limited oxygen index
MAG	magadiite (silicic acid)
MA	maleic anhydride
MAS	magic angle spinning (NMR)
MB	master batch
MC	mica
$Mg_xAl\text{-}CO_3$	carboxylic acid salt of LDH, with molar ratio Mg:Al = x
MHMA	methyl α-hydroxy methyl acrylate
MLR	mass-loss rate
MMT	montmorillonite
MSDS	material safety data sheets
MW	molecular weight
Na-DDS	sodium dodecyl sulfate
Na-FH	sodium-FH
Na-MMT	sodium-MMT
NIRT	notched Izod impact strength at room temperature
NMR	nuclear magnetic resonance
OIT	oxidation induction time
OS	octyl-sulfate
phr	concentration in ''parts per hundred weight parts of resin''
PHRR	peak heat release rate (in cone calorimetry)
PNC	polymeric nanocomposite
POSS	polyhedral oligomeric silsesquioxanes
PTES	phenyl-tri-ethoxy silane
SDBS	sodium dodecyl-benzene sulfonate
SDS	sodium dodecyl sulfate
SEM	scanning electron microscopy
SEPAP 12-24	apparatus for photodegradation studies (Service d'Etude du Photovieillissement Accelere des Polymeres)
SSE	single screw extruder
TEM	transmission electron microscopy
TEOS	tetraethyl orthosilicate
TGA	thermogravimetric analysis
TGDDM	tetra-glycidyl 4,4′-di-amino-diphenyl methane
TSE	twin-screw extruder
TSPP	tetra-sodium pyrophosphate
US	ultrasonics
UV	ultraviolet
VBS	vinyl benzene sulfonate sodium salt
XRD	X-ray diffraction
ZrP	zirconium phosphate

Abbreviations for intercalants

2M2DDA	di-methyl di-dodecyl ammonium chloride
2M2HTA	di-methyl di-(hydrogenated tallow) ammonium chloride
2M2ODA	di-methyl di-octadecyl ammonium chloride
2M2TA	di-methyl di-tallow ammonium chloride
2M2TDA	di-methyl di-tetradecyl ammonium chloride
2MBHTA	di-methyl -benzyl-hexadecyl ammonium chloride
2MBODA	di-methyl-benzyl-octadecyl ammonium chloride
2MHDI	1,2-di-methyl-3-*n*-hexadecyl imidazolium bromide
2MHDODA	di-methyl -hexadecyl-octadecyl ammonium chloride
2MVBHDA	di-methyl-(*p*-vinyl benzyl)hexadecyl ammonium chloride (VB-16)
2ODA	di-octadecyl ammonium chloride
3BHDP	tri-butyl-hexadecyl phosphonium bromide
3MDDA	tri-methyl dodecyl ammonium bromide
3MHDA	tri-methyl hexadecyl ammonium bromide
3MODA	tri-methyl octadecyl ammonium chloride
3ODA	tri-octadecyl ammonium chloride
3PHDP	tri-phenyl *n*-hexadecyl phosphonium
4EA	tetraethyl ammonium
4ODA	tetra-octadecyl ammonium chloride
ADA	ω-amino-dodecanoic acid
ATPS	amine-terminated PS
DBS	4-dodecyl benzene sulfonate [$C_{12}H_{25}\text{-}C_6H_4\text{-}SO_3$]
DDA	dodecyl ammonium chloride
DDS	dodecyl sulfate
HDA	hexadecyl ammonium chloride
HEODI	hydroxy-ethyl-di-hydro-imidazolinium chloride
M2EPG	methyl di-ethyl polypropylene glycol ammonium chloride
M3OA	methyl tri-octyl ammonium chloride ammonium chloride
MC2EG	methyl coco di-polyethylene glycol ammonium chloride
MDD2EG	methyl dodecyl di-polyethylene glycol ammonium chloride
MHT2EtOH	methyl hydrogenated tallow di-hydroxy ethyl ammonium chloride
MT2EtOHA	methyl tallow di-hydroxy ethyl ammonium chloride
ODA	octadecyl ammonium chloride
PEA	2-phenylethyl ammonium chloride
PEM FC	polymer electrolyte membranes for fuel cells
RDI	ricinyl di-hydro-imidazolinium chloride
SDBS	sodium dodecyl-benzene sulfonate
TDA	tetra-decyl ammonium chloride
TGDDM	tetra-glycidyl 4,4′-di-amino-di-phenyl methane
W75	1-methyl-2-norstearyl-3-stearinoacid-amid-oethyl-di-hydro-imidazolinium methyl-sulfate

Abbreviations for polymers

ABS	acrylonitrile-butadiene-styrene
CHR	elastomeric copolymer from epichlorohydrin and ethylene oxide
CPE	chlorinated polyethylene
CR	chloroprene
CSM	chlorosulfonated polyethylene

DOI: 10.1002/pat

EP	epoxy
EPR	electron paramagnetic resonance
EVAc-X	poly(ethylene-co-vinyl acetate) with *X* wt% vinyl acelate
HDPE-g-MA	maleated high density PE
LDPE-g-MA	maleated low density PE
LLDPE-g-MA	maleated linear low density PE
PA-12	polyamide-12
PA-6	poly-ε-caprolactam
PAA	poly(acrylic acid)
PAAm	polyacrylamide
PAC	polyacrylate
PANI	polyaniline
PBT	poly(butylene terephthalate)
PC	bisphenol-A polycarbonate
PEEK	poly(ether-ether-ketone)
PE	polyethylene
PE-*g*-MA	maleated PE (grafted with maleic anhydride)
PEG	polyethylene glycol
PEK	poly(ether-ketone)
PEST	thermoplastic polyesters, e.g. PBT, PET, also TPES
PET	poly(ethylene terephthalate)
PI	polyimide
PLA	polylactic acid
PMAA	polymethylacrylic acid
PMMA	polymethyl methacrylate
PNIPA	poly-(*N*-isopropylacrylamide)
PO	polyolefin
POE-g-MA	poly(octene-co-ethylene) grafted with maleic anhydride (a compatibilizer)
PP	poly(propylene) (isotactic)
PPEG	six-arm star poly(propylene glycol-b-ethylene glycol)
PP-g-MA	maleated PP (grafted with maleic anhydride)
PPG	poly- or oligo-propylene glycol
PS	polystyrene
PSS	*p*-sulfonated PS
PU	polyurethane
PVAl	poly(inyl alcohol)
PVC	poly(vinyl chloride)
PVDF	poly(vinylidene fluoride)
PVS	poly(vinyl sulfonate)
SAN	styrene-co-acrylonitrile (acrylonitrite content ranging from about 5 to 40 wt%)
*s*PP	syndiotactic poly(propylene)
TPU	thermoplastic polyurethane

Symbols

$[\eta]$	intrinsic viscosity, a measure of the hydrodynamic volume
A_{sp}	specific surface area (m^2/g)
c_{cr}	critical clay concentration
d_{001}	clay interlayer spacing (nm)
d_3	LDH interlayer spacing
E	tensile (Young's) modulus
E_f	flexural modulus
$E_R = E_c/E_m$	relative tensile modulus
K_{1c}	fracture toughness of the neat resin
L_a	clay platelet size (nm)
M_n, M_w	number- and weight-average molecular weight
$p = d/t$	aspect ratio (d is platelet diameter, and t is its thickness).
T	temperature
T_c	crystallization temperature
T_d	thermal degradation temperature
T_g	glass transition temperature
T_m	melting point
T_{max}	peak temperature in flammability tests
$\Delta T_d = T_d - T_{d(matrix)}$	change of the degradation temperature due to clay presence
Δt_{max}	delay time to reach the peak temperature in flammability tests
ε_b	elongation (or strain) at break
ϕ_m	maximum packing volume fraction of hard spheres
η_r	relative viscosity
σ	tensile strength
σ_f	flexural strength

REFERENCES

1. Utracki LA. *Clay-containing Polymeric Nanocomposites*, vol. 1 & 2. RAPRA: Shawbury, 2004.
2. Itoh T, Ohta N, Shichi T, Yui T, Takagi K. The self-assembling properties of stearate ions in hydrotalcite clay composites. *Langmuir* 2003; **19**: 9120–9126.
3. Greenwell HC, Jones W, Coveney PV, Stackhouse S. On the application of computer simulation techniques to anionic and cationic clays: A materials chemistry perspective. *J. Mater. Chem.* 2006; **16**: 708–723.
4. Usuki A, Koiwai A, Kojima Y, Kawasumi M, Okada A, Kurauchi YT, Kamigaito O. Interaction of nylon 6-clay surface and mechanical properties of nylon 6-clay hybrid. *, J. Appl. Polym. Sci.* 1995; **55**: 119–123.
5. Spiess HW. Advanced solid-state nuclear magnetic resonance for polymer science. *J. Polym. Sci. Part A: Polym. Chem.* 2004; **42**: 5031–5044.
6. Schmidt-Rohr K, Spiess HW. *Multidimensional Solid-State NMR and Polymers*. Academic Press: London, 1994.
7. Kwiatkowski J, Whittaker AK. Molecular motion in nanocomposites of poly(ethylene oxide) and montmorillonite. *J. Polym. Sci. Part B: Polym. Phys.* 2001; **39**: 1678–1685.
8. VanderHart DL, Asano A, Gilman JW. Solid-state NMR investigation of paramagnetic nylon-6 clay nanocomposites. *Chem. Mater.* 2001; **13**: 3781–3796.
9. Schmidt C, Wefing S, Blümich B, Spiess HW. Dynamics of molecular reorientations: Direct determination of rotational angles from two-dimensional NMR of powders. *Chem. Phys. Lett.* 1986; **130**: 84–90.
10. Potrzebowski MJ. What high-resolution solid-state NMR spectroscopy can offer to organic chemists. *Eur. J. Org. Chem.* 2003; 1367–1376.
11. Sozzani P, Bracco S, Comotti A, Simonutti R, Camurati I. Stoichiometric compounds of magnesium dichloride with ethanol for the supported Ziegler-Natta catalysis: First recognition and multidimensional MAS NMR study. *J. Am. Chem. Soc.* 2003; **125**: 12881–12893.
12. Sozzani P, Bracco S, Comotti A, Mauri M, Simonutti R, Valsesia P. Nanoporosity of an organo-clay shown by hyperpolarized xenon and 2D NMR spectroscopy. *Chem. Commun.* 2006; 1921–1923.

DOI: 10.1002/pat

13. Comotti A, Bracco S, Valsesia P. Adsorption properties of nanoporous organoclay and NMR characterization. AIZ Workshop, Alessandria, Italy 1–2 September 2006.
14. Barrer RM, Dicks LWR. Chemistry of soil minerals: Part IV. Synthetic alkyl-ammonium montmorillonites and hectorites. *J. Chem. Soc. A* 1967; 1523–1529.
15. Kloprogge JT. Synthesis of smectites and porous pillared clay catalysts: A review. *J. Porous Mater.* 1998; **5**: 5–41.
16. Kloprogge JT, Komarneni S, Amonette JE. Synthesis of smectite clay minerals: A critical review. *Clays Clay Miner.* 1999; **47**: 529–554.
17. Carrado KA. Synthetic organo- and polymer-clays: Preparation, characterization and materials applications. *Appl. Clay Sci.* 2000; **17**: 1–23.
18. Carrado KA, Petit S, Bergaya F, Lagaly G.Synthetic clay minerals and purification of natural clays. In *Handbook of Clay Science*, Bergaya F, Theng BKG, Lagaly G (eds). Elsevier: Amsterdam, 2006.
19. Duan X, Evans DG (eds). *Layered Double Hydroxides*. Springer Verlag: Berlin, 2006.
20. Alberti G, Casciola M, Costantino U, Vivani R. Layered and pillared metal IV phosphates and phosphonates. *Adv. Mater.* 2004; **84**: 291–303.
21. Orlemann JK. Process for producing synthetic hectorite-type clays. US Patent 3,666,407, 1972.
22. Tateyama H, Tsunematsu K, Kimura K, Hirosue H, Jinnai K, Furusawa T. Method for producing fluorine mica. US patent 5,204,078, 1993.
23. Hénin S. Synthesis of clay minerals at low temperatures. *Intl. Acad. Sci.—Natl. Res. Council* 1956; **456**: 54–60.
24. Caillére S, Hénin S, Esquevin J. Synthèse des minéraux argileux. *Bull. Groupe Franc. Argiles* 1957; **94**: 67–76.
25. Neumann BS. Synthetic hectorite-type clay minerals. US Patent 3,586,478, 1971; US Patent 3,671,190, 1972.
26. Jaffe J. Hydrothermal method for manufacturing a novel catalytic material, catalysis containing said material, and process using said material. US Patent 3,803,026, 1974.
27. Carrado KA, Xu LQ, Csencsits R, Muntean JV. Use of organo- and alkoxy silanes in the synthesis of grafted and pristine clays. *Chem. Mater.* 2001; **13**: 3766–3773.
28. Reinholdt M, Miehé-Brendlé J, Delmotte L, Le Dred R, Tuilier MH. Synthesis and characterization of montmorillonite-type phyllosilicates in a fluoride medium. *Clay Minerals* 2005; **40**: 177–190.
29. Jaber M, Miehé-Brendlé J. Formation mechanism of 2:1 phyllosilicates. *Compte Rendu de Chimie* 2005; **8**(2): 229–234.
30. Jaber M, Miehé-Brendlé J, Delmotte L, Le Dred R. New reange of Al-Mg organoclays with tailored hydrophobicity: Incorporation of fluoride as local probe to study the octahedral character. *Microporous Mesoporous Mater.* 2003; **66**(1): 155–163; Jaber M, Miehe-Brendle J, Delmotte L, Le Dred R. Formation of organoclays by one-step synthesis. *Solid State Sci.* 2005; **7**(5): 610–615.
31. Daimon N, Izawa T. Sol of ultra-fine particles of synthetic hectorite. US Patent 3,936,383, 1976.
32. Zhao Y, Li F, Zhang R, Evans DG, Duan X. Preparation of layered double-hydroxide nanomaterials with a uniform crystallite size using a new method involving separate nucleation and aging steps. *Chem. Mater.* 2002; **14**: 4286–4291.
33. Paredes SP, Fetter G, Bosch P, Bulbulian S. Sol-gel synthesis of hydrotalcite—like compounds. *J. Mater. Sci.* 2006; **41**: 3377–3382.
34. Carrado KA, Csencsits R, Thiyagarajan P, Seifert S, Macha SM, Harwood JS. Crystallization and textural porosity of synthetic clay minerals. *J. Mat. Chem.* 2002; **12**: 3228–3237.
35. Yano K, Usuki A, Okada A, Kurauchi T, Kamigaito O. Synthesis and properties of polyimide–clay hybrid. *J. Polym. Sci., Part A: Polym. Chem.* 1993; **31**: 2493–2498.
36. Liu ZP, Ma R, Osada M, Iyi N, Ebina Y, Takada K, Sasaki T. Synthesis, anion exchange and delamination of Co-Al layered double hydroxide. *JACS* 2006; **128**: 4872–4880.
37. Zilg C, Thomann R, Mülhaupt R, Finter J. Polyurethane nanocomposites containing laminated anisotropic nanoparticles derived from organophilic layered silicates. *Adv. Mat.* 1999; **11**: 49–52.
38. Pavlikova S, Thomann R, Reichert P, Mülhaupt R, Marcincin A, Borsig E. Fiber spinning from polypropylene-organoclay nanocomposite. *J. Appl. Polym. Sci.* 2003; **89**: 604–611.
39. Kaviratna PD, Pinnavaia TJ, Schroeder PA. Dielectric properties of smectite clays. *J. Phys. Chem. Solids* 1996; **57**: 1897–1906.
40. Taylor RS, Mobbs DB, Buck MJ, Shaw DB, Jenness P. Synthetic clays. Patent WO9206783, 1992.
41. Takagi S, Shimada T, Eguchi M, Yui T, Yoshida H, Tryk DA, Inoue H. High-density adsorption of cationic porphyrins on clay layer surfaces without aggregation: The size-matching effect. *Langmuir* 2002; **18**: 2265–2272.
42. Breu J, Seidl W, Stoll AJ, Lange KG, Probst TU. Charge homogeneity in synthetic fluorohectorite. *Chem. Mater.* 2001; **13**: 4213–4220.
43. Breu J, Seidl W, Stoll A. Disorder in smectites in dependence of the interlayer cation. *Z. Anorg. Allg. Chem.* 2003; **629**: 503–515.
44. Iyi N, Kaneko Y, Fujita T, Nagamani SA, Yelamaggad CV. Thermal behavior of a cationic mesogens intercalated into clay interlayer. *Mol. Cryst. Liq. Cryst.* 2004; **414**: 49–61.
45. Miyake M, Suzuki T, Suzuki T. Cation-exchange selectivity for K^+, Mg^{2+}, and Ca^{2+} ions on sodium-substitutes taeniolite. *Chem. Mater.* 1993; **5**: 1327–1331.
46. DiMasi E, Fossum JO, Gog T, Venkataraman C. Orientation order in gravity dispersed clay colloids. *Phys. Rev.* 2001; **64**: 061704-1–061704-7.
47. da Silva GJ, Fossum JO, DiMasi E, Måløy KJ, Lutnæs SB. Synchrotron X-ray scattering studies of water intercalation in layered synthetic silicate. *Phys. Rev.* 2002; **66**: 011303-1–011303-8.
48. da Silva GJ, Fossum JO, DiMasi E, Måløy KJ. Hydration transition in a nanolayer synthetic silicate. *Phys. Rev.* 2003; **67**: 094114-1–094114-6.
49. Knudsen KD, Fossum JO, Helgesen G, Bergaplass V. Pore characteristics and water absorption in synthetic smectite clay. *J. Appl. Crystallography* 2003; **36**: 587–591.
50. Beall GH, Grossman DG, Hoda SN, Kubinski KR. Inorganic gels and ceramic papers, films, fibers, boards, and coating made there from. US Patent 4,339,540, 1982.
51. Beall GH. Personal communication, 2003.05.08 8 May 2003.
52. Granquist WT, Pollack SS. A study of the synthesis of hectorite. *Proc. Natl. Conf. Clays Clay Minerals* 1960; **8**: 150–169.
53. Stridde GE. Process for alkylating aromatic hydrocarbons with synthetic hectorite-type clay catalyst. US Patent 4,046,826, 1977; US Patent 3,965,043, 1976.
54. Granquist WT. Synthetic silicate minerals. US Patent 3,252,757, 1966.
55. Wright AC, Granquist WT.Kennedy J. Catalysis by layer lattice silicates I. The structural and thermal modification of a synthetic ammonium di-octahedral clay. *J. Catalysis* 1972; **25**: 65–80.
56. van Olphen H, Fripiat JJ (eds). *Data Handbook for Clay Minerals and Other Non-metallic Minerals*. Pergamon Press: Elmsford, NY, 1979.
57. The Source Clays Repository website. http://cms.lanl.gov
58. Garza NB. Personal communication, 2005.01.28. 28 January 2005. Available at Norberto.Garza@Halliburton.com
59. Eugster HP. Hydrous sodium silicates from lake Magadi, Kenya: Precursors of bedded chert. *Science* 1967; **157**: 1177–1180.
60. Fudala A, Konya Z, Kiyozumi Y, Niwa SI, Toba M, Mizukami F, Lentz PB, Nagy J, Kiricsi I. Preparation, characterization and application of the magadiite based mesoporous composite material of catalytic interest. *Microporous Mesoporous Mater.* 2000; **35–36**: 631–641.
61. Lagaly G, Beneke K, Weiss A. Magadiite and H-magadiite: I. Sodium magadiite and some of its derivatives. *Am. Miner.* 1975; **60**: 642–650.
62. Lagaly G, Beneke K, Weiss A. Magadiite and H-magadiite: II. H-magadiite and its intercalation compounds. *Am. Miner.* 1975; **60**: 642–650.
63. Brenn U, Ernst H, Freude D, Herrmann R, Jahnig R, Karge HG, Karger J, Konig T, Madler B, Pingel UT, Prochnow D, Schwieger W. Synthesis and characterization of the layered sodium silicate ilerite. *Microporous Mesoporous Mater.* 2000; **40**(1–3): 43–52.
64. Wang YR, Wang SF, Chang LC. Hydrothermal synthesis of magadiite. *Appl. Clay Sci.* 2006; **33**(1): 73–77.

DOI: 10.1002/pat

65. Binette MJ, Detellier C. Lamellar polysilicate nanocomposite materials: Intercalation of polyethylene glycols into protonated magadiite. *Can. J. Chem.* 2002; **80**: 1708–1714.
66. Kwon OY, Park KW. Synthesis of layered silicates from sodium silicate solution. *Bull. Korean Chem. Soc.* 2004; **251**: 25–26.
67. Scholzen G, Beneke K, Lagaly G. Diversity of magadiite. *Z. Anorg. Allg. Chem.* 1991; **597**: 183–196.
68. Iwasaki T, Kuroda T, Ichio S, Satoh M, Fujita T. Seeding effect on crystal growth in hydrothermal synthesis of layered octosilicate. *Chem. Eng. Commun.* 2006; **193**(1): 69–76.
69. Feng FX, Balkus KJ. Synthesis of kenyaite, magadiite and octosilicate using poly(ethylene glycol) as a template. *J. Porous Mater.* 2003; **10**(1): 5–15.
70. Pastore HO, Munsignatti M, Mascarenhas AJS. One-step synthesis of alkyltrimethylammonium-intercalated magadiite. *Clays Clay Miner.* 2000; **48**(2): 224–229.
71. Crone IA, Franklin KR, Graham PA. New route for the preparation of hydrated alkali-metal silicates. *J. Mater. Chem.* 1995; **5**(11): 2007–2011.
72. Beneke K, Thiesen P, Lagaly G. Synthesis and properties of the sodium-lithium silicate silinaite. *Inorg. Chem.* 1995; **34**(4): 900–907.
73. Fukushima Y, Tani M. An organic/inorganic hybrid layered polymer: Methacrylate-magnesium(nickel) phyllosilicate. *J. Chem. Soc., Chem. Commun.* 1995: 241–242.
74. Mann S, Burkett SL, Davis SA, Fowler CE, Mendelson NH, Sims SD, Walsh D, Whilton NT. Sol-gel synthesis of organized matter. *Chem. Mater.* 1997; **9**: 2300–2310.
75. Silva CR, Fonseca MG, Barone JS, Airoldi C. Layered inorganic-organic talc-like nanocomposites. *Chem. Mater.* 2002; **14**: 175–179; Silva CR, Airoldi C. Brazilian patent application PI 9903110-8, 1999.
76. Schwieger W, Pohl K, Brenn U, Fyfe CA, Grondey H, Fu G, Kokotailo GT. Isomorphous substitution of silicon by boron or aluminum in layered silicates. *Catal. Microporous Mater. Stud. Surf. Sci. Catal.* 1995; **94**: 47–54.
77. Macedo TR, Airoldi C. Structural features of interlamellar functionalized octosilicate, poster communication, AIZ workshop 2006 ''Innovative Applications of Layered Material: From Catalysis to Nanotechnology'', Alessandria, 31 August–2 September 2006; 155-156.
78. Ogawa M, Miyoshi M, Kuroda K. Perfluoroalkylsilylation of the interlayer silanol groups of a layered silicate, magadiite. *Chem. Mater.* 1998; **10**(12): 3787.
79. Okutomo S, Kuroda K, Ogawa M. Preparation and characterization of silylated-magadiites. *Appl. Clay Sci.* 1999; **15**(1–2): 253–264.
80. Fujita I, Kuroda K, Ogawa M. Synthesis of interlamellar silylated derivatives of magadiite and the adsorption behavior for aliphatic alcohols. *Chem. Mater.* 2003; **15**(16): 3134–3141.
81. Ogawa M, Okutomo S, Kuroda K. Control of interlayer microstructures of a layered silicate by surface modification with organochlorosilanes. *J. Am. Chem. Soc.* 1998; **120**(29): 7361–7362.
82. Garces JM, Lakso SR. Synthetic platy magadiite and octasilicate. US patent 7,063,825, 2006.
83. Chastek TT, Que EL, Shore JS, Lowy RJ III, Macosko C, Stein A. Hexadecyl-functionalized lamellar mesostructured silicates and aluminosilicates designed for polymer–clay nanocomposites. Part I. Clay synthesis and structure. *Polymer* 2005; **46**: 4421–4430.
84. Cheng SF, Tzeng JN, Hsu BY. Synthesis and characterization of a novel layered aluminophosphate of kanemite-like structure. *Chem. Mater.* 1997; **9**(8): 1788–1796.
85. Luna-Xavier JL, Guyot A, Bourgeat-Lami E. Preparation of nano-sized silica/PMMA composite latexes by heterocoagulation. *Polym. Int.* 2004; **53**: 609–617.
86. Clearfield A, Duax WL, Medina AS, Smith GD, Thomas JR. On the mechanism of ion exchange in crystalline Zirconium phosphates. Part 1. *J. Phys. Chem.* 1969; **73**: 3424–3430; Part 6, *Ion Exchange Membranes.* 1972; **1**: 91–107.
87. Costantino U, Nocchetti N, Marmottini F, Vivani R. Amino acid derivatives of layered zirconium phosphates-s-α-zirconium L-+-serinephosphate and zirconium L-+-serinephosphate phosphates. *Eur. J. Inorg. Chem.* 1998; **10**: 1447–1452.
88. Özdilek C, Kazimierczak K, van der Beek D, Piken SJ. Preparation and properties of polyamide-6/boehemite nanocomposites. *Polymer* 2004; **45**: 5207–5214.
89. Zanetti M, Camino G, Mülhaupt R. Combustion behaviour of EVA/fluorohectorite nanocomposites. *Polym. Degrad. Stab.* 2001; **74**: 413–417.
90. Zanetti M, Camino G, Zilg C, Mülhaupt R. Thermal degradation and combustion behaviour of EVA/fluorohectorite nanocomposites. First MoDeSt Conference, Palermo, 3-7 September 2000.
91. Reichert P, Nitz H, Klinke S, Brandsch R, Thomann R, Mülhaupt R. Polypropylene/organoclay nanocomposite formation: Influence of compatibilizer functionality and organoclay modification. *Macromol. Mater. Eng.* 2000; **275**: 8–17.
92. Yasue K, Tamura T, Katahira S, Watanabe M. Reinforced polyamide resin composition and process for producing the same. US Patent 5,414,042, 1995.
93. Kim GM, Lee DH, Hoffmann B, Kressler J, Stöppelmann G. Influence of nanofillers on the deformation process in layered silicate/polyamide-12 nanocomposites. *Polymer* 2001; **42**: 1095–1100.
94. McNally T, Murphy WR, Lew CY, Turner RJ, Brennan GP. Polyamide-12 layered silicate nanocomposite by melt blending. *Polymer* 2003; **44**: 2761–2772.
95. Inoue H, Tamura K, Ebata T, Noguchi M. Highly-rigid, flame-resistant polyamide composite material. US Patent 6,294,599, 2002.
96. Lew CY, Murphy WR, McNally GM, Abe K, Yanai S, Brennan GP. Mechanism of clay exfoliation in a polymer matrix during extrusion process. *SPE-ANTEC* 2003; 1418–1423.
97. Vlasveld DPN, Bersee HEN, Picken SJ. Creep and physical aging behaviour of PA6 nanocomposites. *Polymer* 2005; **46**: 12539–12545; Vlasveld DPN, Groenewold J, Bersee HEN, Picken SJ. Moisture absorption in polyamide-6 silicate nanocomposites and its influence on the mechanical properties. *Polymer* 2005; **46**: 12567–12576.
98. Utracki LA (ed.). *Polymer Blends Handbook*. Kluwer Academic Publishers: Dordrecht, 2002; 1442.
99. Lai SM, Liao YC, Chen TW. Properties and preparation of compatibilized nylon 6 nanocomposites/abs blends using functionalized metallocene polyolefin elastomer. I. Impact properties. *J. Appl. Polym. Sci.* 2006; **100**: 1364–1371.
100. Li Y, Shimizu H. Effects of spacing between the exfoliated clay platelets on the crystallization behavior of polyamide-6 in polyamide-6/clay nanocomposites. *J. Polym. Sci. Part B: Polym. Phys.* 2006; **44**: 284–290.
101. Utracki LA, Sepehr M, Li J. Melt compounding of polymeric nanocomposites. *Inter. Polym. Process.* 2006; **21**: 3–16.
102. Sepehr M, Utracki LA. Unpublished 2006.
103. Kawasumi M, Hasegawa N, Kato M, Usuki A, Okada A. Preparation and mechanical properties of polypropylene-clay hybrids. *Macromolecules* 1997; **30**: 6333–6338.
104. Heinemann J, Reichert P, Thomann R, Mülhaupt R. Polyolefin nanocomposites formed by melt compounding and transition metal catalyzed homo- and copolymerization in the presence of layered silicates. *Macromol. Rapid Commun.* 1999; **20**: 423–430.
105. Reichert P, Hoffmann B, Bock T, Thomann R, Mülhaupt R, Friedrich C. Morphological stability of polypropylene nanocomposites. *Macromol. Rapid Commun.* 2001; **22**: 519–523.
106. Zanetti M, Camino G, Reichert P, Mülhaupt R. Thermal behaviour of polypropylene layered silicate nanocomposites. *Macromol. Rapid Commun.* 2001; **22**: 176–180.
107. Oya A, Kurokawa Y, Yasuda H. Factors controlling mechanical properties of clay mineral/polypropylene nanocomposites. *J. Mater. Sci.* 2000; **35**: 1045–1050.
108. Morgan AB, Harris JD. Effects of organoclay Soxhlet extraction on mechanical properties, flammability properties and organoclay dispersion of polypropylene nanocomposites. *Polymer* 2003; **44**: 2313–2320.
109. Gorrasi G, Tortora M, Vittoria V, Kaempfer D, Mülhaupt R. Transport properties of organic vapors in nanocomposites

DOI: 10.1002/pat

of organophilic layered silicate and syndiotactic polypropylene. *Polymer* 2003; **44**: 3679–3685.
110. Varghese S, Karger-Kocsis J, Pannikottu A. Rubber nanocomposites via solution and melt intercalation. *Rubber World* 2004; **230**: 32–38.
111. Varghese S, Karger-Kocsis J.Layered silicate/rubber nanocomposites via latex and solution intercalations. In *Polymer Composites from nano- to macro-scale*, Friedrich K, Fakirov S, Zhang Z (eds). Springer Verlag: New York, 2005.
112. Suzuki N, Oohara Y. Thermoplastic resin compositions containing clay composite and manufacturing thereof with excellent mechanical properties, heat resistance, and molding. Patent WO9743343, 1997.
113. Suzuki N, Oohara Y. Thermoplastic resin composition containing silane-treated foliated phyllosilicate, and method for producing the same. US Patent 6,239,195 B1, 2001.
114. Suzuki N. Thermoplastic polyester resin containing silane/clay composite. Patent WO9923162, 1999; Patent EP1026203, 2000.
115. Oohara Y, Suzuki N. Thermoplastic resin composition containing clay composite and process for preparing the same. Patent EP0899308, 1999; Patent WO9743343, 1997.
116. Suzuki N, Noma T, Kourogi M. Resin compositions and process for producing them. Patent WO2000022042, 2000.
117. Kourogi M, Noma T, Suzuki N. Resin compositions and process for producing the same. Patent WO0022042, 2000.
118. Imai Y, Satoshi N, Abe E, Tateyama H, Abiko A, Yamaguchi A, Aoyama T, Taguchi H. High-modulus polyethylene terephthalate/expandable fluorine mica nanocomposites with a novel reactive compatibilizer. *Chem. Mater.* 2002; **14**: 477–479.
119. Maiti P, Yamada K, Okamoto M, Ueda K, Okamoto K. Polylactide/layered silicate nanocomposites: Role of organoclays. *Chem. Mater.* 2002; **14**: 4654–4661.
120. Ray SS, Yamada K, Ogami A, Okamoto M, Ueda K. New polylactide/layered silicate nanocomposite: Nanoscale control over multiple properties. *Macromol. Rapid Commun.* 2002; **23**: 943–947.
121. Chang JH, An YU, Cho D, Giannelis EP. Polylactic acid nanocomposites: Comparison of their properties with montmorillonite and synthetic mica II. *Polymer* 2003; **44**: 3715–3720.
122. Kiersnowski A, Dąbrowski P, Budde H, Kressler J, Pigłowski J. Synthesis and structure of poly-ε-caprolactone/synthetic montmorillonite nano-intercalates. *Eur. Polym. J.* 2004; **40**: 2591–2598.
123. Hoffman B, Dietrich C, Thomann R, Friedrich C, Mülhaupt R. Morphology and rheology of polystyrene nanocomposites based upon organoclay. *Macromol. Rapid Commun.* 2000; **21**: 57–61.
124. Balazs AC, Singh C, Zhulina E, Lyatskaya Y. Modeling the phase behavior of polymer/clay nanocomposites. *Acc. Chem. Res.* 1999; **32**: 651–657.
125. Kuznetsov DV, Balazs AC. Scaling theory for end-functionalized polymers confined between two surfaces: Predictions for fabricating polymer/clay nanocomposites. *J. Chem. Phys.* 2000; **112**: 4365–4375.
126. Kim K, Utracki LA, Kamal MR. Numerical simulation of polymer nanocomposites using a self-consistent mean-field model. *J. Chem. Phys.* 2004; **121**: 10766–10777.
127. Morgan AB, Harris JD. Exfoliated polystyrene-clay nanocomposites synthesized by solvent blending with sonication. *Polymer* 2004; **45**: 8695–8703.
128. Zhao J, Morgan AB, Harris JD. Rheological characterization of polystyrene-clay nanocomposites to compare the degree of exfoliation and dispersion. *Polymer* 2005; **46**: 8641–8660.
129. Chu LL, Anderson SK, Harris JD, Beach MW, Morgan AB. Styrene-acrylonitrile SAN layered silicate nanocomposites prepared by melt compounding. *Polymer* 2004; **45**: 4051–4061.
130. Morgan AB, Chu LL, Harris JD. A flammability performance comparison between synthetic and natural clays in polystyrene nanocomposites. *Fire Mater.* 2005; **29**: 213–229.
131. Panek G, Schleidt S, Mao Q, Wolkenhauer M, Spiess HW, Jeschke G. Heterogeneity of the surfactant layer in organically modified silicates and polymer/layered silicate composites. *Macromolecules* 2006; **39**: 2191–2200.
132. Zilg C, Mülhaupt R, Finter J. Morphology and toughness/stiffness balance of nanocomposites based upon anhydride-cured epoxy resins and layered silicates. *Macromol. Chem. Phys.* 1999; **200**: 661–670.
133. Kornmann X, Thomann R, Mülhaupt R, Finter J, Berglund LA. High performance epoxy-layered silicate nanocomposites. Proceedings Nanocomposites-2001 International Symposium, Boucherville, QC, Canada, 16–18 Novermber 2001; *Polym. Eng. Sci.* 2002; **42**: 1815–1826.
134. Fröhlich J, Thomann R, Gryshchuk O, Karger-Kocsis J, Mülhaupt R. High-performance epoxy hybrid nanocomposites containing organophilic layered silicates and compatibilized liquid rubber. *J. Appl. Polym. Sci.* 2004; **92**: 3088–3096.
135. Kosiński LER, Rajendran GP, Reitz RR. Polyurethane fibers and films containing clay. Patent WO 9749847, 1997; US Patent 6,533,975, 2003.
136. Rossetti F. *Meccanismi di degradazione termica e di ritardo all fiamma di nanocomposite polimerici*. Thesis, University of Torino, 1999/2000.
137. Gilman JW, Kashiwagi T, Morgan AB, Harris HR Jr, Brassell L, Vanlandingham M, Jackson CL. *Flammability of Polymer Clay Nanocomposites Consortium*. Year One Annual Report, US Department Commerce, Technology Administration, National Institute of Standards and Technology, Report NISTIR #6531, Gaithersburg, 2000; 55 pages.
138. Zanetti M, Camino G, Thomann R, Mülhaupt R. Synthesis and thermal behaviour of layered silicate-EVA nanocomposites. *Polymer* 2001; **42**: 4501–4507.
139. Riva A, Zanetti M, Braglia M, Camino G, Falqui L. Thermal degradation and rheological behaviour of EVA/montmorillonite nanocomposites. *Polym. Degrad. Stab.* 2002; **77**: 299–304.
140. Bellucci F, Camino G, Frache A, Ristori V, Sorrentino L, Iannace S, Bian X, Guardasole M, Vaccaro S. Effect of organoclay impurities on mechanical properties of EVA-layered silicate nanocomposites. *e-Polymers* 2006; 014.
141. Kuwabara S, Nagata K, Kazuhisa Y, Imashiro Y, Sasaki E. Stock solution composition for use in production of hard polyurethane foam. US Patent 5, 779,775, 1998.
142. Si M, Goldman M, Rudomen G, Gelfer MY, Sokolov JC, Rafailovich MH. Effect of clay type on structure and properties of polymethyl methacrylate/clay nanocomposites. *Macromol. Mater. Eng.* 2006; **291**: 602–611.
143. McCarthy DC, Taber DC, Bowers DD. Synthetic hectorite coated flexible film. US Patent 5,523,338, 1996.
144. Doeff MM, Reed JS. Li ion conductors based on Laponite/polyethylene oxide composites. *Solid State Ionics* 1998; **113-115**: 109–115.
145. Inan G, Patra PK, Warner SB. *In-situ* polymerized fire resistant nylon 6/clay nanocomposites. *Polym. Mater. Sci. Eng.* 2003; **89**: 725–726.
146. Shemper BS, Morizur JF, Alirol M, Domenech A, Hulin V, Mathias LJ. Synthetic clay nanocomposite-based coatings prepared by UV-cure photopolymerization. *J. Appl. Polym. Sci.* 2004; **93**: 1252–1263.
147. Xu Y, Brittain WJ, Xue Ch, Eby RK. Effect of clay type on morphology and thermal stability of PMMA-clay nanocomposites prepared by heterocoagulation method. *Polymer* 2004; **45**: 3735–3746.
148. Sun Q, Deng Y, Wang ZL. Synthesis and characterization of polystyrene-encapsulated Laponite composites via miniemulsion polymerization. *Macromol. Mater. Eng.* 2004; **289**: 288–295.
149. Haraguchi K, Li HJ. Mechanical properties and structure of polymer-clay nanocomposite gels with high clay content. *Macromolecules* 2006; **39**: 1898–1905.
150. Galiano H, Caravanier-Callion M, Bebin P, Hourquebie P, Poncin-Epaillard F, Lafleche F, Bergaya F. Method for production of proton-conducting clay particles and composite material comprising said particles. Patent WO2005101552, 2005.
151. Osman MA, Rupp JEP, Suter UW. Tensile properties of polyethylene-layered silicate nanocomposites. *Polymer* 2005; **46**: 1653–1660.
152. Wu TM, Liao CS. Polymorphism in nylon-6/clay nanocomposites. *Macromol. Chem. Phys.* 2000; **201**: 2820–2825.

DOI: 10.1002/pat

153. de Siqueira AV, Lobban C, Skipper NT, Willams GD, Soper AK, Done R, Dreyer JW, Humphreys RJ, Bones JAR. The structure of pore fluids in swelling clays at elevated pressures and temperatures. *J. Phys.: Condens. Matter.* 1999; **11**: 9179–9188.
154. Wang Z, Pinnavaia TJ. Clay-polymer nanocomposites formed from acidic derivatives of montmorillonite and an epoxy resin. *Chem. Mater.* 1994; **6**: 468–474.
155. Wang Z, Pinnavaia TJ. Hybrid organic-inorganic nanocomposites: Exfoliation of magadiite nanolayers in an elastomeric epoxy polymer. *Chem. Mater.* 1998; **10**: 1820–1826.
156. Pinnavaia TJ, Lan T, Wang Z, Shi HZ, Kaviratna PD. Clay-reinforced epoxy nanocomposites. *Chem. Mater.* 1996; **8**: 1584–1587.
157. Pinnavaia TJ, Lan T. Flexible resin-clay composite, method of preparation and use. US Patent, 5,801,216, 1998.
158. Wang Z, Lan T, Pinnavaia TJ. Hybrid organic-inorganic nanocomposites formed from an epoxy polymer and a layered silicic acid magadiite. *Chem. Mater.* 1996; **8**: 2200–2204.
159. Bongiovanni R, Turcato EA, Mazza D, Ronchetti S, Priola A, Superti GB, Pastore HO, Marchese L. Use of synthetic lamellar silicates as fillers for the preparation of epoxy coatings via cationic UV-curing, AIZ Workshop 2006 ''Innovative Applications of Layered Material: From Catalysis to Nanotechnology'', Alessandria, 31 August–2 September 2006; 97–98.
160. Ogawa M, Ishii T, Miyamoto N, Kuroda K. Photocontrol of the basal spacing of azobenzene-magadiite intercalation compound. *Adv. Mater.* 2001; **13**: 1107–1109.
161. Wang D, Jiang DD, Pabst J, Han Z, Wang J, Wilkie CA. Polystyrene magadiite nanocomposites. *Polym. Eng. Sci.* 2004; **44**: 1122–1131.
162. Chigwada G, Jash P, Jiang DD, Wilkie CA. Fire retardancy of vinyl ester nanocomposites: Synergy with phosphorus-based fire retardants. *Polym. Degrad. Stab.* 2005; **89**: 85–100.
163. Costache MC, Jiang DD, Wilkie CA. Thermal degradation of ethylene-vinyl acetate copolymer nanocomposites. *Polymer* 2005; **46**: 6947–6958.
164. Morgan AB, Whaley PD, Lin TS, Cogen JM.The effects of inorganic-organic cations on EVA-magadiite nanocomposite flammability. In *Fire and Polymers: Materials and Concepts for Hazard Prevention*, Wilkie CA, Nelson GL (eds). ACS Symposium Series 922. Oxford University Press: Oxford, 2006; Chapter 5.
165. Kloprogge JT, Breukelaar J, Jansen JB, Geus JW. Development of ammonium-saponites from gels with variable ammonium concentration and water content at low temperatures. *Clays Clay Miner.* 1993; **41**: 103–110.
166. Kloprogge JT, Breukelaar J, Jansen JB, Geus JW. Characterisation of Mg-saponites synthesized from gels containing amounts of Na^+, K^+, Rb^+, Ca^{2+}, Ba^{2+}, or Ce^{4+} equivalent to the CEC of the saponite. *Clays Clay Miner.* 1994; **42**: 18–22.
167. Boccaleri E, Lolaico G, Bisio C, Marchese L, Superti GB, Pastore HO. Saponite-like materials: Synthesis and physico-chemical properties. *Microporous Mesoporous Mater.* 2006; submitted for publication.
168. Carrado KA, Xu L. *In situ* synthesis of polymer-clay nanocomposites from silicate gels. *Chem. Mater.* 1998; **10**: 1440–1445.
169. Higashi S, Miki K, Komarneni S. Hydrothermal synthesis of Zn-smectite. *Clays Clay Miner.* 2002; **50**: 299–305.
170. Frache A, Boccaleri E, Garibaldi F, Canepa F, Marchese L, Camino G. On the thermal behaviour of polymer-clay nanocomposites based on surfactant-modified natural and synthetic clays. International Conference on Interfaces & Interphases in Multicomponent Materials, Villeurbanne-Lyon, 12–14 September 2005.
171. Pinnavaia TJ, Xue S. Synthetic clays for polymer reinforcement. AIZ Workshop 2006 ''Innovative Applications of Layered Material: From Catalysis to Nanotechnology'', Alessandria, 31 August–2 September 2006; 67–68
172. Feitknecht W. Zur Kenntnis der Doppelhydroxyde und basischen Doppelsalze. *Helv. Chim. Acta* 1942; **25**: 106–137.
173. Miyata S, Kumura T, Shimada M. Composite metal hydroxides. US Patent 3,796,792, 1974.
174. Clearfield A, Kieke M, Kwan J, Colon JL, Wang RC. Intercalation of dodecyl sulfate into layered double hydroxides. *J. Inclusion Phenom. Mol. Recognit.* 1991; **11**: 361–378.
175. Stamires D, O'Connor P, Jones W, Brady M. Process for producing anionic clay using boehmite which has been peptized with an acid. US Patent 6,800,578 B2, 2004.
176. Miyata S. Anion-exchange properties of hydrotalcite-like compounds. *Clays Clay Miner.* 1983; **31**: 305.
177. Trifirò F, Vaccari A. *Solid State Supramolecular Chemistry: Two- and Three-dimensional Inorganic Network*, Alberti G, Bein T (eds). Comprehensive Supramolecular Chemistry, vol. 7; Pergamon, Elsevier Science: Oxford, 1996.
178. Perrotta AJ, Williams FS, Stonehouse L. Layered double hydroxides for treatment of Bayer process lake water. *Light Metals* 1997; 37–48; A collection of papers from the TMS annual meeting, Orlando, FL, 9–13 February 1997.
179. Rives V (ed.). *Layered Double Hydroxides: Present and Future.* Nova Science Publishers: New York, 2001.
180. Jones W, Rao CNR (eds). *Supramolecular Organization and Materials Design*. Cambridge University Press: Cambridge, 2002.
181. Newman SP, Jones W. Synthesis, characterization and application of layered double hydroxides containing organic guest. *New J. Chem.* 1998; **22**: 105–115.
182. Leroux F, Besse JP. Polymer interleaved layered double hydroxide: A new emerging class of nanocomposites. *Chem. Mater.* 2001; **13**: 3507–3515.
183. Bravo-Suárez JJ, Páez-Mozo EA, Oyama ST. Review of the synthesis of layered double hydroxides: A thermodynamic approach. *Quim. Nova* 2004; **27**: 601–614.
184. Evans DG, Duan X. Preparation of layered double hydroxides and their applications as additives in polymers, as precursors to magnetic materials and in biology and medicine. *Chem. Commun.* 2006; 485–496.
185. Costantino U, Marmottini F, Nocchetti M, Vivani R. New synthetic routes to hydrotalcite-like compounds—characterisation and properties of the obtained materials. *Eur. J. Inorg. Chem.* 1998; **10**: 1439–1446.
186. Kirkpatrick RJ, Andrey G, Kalinicheve AG, Wang JW, Hou XQ, Amonette JE.Molecular modeling of the vibrational spectra of interlayer and surface species of layered double hydroxides. In *The Application of Vibrational Spectroscopy to Clay Minerals and Layered Double Hydroxides*, Kloprogge T (ed.). CMS Workshop lectures, vol. 13. The Clay Mineral Society: Aurora, CO, 2004.
187. Ennadi A, Legrouri A, De Roy A, Besse JP. X-Ray diffraction pattern simulation for thermally treated [Zn-Al-Cl] layered double hydroxide. *J. Solid State Chem.* 2000; **152**: 568–572.
188. Wilson OC, Olorunyolemi T, Jaworski A, Borum L, Young D, Siriwat A, Dikens E, Oriakhi C, Lerner M. Surface and interfacial properties of polymer-intercalated layered double hydroxide nanocomposites. *Appl. Clay Sci.* 1999; **15**: 265–279.
189. Moujahid EM, Leroux F, Dubois M, Besse JP. *In situ* polymerisation of monomers in layered double hydroxides. *C.R. Chimie* 2003; **62**: 259–264.
190. Ding P, Qu B. Synthesis and characterization of polystyrene/layered double-hydroxide nanocomposites via *in situ* emulsion and suspension polymerization. *J. Appl. Polym. Sci.* 2006; **101**: 3758–3766.
191. Vieille L, Moujahid EM, Taviot-Gue'ho C, Cellier J, Besse JP, Leroux F. *In situ* polymerization of interleaved monomers: A comparative study between hydrotalcite and hydrocalumite host structures. *J. Phys. Chem. Solids* 2004; **65**: 385–393.
192. Costantino U, Montanari F, Nocchetti M, Sisani M. Polymeric composites constituted by polystyrene and Zn-Al/hydrotalcites grafted with benzenephosphonate. AIZ Workshop 2006 ''Innovative Applications of Layered Material: From Catalysis to Nanotechnology'', Alessandria, 31 August–2 September 2006; 89–90.
193. Camino G, Maffezzoli A, Braglia M, De Lazzaro M, Zammarano M. Effect of hydroxides and hydroxycarbonate structure on fire retardant effectiveness and mechanical properties in ethylene-vinyl acetate copolymer. *Polym. Degrad. Stab.* 2001; **74**: 457–464.

DOI: 10.1002/pat

194. Jiao CM, Wang ZZ, Ye Z, Hu Y, Fan WC. Flame retardation of ethylene-vinyl acetate copolymer using nano magnesium hydroxide and nano hydrotalcite. *J. Fire Sci.* 2006; **24**: 47–64.
195. O'Leary S, O'Hare D, Seeley G. Delamination of layered double hydroxides in polar monomers: New LDH-acrylate nanocomposites. *Chem. Commun.* 2002; 1506–1507.
196. Liao CS, Ye WB. Structure and conductive properties of polyethylene oxide/layered double hydroxide nanocomposite polymer electrolytes. *Electrochim. Acta* 2004; **49**: 4993–4998.
197. Fischer HR, Gielgens LH, Koster TPM. Nanocomposites from polymers and layered materials. *Acta Polym.* 1999; **50**: 122–126.
198. Costache MC, Wang D, Heidecker MJ, Manias E, Wilkie CA. The thermal degradation of polymethyl methacrylate nanocomposites with montmorillonite, layered double hydroxides and carbon nanotubes. *Polym. Adv. Technol.* 2006; **17**: 272–280.
199. Fischer HR, Gielgens LH. Nanocomposite material. US Patent 6,365,661, 2002.
200. Fischer HR, Gielgens LH. Nanocomposite material. US Patent 6,372,837, 2002.
201. Zammarano M, Bellayer S, Gilman JW, Franceschi M, Beyer FL, Harris RH, Meriani S. Delamination of organo-modified layered double hydroxides in polyamide 6 by melt processing. *Polymer* 2006; **47**: 652–662.
202. Lee WD, Im SS, Lim HM, Kim KJ. Preparation and properties of layered double hydroxide/polyethylene terephthalate nanocomposites by direct melt compounding. *Polymer* 2006; **47**: 1364–1371.
203. Chen W, Qu B. Structural characteristics and thermal properties of PE-g-MA/MgAl-LDH exfoliation nanocomposites synthesized by solution intercalation. *Chem. Mater.* 2003; **15**: 3208–3213.
204. Chen W, Feng L, Qu B. Preparation of nanocomposites by exfoliation of ZnAl layered double hydroxides in nonpolar LLDPE solution. *Chem. Mater.* 2004; **16**: 368–370.
205. Costantino U, Gallipoli A, Rocchetti M, Camino G, Bellucci F, Frache A. New nanocomposites constituted of polyethylene and organically modied ZnAl-hydrotalcites. *Polym. Degrad. Stab.* 2005; **90**: 586–590.
206. Qiu L, Chen W, Qu B. Morphology and thermal stabilization mechanism of LLDPE/MMT and LLDPE/LDH nanocomposites. *Polymer* 2006; **47**: 922–930.
207. Costa FR, Goad MA, Wagenknecht U, Heinrich G. Nanocomposites based on polyethylene and Mg-Al layered double hydroxide. Part I. Synthesis and characterization. *Polymer* 2005; **46**: 4447–4453.
208. Costa FR, Wagenknecht U, Jehnichen D, Goad MA, Heinrich G. Nanocomposites based on polyethylene and Mg-Al layered double hydroxide. Part II. Rheological characterization. *Polymer* 2006; **47**: 1649–1660.
209. Ding P, Qu B. Synthesis of exfoliated PP/LDH nanocomposites via melt-intercalation: Structure, thermal properties, and photo-oxidative behavior in comparison With PP/MMT nanocomposites. *Polym. Eng. Sci.* 2006; **46**: 1153–1159.
210. Bocchini S, Morlat Therias S, Gardette JL, Camino G. Influence of hydrotalcite on polypropylene photooxidation. AIZ Workshop 2006 ''Innovative Applications of Layered Material: From Catalysis to Nanotechnology'', Alessandria 31 August–2 September 2006; 93–94.
211. Hsueh HB, Chen CY. Preparation and properties of LDHs/polyimide nanocomposites. *Polymer* 2003; **44**: 1151–1161.
212. Hsueh HB, Chen CY. Preparation and properties of LDHs/epoxy nanocomposites. *Polymer* 2003; **44**: 5275–5283.
213. Zammarano M, Franceschi M, Mantovani F, Minigher A, Celotto M, Meriani S. Flame resistance properties of layered-double-hydroxides/epoxy nanocomposites. 9th European Meeting on Fire Retardancy and Protection of Materials, FRPM'03, Lille, 17–19 September 2003.
214. Zammarano M, Franceschi M, Bellayer S, Gilman JW, Meriani S. Preparation and flame resistance properties of revolutionary self-extinguishing epoxy nanocomposites based on layered double hydroxides. *Polymer* 2005; **46**: 9314–9328.
215. Liu YJ, DeGroot DC, Schindler JL, Kannewurf CR, Kanatzidis MG. Stabilization of anilinium in vanadiumV oxide xerogel and its post-intercalative polymerization to polyaniline in air. *J. Chem. Soc., Chem. Commun.* 1993; 593–596.
216. Murphy DW, Di Salvo FJ, Hull GW, Waszczak JV. Convenient preparation and physical properties of lithium intercalation compounds of Group 4B and 5B layered transition metal dichalcogenides. *Inorg. Chem.* 1976; **151**: 17–21.
217. Lemmon JP, Lerner MM. Preparation and characterization of nanocomposites of polyethers and molybdenum disulfide. *Chem. Mater.* 1994; **6**: 207–210.
218. Lerner M, Oriakhi C.Layered metal chalcogenides. In *Handbook of Layered Materials*, Auerbach S, Carrado KA, Dutta P (eds). Marcel Dekker: New York, 2004.
219. Benavente E, Santa Ana MA, Gonzalez G. Electrical conductivity of MoS2 based organic-inorganic nanocomposites. *Phys. Status Solidi B-Basic Res.* 2004; **241**: 2444–2447.
220. Mirabal N, Aguirre P, Santa Ana MA, Benavente E, Gonzalez G. Thermal stability and electrical conductivity in polyethers-molybdenum disulfide nanocomposites. *Electrochim. Acta* 2003; **48**: 2123–2127.
221. Santa Ana MA, Benavente E, Gómez-Romero P, González G. Polyacrylonitrile-molybdenum disulfide polymer electrolyte nanocomposite. *J. Mater. Chem.* 2006; **16**: 307–3113.
222. Alberti G, Allulli S, Costantino U, Tomassini N. Crystalline ZrR-PO32 and ZrR-OPO32 compounds R-organic radical: A new class of materials having layered structure of the zirconium phosphate type. *J. Inorg. Nucl. Chem.* 1978; **40**: 1113–1117.
223. Ortiz-Avila C, Clearfield A. Polyether derivatives of zirconium phosphate. *Inorg. Chem.* 1985; **24**: 1773–1778.
224. Zappelli P, Alberti G, Casciola M, Marmottini F, Vivani R. Mesoporous crystalline composition with a high surface area of a tetravalent metal which can be used as catalyst. US Patent 5,993,768, 1999.
225. Casciola M, Donnadio A. Enhanced thermal properties of polymer nanocomposites based on exfoliated Zirconium phosphate. AIZ Workshop 2006 ''Innovative Applications of Layered Material: From Catalysis to Nanotechnology'', Alessandria, 31 August–2 September 2006; 95–96.
226. Alberti G, Casciola M, Pica M, Di Cesare G. Preparation of nano-structured polymeric proton conducting membranes for use in fuel cells. *Ann. N.Y. Acad. Sci.* 2003; **984**: 208–225.
227. Bauer B, Roziere J, Jones D, Alberti G, Cascila M, Pica M. Ion conducting composite membrane materials containing an optionally modified zirconium phosphate dispersed in a polymeric matrix, method for preparation of the membrane material and its use. US Patent Application 2005/0118480 A1, 2005.
228. Casciola M, Donnadio A, Pica M, Valentini V, Piaggio P. Characterization of Zr phosphate/PVDF nanocomposites by vibrational spectroscopy. *Macromol. Symp.* 2005; **230**: 95–104.
229. Gatta GD, Masci S, Vivani R. Dimensional reduction in zirconium phosphate; from layers to ribbons to chains. *J. Mater. Chem.* 2003; **13**: 1215–1222.
230. Alberti G. Layered and pillared metal phosphates and phosphonates: Structures, properties and applications. AIZ Workshop 2006, Alessandria, 1–2 September 2006.
231. Musina Z, Monticelli O, Russo S, Superti GB, Pastore HO. Synthesis and characterisation of kanemite-based polystyrene nanocomposites. AIZ workshop 2006 ''Innovative Applications of Layered Material: From Catalysis to Nanotechnology'', Alessandria, 31 August–2 September 2006; 107–108.
232. Canepa F, Frache A, Camino G, Superti GB, Pastore HO. Effect of transition metals on thermal behaviour of polypropylene-ALPO kanemite nanocomposites, poster communication. AIZ workshop 2006, ''Innovative Applications of Layered Material: From Catalysis to Nanotechnology'', Alessandria, 31 August–2 September 2006; 101–102.

DOI: 10.1002/pat